INSTITUTE OF PATHOLOGY,
OSLO UNIVERSITY HOSPITAL RIKSHOSPITALET

Molecular studies on bone with focus on fracture healing in experimental osteoporosis

PhD thesis

Gunhild Melhus
cand. med.
2/1/2010

Series of dissertations submitted to the
Faculty of Medicine, University of Oslo
No. 941

ISBN 978-82-8072-509-7

Cover: Inger Sandved Anfinsen.
Printed in Norway: AiT e-dit AS.

Produced in co-operation with Unipub.
The thesis is produced by Unipub merely in connection with the
thesis defence. Kindly direct all inquiries regarding the thesis to the copyright
holder or the unit which grants the doctorate.

TABLE OF CONTENTS

ACKNOWLEDGEMENTS

The present study has been carried out at the Laboratory for Electron Microscopy and Laboratory for Immunohistochemistry and Immunopathology (LIPAT), Institute of Pathology, Oslo University Hospital Rikshospitalet. I started this work by participating in The Medical Student Research Program (MSR) in August 2003 to June 2006, which was jointly financed by the University of Oslo and The Research Council of Norway. I am grateful for the support and enthusiasm the head of the program *Professor Jarle Breivik* and the administrator and senior executive officer *Maje Siebke* have shown throughout these 3 years. After graduating from Faculty of Medicine at University of Oslo in June 2007, I was granted a PhD scholarship by the Norwegian South-Eastern Regional Health Authority extending to December 2009. I would like to express my gratitude toward both institutions.

The insights and comments of a great number of people have proved invaluable to the different aspects of this work. The thesis has benefited greatly from your generous support, criticism, and technical assistance. The following people, however, deserve special recognition.

Professor Finn P. Reinholt, my eminent and inspiring tutor, has been hands-on throughout the entire project. His enthusiasm and genuine interest proved durable and lasting; his office door was never shut and his cell phone was never off. He has generously shared his insight and knowledge, which extend far beyond the field of pathology, and asked all the right questions that helped move this project forward. I thank Finn for his medical and scientific competence, his perspective on life, and not least, his unforgettable one-liners.

Lars Nordsletten, Jan Erik Madsen, Sigbjørn Dimmen, Lene Solberg, Göran Andersson, Dick Heinegård, Lovisa Hessle, Christiane Petzold, Rune Jemtland, Christina Wenglen, Mikael Wendel, Espen S Bækkevold and Sverre-Henning Brorson, my co-authors, have all greatly contributed to the work. By sharing their extensive knowledge they have enriched and helped develop the project. I would like to give special thanks to Espen, who taught a much appreciated crash course on *in situ* hybridization and with great patience spent hours supervising the setting up of the protocol, and Sverre, my second tutor, who in virtue of his genuine interest for electron microscopy and infinite patience has been a solid source of help and inspiration at all times, and Lene, for sharing the ups and downs of the working days in the research program, and for making it cool to be a nerd.

Furthermore, a big thank-you goes to *Linda Dorg*, whose wit and honest feedback turned the strenuous lab-work into, if not a walk in the park, at least a pleasant hike, and *Aileen Murdoch-Larsen*, for her great attitude and her never-ending willingness to help with the electron microscope and preparation of the material, and *Linda I. Solfjell*, for answering mundane questions and helping a despaired physician through the jungle of molecular biology (and for teaching me all about the social importance of soccer…).
Furthermore, statistician *John Michael Gran* suggested valuable solutions to statistical challenges and provided excellent advices.

Lastly, my best friend and soon-to-be husband, *Petter A. Stordalen*, a closeted academic with a well-hidden desire for a doctoral title (at least in the family), has endured my hardship. He put up with me through tough times and supported this project in every way conceivable. He has spent days and nights stimulating his self-declared insatiable interest in metabolic bone diseases, thereby gaining an insight into the research questions and an appreciation of the challenges along the way. Not once has he expressed any negative feelings toward the project or any wish for me to become a stay-at-home wife. His disposition and outlook have helped me transform my frustrations into optimism and confidence. As my rock-solid mentor and inexhaustible source of positivity and inspiration, Petter, who in keeping with his feminist mindset now has earned the right to call himself *Herr Doktor Melhus,* added the finishing touch by writing the concluding paragraph himself.

ABBREVIATIONS

$1,25(OH)_2D_3$	1,25-dihydroxyvitamin D_3
25(OH)D	25-hydroxyvitamin D
ALP	Alkaline phosphatase
ANOVA	Analysis of variance
BMD	Bone mineral density
BMPs	Bone morphogenic proteins
BMUs	Basic multicellular units
BSP	Bone sialoprotein
BSA	Bovine serum albumin
BV_1	Low-density bone
BV/TV	Normalized volume of high-density bone
Cbfa1/Runx2	Runt-related transcription factor 2
cDNA	Complimentary DNA
CHAD	Chondroadherin
COMP	Cartilage oligomeric matrix protein
COX-2	Cyclooxygenase 2
cRNA	Complementary RNA
CS	Chondroitin sulphate
CTK	Cathepsin K
DAB+	Diaminobenzidine
DIG	Digoxigenin
DMP1	Dentin matrix protein 1
DXA	Dual X-ray absorptiometry
ECM	Extracellular matrix
FC	Fold changes
FDA	U.S. Food and Drug Administration
FGFR	Fibroblast growth factor receptor
FGF	Fibroblast growth factor
FS	Freeze-substitution
GAG	Glycosaminoglycan
HAP	Hydroxyapatite
HPF	High-pressure freezing
HPF-FS	High-pressure freezing with freeze-substitution
HPR	Horseradish peroxidise
IGF	Insulin-like growth factor
IHC	Immunohistochemistry
Ihh	Indian hedgehog
IL	Interleukin

ISH	*In situ* hybridization
KO	Knockout mice
LM	Light microscopy
LRR	Leucine-rich repeat
MANOVA	Multivariate analysis of variance
M-CSF	Macrophage-colony stimulating factor
MEPE	Matrix extracellular phosphoglycoprotein
Micro-CT	Micro-computer tomography
MMPs	Metalloproteinases
MSC	Mesenchymal stem cell
NCPs	Non-collagenous proteins
NPP1/PC-1	Nucleotide pyrophosphatase phosphodiesterase
NSAIDs	Non-steroid anti-inflammatory drugs
NUC	Nucleobindin
OPG	Osteoprotegerin
OPN	Osteopontin
OSAD	Osteoadherin
OVX	Ovariectomy/ovariectomized
PCR	Polymerase chain reaction
PDGF	Platelet derived growth factor
PF	Paraformaldehyde
PGs	Proteoglycans
Pi	Inorganic phosphate
PPi	Pyrophosphate
pQCT	Peripheral quantitative computed tomography
PS	Phosphatidyl serine
PTH	Parathyroid hormone
PTHrP	PTH related peptide
RANK	Receptor activator of nuclear factor κβ
RANKL	Receptor activator of nuclear factor κβ ligand
ROI	Region of interest
SD	Standard deviation
SIBLING	Small integrin-binding ligand, N-glycosylated protein
SLRP	Small leucine-rich proteoglycan
TEM	Transmission electron microscopy
TGF-β	Transforming growth factor β
TNAP	Tissue non-specific alkaline phosphatase
TNFα	Tumor necrosis factor α
TRAP	Tartrate-resistant acid phosphatase
VEGF	Vascular endothelial growth factor
VvTB	Volume density of trabecular bone
WT	Wild type mice

PUBLICATIONS INCLUDED

I. Experimental osteoporosis induced by ovariectomy and vitamin D deficient diet does not markedly affect fracture healing in rats.
Melhus G*, Solberg LB*, Dimmen S, Madsen JE, Nordsletten L, Reinholt FP.
* The authors contributed equally to the manuscript

Acta Orthop. 2007 Jun;78(3):393-403.

II. Heat-induced retrieval of immunogold labelling for nucleobindin and osteoadherin from Lowicryl sections of bone
Solberg LB*, Melhus G*, Brorson SH, Wendel M, Reinholt FP.
* The authors contributed equally to the manuscript

Micron. 2006;37(4):347-54. Epub 2005 Dec 9.

III. Key bone remodelling markers in the callus of vitamin D depleted ovariectomized rats
Melhus G, Brorson SH, Baekkevold ES, Jemtland R, Andersson G, Reinholt FP

Calcif Tissue Int. (submitted)

IV. Chondroadherin-deficient mice display a distinct skeletal phenotype
Melhus G*, Hessle L*, Wenglen C, Petzold C, Brorson SH, Baekkevold ES, Reinholt FP, Heinegard D
* The authors contributed equally to the manuscript

Manuscript, 2010

1 INTRODUCTION

1.1 BONE

Bone is a dynamic mineralized connective tissue that together with cartilage forms the skeletal system which provides both structural and metabolic functions. Anatomically, bones can be classified as either long (humerus, tibia, femur) or flat (skull bones and mandible, scapula, rib cage, pelvis and sacrum). At the morphological level, bone can be divided into woven and lamellar. Woven bone is formed during embryonic growth and during fracture healing, and is made up of irregularly deposited collagen fibers. Woven bone is replaced with mature lamellar bone with orderly deposition of the collagen fibers in a highly organized parallel or concentric layered structure. Lamellar bone exists as either cortical (compact) or trabecular (spongy or cancellous) bone. Cortical bone makes up the hard outer shell of flat bones and the diaphyses of long bones, accounting for approximately 80% of the total bone mass in the adult. It is characterized by a slow turnover rate and high resistance to bending and torsion. The remaining 20 % is trabecular bone, with low density but high surface area, is found in the interior of flat bones and in the metaphyses of long bones. Rod- and plate-like bone elements compose a spongy network housing the red bone marrow, which plays an important role in haematopoiesis. Trabecular bone is less dense, more elastic and has a higher turnover rate than cortical bone, providing the initial supplies of mineral to the systemic circulation in states of acute deficiency.

A long bone consists of two epiphyses, connected by the diaphysis (shaft) via the metaphyses (fig 1.1). During bone growth, a cartilaginous growth plate is present at the epiphysis/metaphysis interface. After onset of puberty, the growth plate closes, leaving a thin residual growth line in the adult. The diaphysis is a cortical cylinder containing bone marrow. The epiphyses consist of trabecular bone covered with a thin cortical layer. The periosteum lines the outer bone surface, except at articular surfaces and insertion sites for ligaments and tendons. Endosteum lines the marrow cavity.

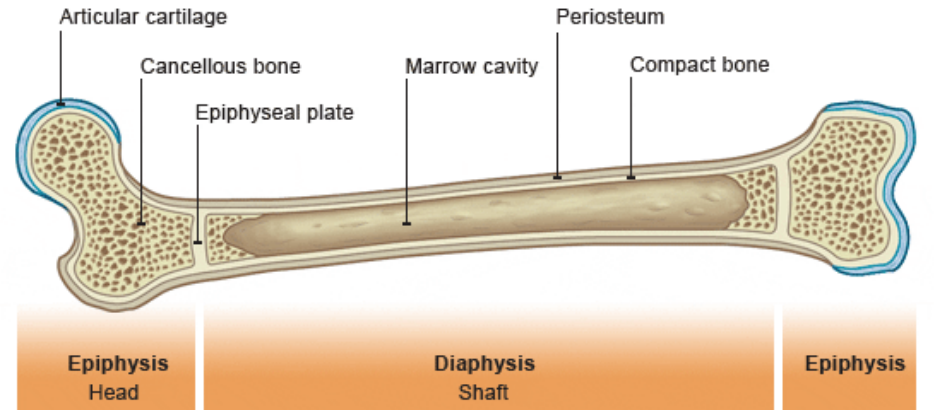

Fig. 1.1 (from *http://www.bbc.co.uk/schools/gcsebitesize/pe/images/bone_anatomy.gif*)

1.1.1 Bone cells

Bone cells originate from two different sources; mesenchymal progenitor cells which give rise to the osteoblastic lineage (osteoblasts, osteocytes and lining cells), and precursor cells related to the monocyte-macrophage cell line from the bone marrow differentiating into osteoclasts.

The *osteoblast* is a cuboidal mononuclear cell, responsible for bone formation by synthesizing the main components of the extracellular matrix (ECM), i.e. collagen and non-collagenous proteins. Osteoblasts are found in clusters along the bone surfaces, lining the layer of bone matrix they are synthesizing. Runt-related transcription factor 2 (Cbfa1/Runx2) and a downstream factor, osterix, are essential to osteoblast differentiation. In the process of bone formation, some osteoblasts become embedded in their own synthesized osteoid, and subsequently differentiate into the terminal stage of the osteoblastic cell lineage, becoming an osteocyte. Simultaneously, other cells undergo apoptosis or remain on the bone surface, becoming flattened lining cells. Morphologically, osteoblasts are characterized by a rounded nucleus, abundant rough endoplasmatic reticulum, an extensive Golgi apparatus as well as lysosomes. The expression of alkaline phosphatase (ALP) in the mature osteoblast disappears if the cell differentiates into an osteocyte.

The osteocyte is the most abundant cell type in bone. Osteocytes are contained in separate lacunae throughout the bone, but create a functional communicative network enabling cross-talk between the various types of bone cells by sending out thin cytoplasmatic extensions traversing mineralized bone via thin canals, so-called canaliculi. Osteocytes are involved in the biomechanical regulation of bone mass and structure, probably by sensing bone deformation, pressure, fluid flows and streaming potentials. Osteocytes typically express molecules such as

dentin matrix protein 1 (DMP1) (4) and matrix extracellular phosphoglycoprotein (MEPE) (5). MEPE is an inhibitor of mineralization (6), whereas DMP1 is produced by the osteocyte in a mechanically sensitive manner (7), and influences phosphate homeostasis through control of fibroblast growth factor 23 (FGF23).

The *bone lining cells* are flat elongated cells covering quiescent bone surfaces. Their function is not fully understood, but they may 1) participate in the regulation of substrate exchange between the bone fluid compartment and the extracellular fluid of bone marrow, 2) respond to mechanical signals and mediate communication between the osteocyte network and the pool of osteoclasts and thereby initiating bone resorption or 3) serve catabolic functions (8).

Osteoclasts are giant multinucleated cells responsible for bone resorption, formed by fusion of mononuclear progenitors of the monocyte-macrophage lineage. Two hematopoietic cytokines, macrophage-colony stimulating factor (M-CSF) and receptor activator of nuclear factor κβ ligand (RANKL) are necessary and sufficient for differentiation of macrophage precursors into mature osteoclasts. Osteoclasts contain abundant Golgi complexes, mitochondria and transport vesicles loaded with lysosomal enzymes. Non-resorbing osteoclasts are motile and show no distinct membrane domains. Prior to bone resorption, the osteoclast polarizes due to changes in the cytoskeleton and forms three distinct plasma membrane domains, i.e. the *clear (sealing) zone* on the apical side where the cell membrane pastes tightly to the bone surface, sealing off a compartment underneath the cell. In the cell membrane overlying this isolated compartment, numerous thin finger-like extensions form and make up the *ruffled border*, where the actual bone resorption occurs. Simultaneously, a functional secretory domain forms on the basolateral side of the cell. The initial attachment of osteoclasts to bone surfaces involves binding of integrins to specific amino acid sequences (RGD) within proteins such as osteopontin (OPN) at the matrix surface (9). Carbonic anhydrase II generates protons (H^+) in the osteoclast cytoplasm, and these protons are transported into acidic vesicles through the action of a vacuolar-type ATPase proton pump (V-ATPase) localized in the membrane of the vesicles (10). The migration and subsequent fusion of these acid-containing vesicles with the cell membrane form the ruffled border, and the contents of the vesicles are released into the resorption (Howship's) lacuna. The active secretion of protons acidifies the environment and solubilises the mineral crystals, exposing the organic matrix for degrading proteases, and providing the pH optimum for the action of these proteases. of the organic matrix is cathepsin K (CTK) (11). The degradation products are endocytosed from the ruffled border, transported through the cell, and finally secreted into the extracellular space through the functional secretory domain (12-13). Osteoclasts also contain large amounts of tartrate-resistant acid phosphatase (TRAP), a metallophosphatase secreted into

the resorption lacunae. When activated by proteolytic processing, TRAP exhibits protein phosphatase activity towards matrix proteins such as OPN (14), and TRAP has recently been suggested to regulate osteoclast motility by dephosphorylation of OPN in the matrix (15).

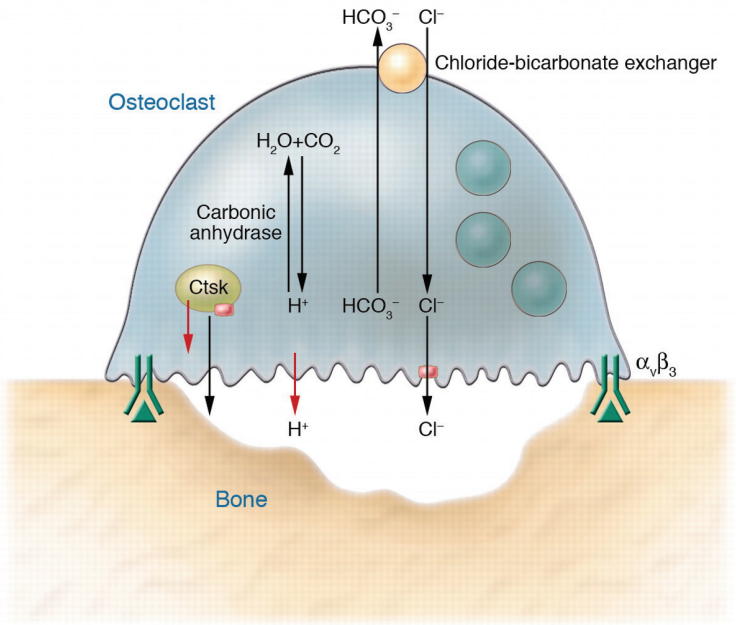

Figure 1.2: Osteoclastic bone resorption
The osteoclast adheres to bone via binding of RGD-containing proteins (green triangle) to the integrin $\alpha_v\beta_3$, initiating signals that lead to insertion into the plasma membrane of lysosomal vesicles that contain cathepsin K (Ctsk). Consequently, the cells generate a ruffled border above the resorption lacuna, into which is secreted hydrochloric acid and acidic proteases such as cathepsin K. The acid is generated by the combined actions of a vacuolar H^+ ATPase (red arrow), its coupled Cl^- channel (pink box), and a basolateral chloride/bicarbonate exchanger. Carbonic anhydrase converts CO_2 and H_2O into H^+ and HCO_3^-.
(From *http://www.biology-online.org/articles/skin_bone/figures.html*)

1.1.2 Bone and cartilage extracellular matrix

Bone cells are surrounded by an organic ECM, strengthened by mineral deposits, mainly present in the form of hydroxyapatite (HAP) crystals [$Ca_{10}(PO_4)_6(OH)_2$]. Bone mineral comprises approximately 70% of the dry weight of bone. The organic phase contains mainly type I collagen fibers (which comprises 90% of the organic bone matrix), various noncollagenous proteins (NCPs), serum proteins and proteoglycans (PGs). In addition, small amounts of water and lipids are present. In a similar manner, cartilage cells are embedded in an abundant ECM, where collagen type II is the dominating collagen (for references, see (16)).

Collagens (table 1A)

Collagen is a triple helical molecule containing three identical or two or three different α chains depending on the collagen type. Collagen α chains is characterized by a Gly-X-Y repeating triplet where Y is often proline. Each of the different collagen chains has its own unique structure of this repeating triplet. After synthesis, the chains are extensively modified inside the cell by enzymes that add a variety of additional molecules (i.e. post-translational modifications). After assembly into fibrils, collagen chains exit the cell, and globular regions at both ends of the triple helix are cleaved by specific proteases leaving a shortened triple helical chain. Extracellularly, the triplex undergoes further modification with intra- and intermolecular crosslinks. The fibrils are then further arranged in collagen fibers forming a highly ordered network providing elasticity and flexibility. In addition, different types of collagen often interact at fibril surfaces also exposing domains for interaction with other extracellular matrix components. A variety of the NCPs influence the fibril formation

Table 1A. Collagens in bone and cartilage

Protein	Gene	Distribution and suggested function
Type I	COL1A1, COL1A2	Most abundant protein in bone, serves as scaffold, binds and orients other proteins regulating central processes like mineralization
Type II	COL2A1	The key component of hyaline cartilage; contributes to the regulation of chondrocyte function, including differentiation, proliferation, and survival through cell-surface signalling mechanisms. Predominates in interterritorial matrix (composed of fibrillar collagen network providing tensile

		strength) with type XI and type IX (17)
Type III	COL3A1	Present in bone in trace amounts, may regulate collagen fibril diameter, paucity in bone may explain the large diameter size of bone collagen fibrils
Type V	COL5A1, COL5A2, COL5A3	Found in tissues containing type I, and tends to regulate the assembly of heterotypic fibers composed of both type I and type V
Type VI		Predominates in the territorial matrix (close to the cell, consists of little or no fibrillar collagen) as microfibrils
Type IX	COL9A1 COL9A2 COL9A3	Major component of hyaline cartilage
Type X	COL10A1	Present in hypertrophic and mineralizing cartilage, expressed by hypertrophic chondrocytes during endochondral bone formation and in the growth plate
Type XI	COL11A1	Produced by chondrocytes in the upper growth plate zones
Type XXVII	COL27A1	A novel member of the fibrillar collagen family, contributes to a stable cartilage matrix (18).

Noncollagenous proteins in bone and cartilage

Various NCPs account for the remaining 10% of the organic matrix, and are a heterogeneous group of proteins varying from entrapped serum protein to glycoproteins, which are unique to bone and/or cartilage. The NCPs are embedded in the matrix during bone and cartilage formation (some of them bind to collagen) and are released during resorption, participating in the remodelling process. Approximately 25% of the total NCP content is exogenously derived (table 1B,6). The remaining NCPs are locally produced by the cells, which synthesize collagen and NCP molecules in a 1:1 ratio. These NCPs can be divided into 5 groups: 1) PGs, 2) glycosylated proteins, 3) glycosylated proteins with cell attachment activities, and 4) γ-carboxylated (gla) proteins (19). In addition, the matrilins are regarded as a separate group of NCPs (table 1B,1-5). In cartilage, the collagen fibers are embedded in a hydrated gel of PGs and other glycoproteins. The PGs are essential for protecting the collagen network. The predominant glycosaminoglycan (GAG) of PGs in articular cartilage is

chondroitinsulfate (CS), along with aggrecan being the most abundant CS proteoglycan in the matrix of articular cartilage. Aggrecan forms complexes with hyaluronic acid, providing compressive resistance to the tissue. A large number of NCPs present in bone are also expressed in cartilage. However, some cartilage-NCPs are not expressed in bone, e.g. cartilage oligomeric matrix protein (COMP) and perlecan. The NCPs are regulated by several other molecules such as matrix metalloproteinases (MMPs), growth factors, transforming growth factor β (TGF-β), and bone morphogenic proteins (BMPs).

1) Proteoglycans
The PGs are macromolecules with acidic sugar side chains attached to a central core protein, which modulate cellular behaviour either through the attached GAG chains or by direct protein-protein interactions via the core protein sequences. In this group, we find among others, versican, decorin, biglycan, hyaluronan (a GAG, i.e. not attached to a protein core) and perlecan. In addition, there are other small leucine-rich proteoglycans (SLRPs) in bone, such as osteoglycin, osteoadherin, lumican, asporin and fibromodulin. The distinguishing feature of SLRPs is the presence of a central domain containing leucine-rich repeats (LRRs) in the protein core. The SLRPs play roles in biological processes, such as skeletal growth, craniofacial structure, and collagen fibrillogenesis (20).

2) Glycosylated proteins
ALP is a glycoprotein-enzyme highly expressed in bone, and believed to play a role in mineral deposition. Osteonectin, the most abundant protein in bone, is also a phosphorylated glycoprotein.

3) Glycosylated proteins with cell attachment activities
Bone cells synthesize at least 12 proteins that may mediate cell attachment: the 5 members of the small Integrin-binding ligand, N-glycosylated protein (SIBLING) family, type I collagen, fibronectin, thrombospondin(s), vitronectin, fibrillin, BAG-75 and osteoadherin (which is also a PG). Common for most of these proteins is that they contain RGD (arginine–glycine–aspartate), the cell attachment sequence that binds to integrins in cell membranes. *The SIBLING* family includes OPN, bone sialoprotein (BSP), DMP1, dentin sialophosphoprotein and MEPE. Except from MEPE, these proteins are acidic, phosphorylated and secreted proteins. SIBLINGs bind strongly to bone mineral, and contain the RGD motif (21). The SIBLINGs are believed to play key biological roles in the development, turnover and mineralization of bone and dentin.

4) Gla-containing proteins
Matrix Gla-protein, osteocalcin and protein S (primarily synthesized by the liver, but also by bone cells) are post-translationally modified by the action of vitamin

K-dependent γ-carboxylases. The di-carboxylic glutamyl (gla) residues enhance calcium binding.

Table 1B. Noncollagenous proteins in bone and cartilage[1]

1) Proteoglycans

Protein (gene symbol)	Tissue distribution	Suggested function(s) in bone and/or cartilage
Decorin (Dcn)	Widely distributed	Role in ECM assembly
Biglycan (Bgn)	Bone and connective tissues	Modulation of matrix mineralization by modulating collagen assembly (22)
Versican (Vcan)	Secreted by many cell types	Important in chondrogenesis (23)
Perlecan (Hspg2)	Cartilaginous tissues	Interaction with matrix components to regulate cell signalling (24)
Fibromodulin (Fmod)	Widely distributed in connective tissues	Binding to collagen type I, regulation of collagen fibril formation
Asporin (Aspn)	Periosteum and dental follicles during development	Regulation of the initial deposition of hydroxyapatite in the collagen gap regions *in vitro* (25)
Lumican (Lum)	Widely distributed in connective tissues	Collagen binding, regulate collagen organization (26)
Chondroadherin (Chad)	Mainly in cartilage matrix, but also in bone and other tissues	Role in regulation of chondrocyte growth and proliferation
Aggrecan (Acan)	Cartilage-specific	Mediation of cell – cell and cell – matrix interactions, inhibitor of mineralization

2) Glycosylated proteins

Protein (gene symbol)	Tissue distribution	Suggested function(s) in bone and/or cartilage
Osteonectin (Sparc)	Widely distributed, particularly at sites of remodelling and matrix assembly	Regulation of collagen organization, regulation of bone formation and remodelling (27)
Alkaline	Bone, liver, kidney	Potential calcium ion carrier,

phosphatase (Alpl)		hydrolyzes inhibitors of mineral deposition

3) Glycosylated proteins with cell attachment activities

Protein (gene symbol)	Tissue distribution	Suggested function(s) in bone and/or cartilage
Osteopontin (Spp1)	Widely distributed	Cell (osteoclast) binding, regulator of mineralization
Bone sialoprotein (Ibsp)	Mineralized tissues	Cell binding, initiation of mineralization
Dentin matrix protein-1 (Dmp1)	Bone, dentin and non-mineralized tissues	Regulatory role in dentin mineralization and Pi homeostasis (28), no known function in bone
Dentin sialophospho-protein (Dspp)	Tooth, bone, kidney and salivary glands	Role in initial mineralization and remodelling of bone (29).
Matrix extracellular phosphoglyco-protein (Mepe)	Bone and teeth	Role in bone homeostasis
Fibronectin (Fn)	Expressed in a variety of tissues	Cell adhesion, growth, migration and differentiation
Thrombo-spondin-2 (Thbs2)	Expressed in a variety of tissues	Promotion of mineralization (30)
Vitronectin (Vtn)	Mineralized bone, and several other tissues	Regulation of bone metabolism (31)
Fibrillins	Expressed in a variety of tissues	Role in cartilage development (32)
Bone acidic glycoprotein-75	Restricted to actively forming primary or woven bone and dentin	Delineation of future extracellular sites of mineralization together with BSP (33)
Osteoadherin/ Osteomodulin (Omd)	Specific to mineralized tissues	Cell binding, role in mineralization (is also a PG)
Cartilage oligomeric matrix protein (Comp)	Expressed in cartilage, ligament, and tendon	Interaction with fibronectin, a role in ECM assembly by molecular interactions

4) Gla-containing proteins

Protein (gene symbol)	Tissue distribution	Suggested function(s) in bone and/or cartilage
Matrix Gla protein (Mgp)	Bone and cartilage, but expressed in many connective tissues	Inhibitor of extracellular matrix calcification (34)
Osteocalcin (Bglap)	Most abundant NCP in bone, secreted by mineralized tissues	Participation in mineralization and cell signalling, recruiting osteoblasts and osteoclasts (35)

5) Matrilins

Protein (gene symbol)	Tissue distribution	Suggested function(s) in bone and/or cartilage
Matrilins (Matn)	Matrilin-1 and -3 specific to cartilage	Role as adaptor proteins mediating interactions between collagens and proteoglycans (36-37)

6) Exogenously derived serum proteins

Protein (gene symbol)	Tissue distribution	Suggested function(s) in bone and/or cartilage
α_2HS-glycoprotein (Ahsg)	Widely distributed protein from liver	Regulation of bone mineralization
Albumin	Widely distributed protein from liver	Inhibition of growth of bone mineral crystals

[1] The exact role of most proteins is not known, and the official gene symbols (for *Rattus norvegicus*) and suggested functions are referred from www.ncbi.nlm.nih.gov/gene if no other reference is given.

1.1.3 Bone mineralization

Mineralization occurs by the orderly deposition of HAP at discrete sites in the collagenous network, where mineralization nodular complexes form within 48 – 72 h (38). Crystals are always deposited so that their longest dimension lies parallel to the axis of the collagen fibrils. Formation of the initial HAP crystal, i.e. the "critical nucleus", is the most energy demanding step in the process, requiring the ions of the future crystal to fuse with proper direction and sufficient energy, and is believed to occur at the gap ("hole") zones between collagen fibrils.

Because body fluids are undersaturated with respect to HAP, crystals will not precipitate spontaneously. Thus, promoters and/or local factors in the ECM are

required to facilitate initiate crystal formation. Two current hypotheses of critical nucleus formation exist; 1) Passive *de novo* formation, where local mineralization inhibitors are overwhelmed (39), and 2) heterogeneous nucleation, i.e. active contribution to crystal formation by local extracellular nucleation complexes such as mineralization foci (40), crystal ghosts (41), matrix vesicles (41-42), or ECM phosphoproteins (42-43).

Matrix vesicles

Matrix vesicles are generally accepted to play a role during mineralization of vertebral hard tissues, although to a lesser extent in bone compared to cartilage and tendon (44). They are small (20 – 200 nm) spherical bodies observed in the pre-mineralized matrix of dentin, cartilage and bone, derived from the plasma membrane of chondrocytes, osteoblasts and odontoblasts. They contain a nucleation core consisting of acidic phospholipids, calcium, inorganic phosphate (Pi), annexins (Ca-transport proteins), and are also enriched in tissue non-specific alkaline phosphatase (TNAP), nucleotide pyrophosphatase phosphodiesterase and phosphatidyl serine in addition to several MMPs. The vesicles may provide protected areas to enhance the concentration of Pi and calcium, and/or remove the inhibitory effect of pyrophosphate (PPi) on HAP formation (45-47). On the outer membrane surface, TNAP hydrolyses PPi in the ECM, which inhibits HAP formation and yields free Pi which reacts with calcium to form HAP (42,48). Although regulation of extracellular PPi and Pi concentration is necessary for mineralization, TNAP is important but not sufficient , unless the enzyme is membrane-anchored (49).

However, the mechanisms through which matrix vesicles initiate mineralization remain unclear, especially because they are not directly associated with the collagen fibrils where crystals are finally deposited.

Role of matrix proteins

It is now generally accepted that there are NCPs associated with collagen that can serve as nucleators and regulators of size and shape of HAP crystals. Members of the SIBLING family (in particular BSP and DMP1), osteonectin and BAG75 are all suggested to act as nucleators (44,50). Most of these molecules are acidic and capable of binding calcium ions. BAG75 delineates future sites of mineralization (33), and BSP, BAG75 (50) and TNAP form spherical structures in osteoblast cultures which represent mineralization foci. Other protein such as osteonectin, OPN and osteocalcin do not generally act as nucleators but bind to HAP with high affinity and act as effective inhibitors of crystal proliferation. However, even a highly phosphorylated form of OPN can act as a nucleator, while a small peptide of MEPE can act as an inhibitor of cell-mediated mineralization (51). It is thus likely that many of these proteins are modified locally to modulate the process of mineralization.

Once the critical nucleus is formed and large enough to persist in solution, ions or ion clusters are easily added in the process of crystal growth. In bone, there are obviously many such nucleation sites, as crystals form concurrently at numerous separate loci. Secondary nucleation occurs as new ions form on the initial nucleus in a manner analogous to that of glycogen branching. The new crystal branches separate and provide additional nuclei. When bone matures, the crystals increase in size and become more perfect (i.e. contain less impurities and thus are less soluble). While each of the major hypotheses of the initiation of mineralization is plausible and backed by a substantial body of evidence, the known features of cartilage and bone mineralization are still incompletely understood.

1.2 BONE GROWTH AND REMODELLING

1.2.1 Bone formation

The future bony skeleton in the embryo is composed of either fibrous tissue or hyaline cartilage. Bone formation occurs by two distinct processes; intramembranous and endochondral pathways, which in general form flat and long bones, respectively (for references, see (52)).

Intramembranous bone formation

Mesenchymal cells migrate and condensate into clusters within the fibrous tissue, and differentiate directly into osteoblasts. Such a cluster is known as an ossification center, and the osteoblasts start to secrete matrix, which subsequently mineralize. Matrix synthesis continues until the osteoblasts are completely covered in immature, irregular matrix, forming a trabeculum. The woven bone is subsequently remodelled into mature lamellar bone. Mesenchymal cells continue to differentiate in the periphery. Other trabeculae form in nearby ossification centers and fuse into the open latticework characteristic of trabecular bone, and bone marrow develops in the intertrabecular areas by ingrowth of capillaries. The original connective tissue surrounding the growing bone mass, transforms into the periosteum, and eventually, the surface layers of trabecular bone are transformed into cortical bone. Much of this newly formed bone is subsequently modelled and remodelled until the bone reaches its final adult size and shape.

Endochondral bone formation

Endochondral bone formation occurs via an intermediate step of cartilage, and involves a coordinated set of interactions requiring the transient expression of specific genes and various cell – cell and cell – matrix interactions, which results in the eventual replacement of cartilage with bone. The process starts with proliferation and aggregation of mesenchymal cells at the site of the future bone, which in hypoxic areas differentiate into chondroblasts. The chondroblasts

secrete cartilaginous matrix that lead to development of a cartilage model of the future bone, lined with a membrane known as the perichondrium. Midway along the diaphysis, blood vessels start to penetrate the perichondrium, stimulating cells in the internal layer of the membrane to differentiate into osteoblasts. The osteoblasts deposit bone matrix making a bone collar around the diaphysis of the cartilage model. Thus, the perichondrium is transformed into the periosteum. Simultaneously, the primary ossification center develops centrally in the cartilaginous diaphysis where chondrocytes start to hypertrophy. Typical features of hypertrophic chondrocytes are the expression of type X collagen (53), increased synthesis of ALP (54), denaturation and removal of ECM, and a net increase in the production of MMPs over their tissue inhibitors. This is followed by blood vessel invasion and matrix calcification. The hypertrophic cells undergo apoptosis, matrix breaks down and an expanding marrow cavity ensues. Meanwhile, capillaries grow into the cavity and establish contact with bone marrow cells. The calcified matrix is partially resorbed and osteoblasts begin to deposit bone. Periosteal bone formation continues to increase the cortical thickness, while the cartilage model enlarges bilaterally at both ends. Ingrowth of blood vessels also occurs in the epiphyses and trabecular bone is formed, establishing the two secondary ossification centers within the epiphyses. After formation of the secondary ossification centers, the cartilage model is completely replaced by bone except at the articular surfaces, which are permanently covered with cartilage, and at the epiphysis/diaphysis interface, where cartilage persists as the epiphyseal growth plate. Bone elongation occurs by proliferation of cells at the epiphyseal side of the growth plate, where chondrocytes pass through various stages of differentiation, from a resting stage through proliferation, maturation, and finally hypertrophy, leading to replacement of cartilage with bone on the diaphyseal side. Thus, the thickness of the epiphyseal growth plate remains fairly constant but the diaphyseal bone continues to elongate. Increase in cortical diameter occurs by parallel periosteal appositional growth and endosteal resorption. Initially, diaphyseal and epiphyseal ossification form trabecular bone, but this is transformed into cortical bone. In humans, primary and secondary ossification centers fuse after puberty, whereas in adult rodents a narrow region of growth plate cartilage remains.

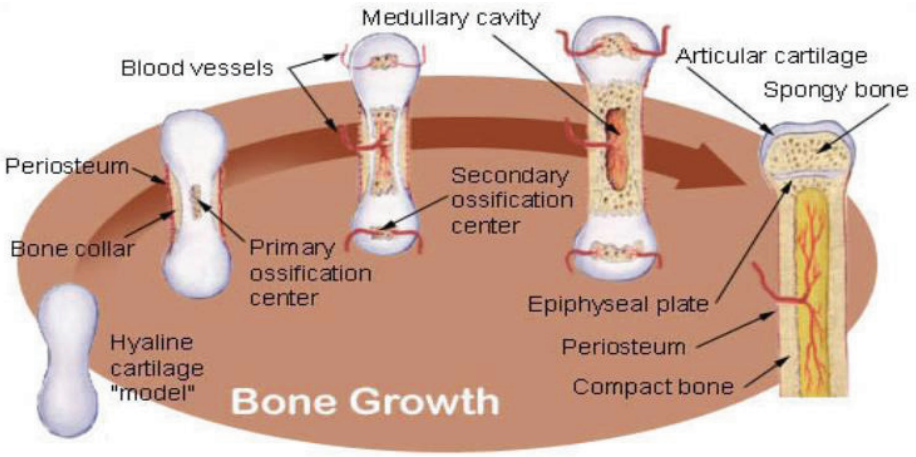

Figure 1.3: Endochondral bone growth
Endochondral bone formation starts at discrete sites in the cartilage (i.e. the primary ossification centers) appearing during fetal development, although some short bones starts ossification post partum. The primary ossification center forms in the diaphyses of long bones, short bones and certain parts of irregular bones. Secondary ossification occurs post partum and forms the epiphyses of long bones and the extremities of irregular and flat bones. The diaphysis and both epiphyses are separated by a growing cartilaginous zone, i.e. the epiphyseal growth plate, which closes during puberty and cessation of longitudinal growth.
http://www.mheresearchfoundation.org/sitebuilder/images/illu_bone_growth-740x379.jpg

1.2.2 The epiphyseal growth plate

The epiphyseal growth plate can be divided in 4 distinct zones. The resting (or reserve) zone is a source of mesenchymal stem cells, responsible for protein synthesis and maintenance of germinal structure. The proliferative zone is characterized by actively proliferating cells, arranged in regular vertical columns which synthesize matrix. The hypertrophic zone (divided in the upper and lower hypertrophic layers) contains chondrocytes that enlarge, separate and subsequently undergo apoptosis. In the calcifying zone, the remaining longitudinal septa of cartilage are subsequently mineralized by increased release of ALP, calcium and matrix vesicles by terminally differentiated chondrocytes. Metaphyseal vessels carrying osteoprogenitor cells grow in and the mineralized matrix is partially resorbed by chondroclasts. The osteoprogenitor cells differentiate and start to deposit woven bone on the cartilaginous septa, forming the primary spongiosa. The woven bone and cartilage are subsequently

remodelled and replaced by lamellar bone. This mature trabecular bone is called the secondary spongiosa. Estrogen secretion in both sexes at the onset of puberty is considered the main cause of cessation of growth by inactivating the growth plate, which is subsequently replaced by trabecular bone in most mammals.

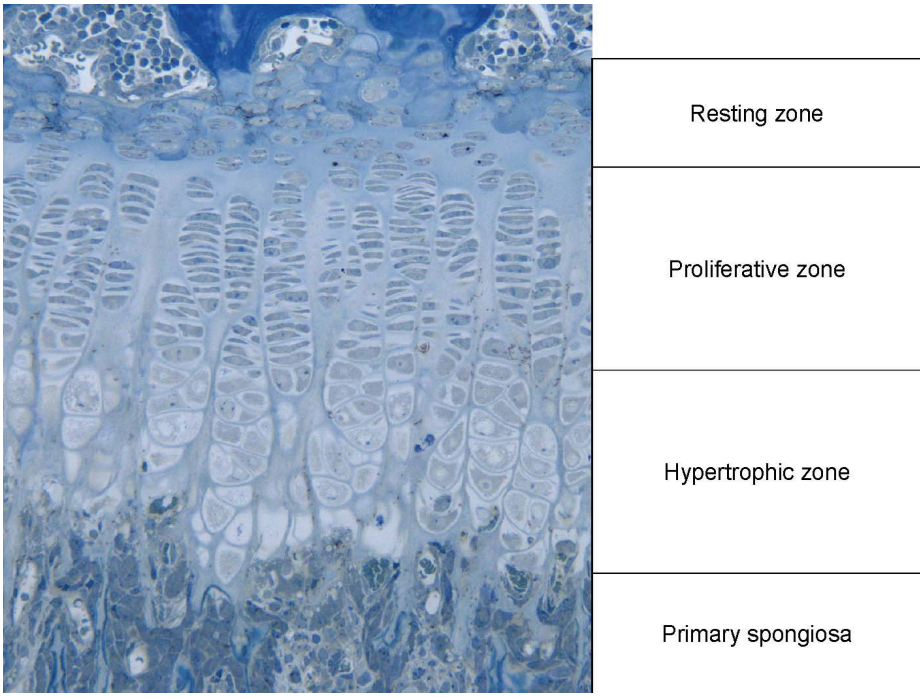

Regulation of the epiphyseal growth plate

Molecular regulation of chondrocyte proliferation and hypertrophy include the "Indian hedgehog" (Ihh), parathyroid hormone (PTH) related peptide (PTHrP), Wnt, Fgf and Bmp signalling pathways (for references, see (52)).

Sox9 and Runx2 are master transcription factors required for developing chondrocytes and osteoblasts from mesenchymal stem cells, respectively. Increased Wnt signalling takes place during intramembranous bone formation and promotes osteoblast differentiation, while decreased Wnt signalling favours chondrocyte differentiation. Ihh signalling is required for osteoblast differentiation. In contrast to Wnt and Ihh, BMP signalling stimulate both osteoblast and chondrocyte differentiation from mesenchymal progenitors. Fibroblast growth factors (FGFs) and FGF receptors (FGFRs) are also important mediators of bone formation although their exact roles are not fully elucidated. Ihh controls the pace of chondrocytes hypertrophy by activating PTHrP, which is synthesized in the perichondrium by terminally differentiated chondrocytes (52). Secondary to activation of PTH/PTHrP receptors, PTHrP stimulates cell proliferation by G protein activation and delays transformation into

prehypertrophic and hypertrophic chondrocytes. The feedback loop between Ihh and PTHrP regulates the balance between proliferating and hypertrophic chondrocytes, maintaining the growth plate at a constant width.

1.2.3 Bone remodelling

Bone remodelling is the process where the skeleton is continuously being renewed throughout its lifetime, allowing the maintenance of the shape, quality and size of the skeleton. Remodelling occurs asynchronously at multiple discrete sites throughout the skeleton, and is coordinated by multiple paracrine and autocrine factors (55). Remodelling occurs in order to 1) repair micro-fractures before they accumulate and lead to fatigue fractures under repeated cyclic loading (targeted remodelling), and 2) provide access to stores of calcium and phosphate, maintaining the mineral homeostasis (random remodelling) (56). Osteoclastic resorption is followed by osteoblastic formation in a tightly coupled process; these cell types work together in basic multicellular units (BMUs). The BMU undergo a stepwise remodelling cycle comprising activation, resorption, and formation, followed by a quiescent stage. In between resorption and formation, there is a reversal phase. Imbalance in the remodelling cycle is essential in the pathogenesis of several bone disorders, such as osteoporosis and Paget's disease (57). The coupling of resorption and formation is based upon the RANK-RANKL-OPG axis. RANKL is a protein synthesized by cells in the osteoblastic lineage, and is present both in a membrane-bound and a soluble form. RANKL binds to its receptor, RANK (receptor activator of nuclear factor κβ), expressed by osteoclast precursors, thereby promoting osteoclast formation (58). A competitive soluble ligand for RANK, osteoprotegerin (OPG), also produced by osteoblastic cells, blocks activation of RANK and thus formation of active osteoclasts.

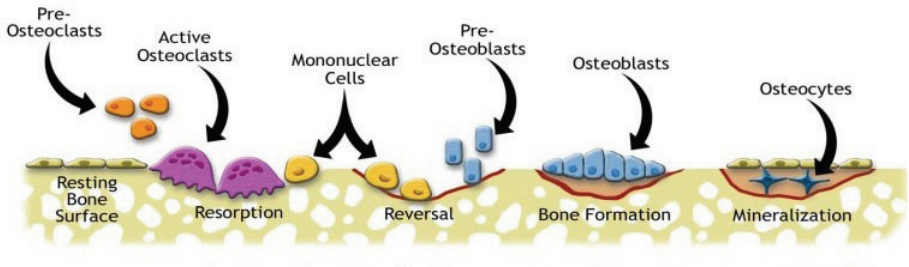

Figure 1.5: Bone remodelling cycle
The remodelling cycle consists of 3 consecutive phases: activation, resorption, during which osteoclasts digest old bone, followed by a reversal phase where mononuclear cells appear on the bone surface, and subsequently formation, when osteoblasts lay down new bone until the resorbed bone is completely replaced.
(*From www.umich.edu/news/Releases/2005/Feb05/bone.html*)

1.2.4 Local and systemic control of bone remodelling

The calcium and phosphate ion storage role of the skeleton is helpful in understanding the complex regulation of bone remodelling.

The main *systemic factors* influencing bone remodelling are PTH and vitamin D_3 ($1,25(OH)_2D_3$). Receptors for these hormones are expressed solely in osteoblasts, and these and other factors regulating bone resorption, signal to the osteoblast/stromal cells, which then translate these signals into different levels of RANKL and OPG expression (58-59). Thus, the "convergence hypothesis" refers to that OPG and RANKL can be the mediators for the stimulatory or inhibitory effects of a variety of systemic hormones, growth factors and cytokines on osteoclastogenesis. The activity of the resorptive and antiresorptive agents "converges" at the level of these two mediators, whose final ratio controls the degree of osteoclast differentiation, activation and apoptosis (60). A third hormone involved in mineral homeostasis, calcitonin, acts directly on osteoclasts, antagonizing the action of PTH and vitamin D_3, thereby inhibiting bone resorption.
Glucocorticoids exert both stimulatory and inhibitory effects on bone cells, being essential for osteoblast maturation by promoting differentiation from mesenchymal progenitors, but decrease osteoblast activity. Furthermore, glucocorticoids sensitize bone cells to regulators of bone remodelling and they augment osteoclast recruitment.

Thyroid hormones stimulate both bone resorption and formation. Thus, hyperthyroidism may increase turnover which may result in bone loss. *Estrogens* protect the adult skeleton against bone loss by slowing the rate of bone remodelling (by attenuating the birth rate of osteoclast/osteoblast progenitors) and by maintaining a focal balance between bone resorption and formation (by exerting a proapoptotic effect on osteoclasts, and antiapoptotic effects on osteoblasts/osteocytes). *Androgens* are essential to skeletal growth and maintenance via receptors present in all types of bone cells (for references, see (61)).

Mature osteoblasts express receptors for and are regulated in an autocrine and paracrine manner by a variety of growth factors such as insulin-like growth factors (IGFs), platelet-derived growth factor (PDGF), FGFs, TGF-β and the BMPs. A number of cytokines such as tumor necrosis factor α (TNF-α) and interleukin 10 (IL-10) modulate the RANK-RANKL-OPG system by stimulating macrophage colony-stimulating factor (M-CSF) production and by directly increasing RANKL expression (62). Furthermore, IL-6, a pleiotropic cytokine secreted by osteoblasts, osteoclasts and stromal cells, appears to be an important regulator of bone remodelling by stimulating osteoclastic bone resorption (63) but also by promoting osteoblast generation in conditions of high bone turnover (64). Furthermore, recent studies have suggested that osteoblast-derived PTHrP promotes the recruitment of osteogenic cells and prevents the apoptotic death of osteoblasts, thus being an important regulator of bone cell function (65).

Table 1C. Effects of cytokines and hormones on bone remodelling through RANKL and OPG secretion

Factor	RANKL	OPG
TGF-β	-	↑
PTH	↑	↓
1,25$(OH)_2$ vitamin D_3	↑	-
Glucocorticoids	↑	↓
Estrogen	-	↑
FGFs	↑	↓
Prostaglandin E	↓	↑

1.3 BONE REPAIR – FRACTURE HEALING

Fracture healing is a unique response to bone injury, which in contrast to repair of many other types of tissues, leads to the complete restoration of both anatomy and function without leaving a scar. In general, fracture healing is completed in

6 – 8 weeks after initial injury. Fracture healing may occur both through direct (intramembranous) or indirect (endochondral) bone formation.

Fracture healing can be divided in four more or less overlapping stages. At the cellular level, inflammatory cells, vascular cells, osteochondral progenitors, and osteoclasts are key players in the repair process. At the molecular level, fracture repair is driven by the 3 main classes of factors: pro-inflammatory cytokines and growth factors, pro-osteogenic factors, and angiogenic factors (66), recruiting cells and stimulating growth and/or differentiation. Thereafter, the damaged soft tissues are repaired and the fracture is bridged by soft callus and later hard callus. The bridging hard callus is eventually remodelled to re-establish the original anatomy and function of the fractured bone.

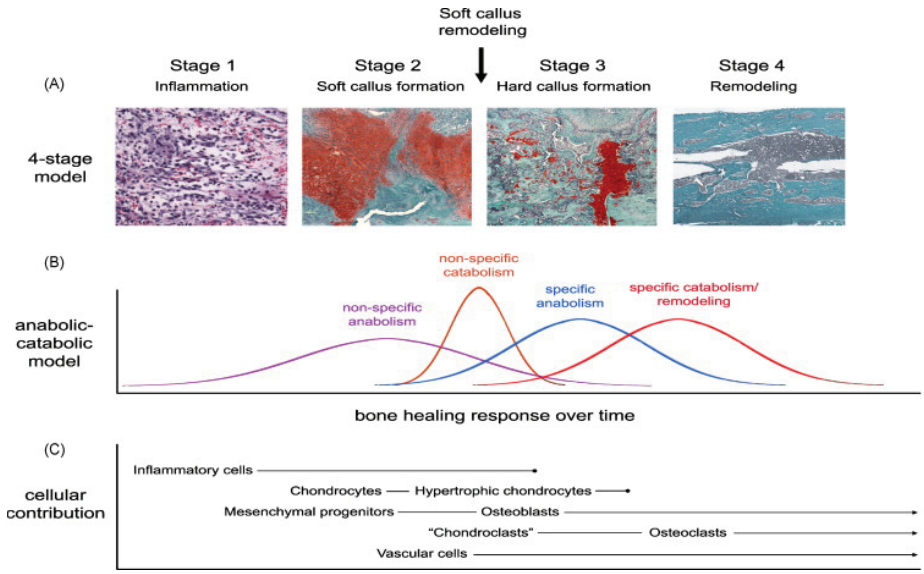

Figure 1.6. Stages of fracture healing
(A) A representative series of images of the 4 stage-model of fracture healing. Between stage 2 and 3, the soft callus is systematically remodelled. (B) A detailed version of the anabolic/catabolic model of fracture repair that incorporates the concepts of non-specific anabolism (the early tissue repair process) and non-specific catabolism (soft callus remodelling). (C) A schematic illustration of the cellular contributors to the fracture repair process. The sources of mesenchymal progenitors that are able to differentiate into osteoblasts remain ambiguous (Figure from (3)).

Stage 1: *Inflammation*
The acute bone injury is typically associated with damage also of soft tissue, interruption of blood vessels and distortion of the marrow cavity, leading to activation of non-specific tissue healing pathways. The first event is haematoma formation within the fracture site, with degranulating platelets, macrophages and inflammatory cells (granulocytes, lymphocytes and monocytes), which secrete cytokines/growth factors and advance formation of a stable fibrinous clot (67). Subsequently the clot is reorganized into granulation tissue with extensive ingrowth of capillaries, allowing macrophages and other phagocytic cells to clear degenerated cells and debris. Important regulators of this first stage include TGF-β, PDGF, FGF-2, vascular endothelial growth factor (VEGF), M-CSF, IL1- and IL-6, BMPs and TNF-α (68). In addition, the expression of cyclooksygenase-2 (COX-2) is critical to early stages of fracture healing (69-70). These factors contribute to further attraction of inflammatory cells, as well as multipotent mesenchymal stem cells (71). Periosteum (72), bone marrow (73), circulating blood (74) and surrounding soft tissue (75) have all been suggested as sources of stem cells.

Stage 2: *Soft callus (fibrocartilage) formation*
In completely stable fractures, healing can occur solely by intramembranous bone formation. However, at most fracture sites, there is some degree of instability between the fracture fragments, promoting endochondral bone healing (67). This stage is dominated on a cellular level by chondrocytes and fibroblasts, producing a semi-rigid soft callus providing mechanical support to the fracture and concurrently acting as a template for the subsequent bony callus. The cartilaginous callus is initially avascular, although replacement with woven bone involve vascular invasion. Mesenchyme-derived chondrocytes synthesize cartilaginous matrix, thereby replacing the granulation tissue with cartilage. In the absence of cartilage formation, fibroblasts replace the haematoma with fibrous tissue. The discrete cartilaginous areas expand to form a central fibrocartilaginous glue between the fracture fragments (66). Finally, the chondrocytes hypertrophy and mineralize the cartilaginous matrix before undergoing apoptosis. The proliferation and differentiation of fibroblasts and chondrocytes are stimulated by growth factors such as TGF-β2 and –β3, PDGF, FGF-1 and IGF. TGF-β1 is also critical, and decreased serum levels are found in humans with delayed fracture healing (76). Additionally, various BMPs contribute to proliferation and chondrogenesis. In response to these factors, chondrocytes produce ECM components, particularly collagen II (and collagen X by hypertrophic chondrocytes) (77). Pro-angiogenic factors such as VEGF, BMPs, FGF-1 and TGF-β attract endothelial cells and stimulate angiogenesis (78). VEGF is important to fracture healing (79). The key bone and cartilage transcription factor Cbfa1/Runx2 is essential for VEGF expression by osteogenic cells (80)

Stage 3: *Hard callus formation (primary bone formation)*
This stage represents the most active period of osteogenesis, with intense osteoblast activity and formation of mineralized bone matrix, which arises directly in the peripheral callus in areas of stability bridging the bone fragments. The soft callus is replaced with woven bone which becomes revascularized. Various BMPs are critical for the proliferation/ differentiation and ECM synthesis in osteoblasts, and are sufficient for *de novo* bone formation (81-82). Although other growth factors are expressed during this stage, their roles in promoting migration/proliferation and/or differentiation of osteoprogenitors remain unclear (67). Sufficient vascularization yielding increased local oxygen tension and thus promoting osteoblast differentiation is critical to formation of hard callus.

Stage 4: *Bone remodelling*
Remodelling of woven bone into its original lamellar cortical and/or trabecular configuration represents the last stage of fracture healing.

Factors influencing fracture healing
Fracture repair is affected by the degree of injury, the specific site, the fracture gap, and by type/stability of an eventual surgical fixation. Local biology, including the condition of the vasculature available at the site, and individual factors in the subject, such as age, gender, medication, and diseases, all affect fracture repair. Additional integral factors include viability of local tissue, vasculature, and access to stem cells.

Factors that negatively affect fracture healing can be classified as injury- related, patient-related and surgery/surgeon-related factors (83). Injury- related factors include high energy trauma (84), soft tissue injury (85), complex fractures (86) and degree of obliquity (87). Patient-related factors include smoking (88), drug (e.g. NSAIDs (89)) and alcohol consumption (90), aging (70,91-92), nutritional state (93) as well as underlying metabolic conditions e.g. diabetes mellitus (94) and hyperhomocysteinemia (95). Surgery-related factors include gap between fracture fragments (87), use of an open instead of a closed surgical technique, and persisting instability between fracture fragments.

1.4 PATHOLOGIC BONE REMODELLING – OSTEOPOROSIS

Osteoporosis is a multifactorial skeletal disease, characterized by reduction in bone mass and disruption of the microarchitectural structure of bone tissue, resulting in loss of mechanical strength and increased risk of fracture. The disorder can be localized or generalized, involving the entire skeleton. In the European Union, osteoporosis is a leading cause of mortality and morbidity in the elderly and a key factor in the high cost of medical care (96). Osteoporosis is defined by the World Health Organization in women as bone mineral density

(BMD) (g/cm^2) 2.5 $\leq$ standard deviations below young adult women (T-score < 2.5), while a T-score between -2.5 and -1 is defined as osteopenia (97). T-score is defined as the measured BMD minus young adult mean BMD divided by the young adult standard deviation. Established osteoporosis includes T score $\leq$ -2.5 and the presence of one or more fragility fractures. Although BMD is strongly correlated to the risk of fracture (98-99), low BMD alone is not a sufficient predictor of fracture risk (100).

Generalized osteoporosis can be classified as either primary or secondary. Primary osteoporosis is further divided into type I, which is postmenopausal in women and "idiopathic" in men, occurring in the 5^{th} to 7^{th} decade of life. Type I osteoporosis mainly affects trabecular areas and contributes in particular to vertebral and wrist fractures. It is associated with low trabecular bone mass and disturbed trabecular architecture. Also cortical bone mass is decreased and the diameter of the medullary cavity is expanded due to increased endocortical bone resorption overriding periosteal apposition. Type II, also known as senile osteoporosis, affects both trabecular and cortical bone in aged individuals (typically from the 7^{th} decade), and predisposes to hip fractures. Secondary osteoporosis is related to other conditions such as hypogonadism, endocrine disorders, renal failure, rheumatic diseases, gastrointestinal disorders, osteomalacia, rickets and Paget's disease (for references see (101-102)).

After achieving peak bone mass in the late twenties, both sexes start to lose bone. Peak bone mass is mainly determined by genetic factors, but also influenced by environmental factors such as diet (vitamin D, calcium) and physical activity. Thus, individuals that do not achieve their genetically optimal bone mass have less bone to lose as a result of normal aging and suffer an increased risk of developing osteoporosis. In general, men have higher bone mass than women (thus more bone to lose), and are therefore prone to later onset of osteoporosis. Osteoporosis could be the consequence of a failure to reach peak bone mass in young adulthood, excessive resorption after peak bone mass is achieved, or impaired bone formation during remodelling (103). Postmenopausal osteoporosis is the consequence of withdrawal of the bone-sparing effect of estrogen, where resorption overrides bone formation.
Age-related bone loss occur at most skeletal sites in both sexes, although pattern, magnitude and underlying cellular mechanisms differ markedly. In men, trabecular bone volume decreases with age and the individual trabeculae become thinner, but remains connected (104). This is associated with decreased rate of matrix deposition and increased duration of the bone formation phase during remodelling (105). The same trabecular thinning is observed in women until menopause, where the rate of bone loss accelerates due to cessation of estrogen production. Estrogen deficiency is associated with an increase in RANKL production by bone marrow osteoblastic, T and B cells (106), thereby enhancing

the bone turnover rate and the osteoclastic resorption. There is also an increase in the activation frequency of BMUs, and the enhanced osteoclast activity could also leads to deeper Howship's lacunae. Thus, trabeculae are perforated and ultimately removed, resulting in reduced trabecular number and connectivity in women (107).
Although an increase in bone diameter is seen with advancing age, the cortices attenuate because periosteal apposition is less than endocortical resorption (108).

2 AIMS OF THE STUDY

The main aim of this thesis was to obtain a better understanding of some of the molecular mechanisms involved in bone remodelling/healing during physiological and a pathological state.

SPECIFIC OBJECTIVES AND HYPOTHESES

1. To examine whether experimental postmenopausal osteoporosis influences the healing of fractures as evaluated by histomorphometric, radiographic and mechanical parameters. Our hypothesis was that the combined withdrawal of estrogen and vitamin D will disturb and/or delay the healing process, resulting in impaired mechanical properties of callus.
2. To enhance immunolabelling in electron microscopic studies of bone by retrieving epitopes by heating Lowicryl sections of paraformaldehyde (PF)-fixed tissues prior to immunolabelling. Our hypothesis was that heating under controlled conditions will reveal more epitopes with retained tissue distribution.
3. To examine whether experimental postmenopausal osteoporosis influences the molecular composition of the ECM in the fracture callus. Our hypothesis was that lack of estrogen and vitamin D deficiency influence global gene expression, as well as synthesis and ultrastructural distribution of ECM molecules in the callus, and consequently, the capacity of fracture repair.
4. To learn more about the ECM protein chondroadherin (CHAD) using a gene knockout mouse model. Our hypothesis was that these knockout mice will show a distinct skeletal phenotype indicating specific roles for the protein in bone and cartilage metabolism.

3 METHODOLOGY

Detailed descriptions of methods are provided in papers I-IV, respectively. General aspects of the main methods used for the work included in the thesis are presented in this section.

Table 3.1 Overview over methods used in the thesis

Paper	Animals	Methods
I	OVX rats fed vitamin D deficient diet Tibial midshaft fracture, intramedullary nail	*In vivo* DXA measurements Bone histomorphometry Three-point cantilever bending test
II	Normal rats	Immunoelectron microscopy (NUC, OSAD) for retrieved and non-retrieved PF-fixed sections, and non-retrieved HPF-Fs sections
III	OVX rats fed vitamin D deficient diet Tibial midshaft fracture, intramedullary nail	*In situ* hybridization (TRAP, CTK, OPN, BSP) Immunoelectron microscopy (TRAP, CTK, OPN, BSP) DNA microarrays
IV	CHAD null mice	Histology Bone histomorphometry *In situ* hybridization (TRAP, CTK, OPN, BSP, COMP) Immunohistochemistry (COMP) Immunoelectron microscopy (OPN, BSP) Micro-CT

3.1 ANIMAL MODELS

All animal procedures were approved by the Norwegian or the Swedish Animal Research Authority.

3.1.1 Animal model of fracture healing in osteoporosis

In paper I and III, female rats, 10 weeks of age, were randomly assigned to 2 groups; bilateral ovariectomy (OVX) and vitamin D_3 deficient diet (OVX-D), or sham operation and normal diet (sham). After 12 weeks, a closed transverse tibial fracture was established in all animals during deep anaesthesia and stabilized with an intramedullary nail. OVX-D and sham animals were killed 3 and 6 weeks after fracture, and blood was collected for serum analyses of estradiol and 25(OH)D.

3.1.2 Chondroadherin null mice (fig. 3.1)

In paper IV, mice with the chondroadherin (CHAD) gene knocked out were examined. In brief, after isolating the CHAD gene from a mouse gene library, a similar but inoperable DNA gene and its neighbour sequence were engineered. Embryonic stem cells were combined with the new CHAD sequence and a targeting vector using electroporation. After growth in culture, positive clones were picked, expanded and purified, and DNA analyzed with Southern blot for confirmation of the correct targeting events. Targeted embryonic stem cells were injected to mouse blastocysts according to standard procedures. Chimeric males were matched with C57BL/6 and males with germ line transmission were further bred with 129/sv females to establish an inbred strand of CHAD null mice.

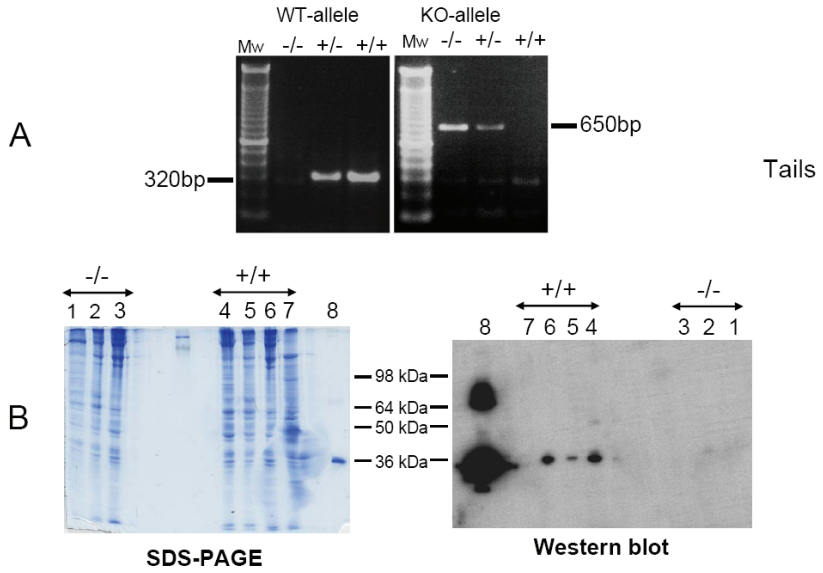

Figure 3.1: Analyses of message and proteins in CHAD-/- and WT mice
A: PCR and agarose electrophoresis of mouse tail samples. B: Protein stained gel (Comassie stained, left) and Western blot (with anti-CHAD, right) of cartilages and liver as a control of non-specific reactions. Different cartilages were extracted with 4M GuHCl, proteins precipitated with ethanol and electrophoresed on 4-16% SDS-PAGE. The lanes represent extracts of null (-/-) and WT (+/+) mice: 1. trachea (-/-); 2. nasal cartilage (-/-); 3. knee cartilage (-/-); 4. trachea (+/+); 5. nasal cartilage (+/+); 6. knee cartilage (+/+); 7. liver (+/+); 8. recombinant CHAD.

3.2 RADIOGRAPHIC AND BIOMECHANICAL ANALYSES

3.2.1 Dual X-ray absorptiometry (DXA)

In paper I, BMD was measured in the right tibial diaphysis prior to fracture. Two, 3 and 6 weeks after fracture, BMD was measured *in vivo* in the fracture area, tibial and femoral diaphysis, femoral neck and the lower lumbal vertebrae. For the fractured tibia, BMD of the extracted intramedullary nail was measured and the value subtracted from the *in vivo* BMD values.

3.2.2 Micro computer tomography

In paper IV, we measured total length of femur, cortical and trabecular thickness, trabecular separation, bone volume and porosity, trabecular connectivity as well as degree of anisotropy and structure model index in mice aged 5 days, 3 weeks and 4 months by micro computer tomography.

3.2.3 Three-point cantilever bending test

In paper I, biomechanical properties of the fracture callus as well as the femoral neck were examined *ex vivo* using a three-point cantilever bending test. Although originally developed for testing of femoral shaft, the mechanical test has later been modified for testing of tibial shaft as well as the femoral neck (109).

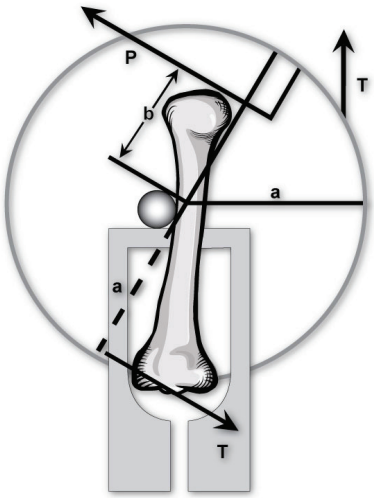

Figure 3.2. Three-point cantilever bending – applied forces
The measured moment (Ta) equals the moment required to bend the distal tibia ventrally (Pb). Thus, the applied force (T) is directly proportional to bending moment (Pb).a = disc radius (2).

3.3 BONE HISTOMORPHOMETRY

In general, tissues were fixed by transcardial *in vivo* perfusion, dehydrated and embedded in resin or paraffin. Both sections of intact calcified bone stained with trichrome and sections of decalcified bone stained with toluidine blue were used. The sampling hierarchy was designed in pilot analyses using cumulative mean plots for deciding sample size at each level below the animal level. At each level

systematic random sampling was performed on coded material. In paper I, total outer diameter, cortical thickness and cortical area for the tibial and femoral diaphyses were estimated along with trabecular bone volume according to stereological principles with point counting as the main method (110). In paper IV, mean height of the epiphyseal growth plate was calculated from measurements along 10 randomly placed vertical arbitrary lines. The relative zone distribution of the epiphyseal growth plate (111)) was estimated on longitudinal sections through the distal femur. Finally, osteoid surface in the proximal tibial metaphysis was estimated using the linear intercept method (110).

3.4 GENE EXPRESSION ANALYSES

3.4.1 *In situ* hybridization

Total RNA was reverse transcribed into cDNA, and gene sequences of interest were amplified from cDNA or directly from IMAGE clones by conventional PCR, using oligonucleotide primers. The sequences were subsequently cloned and sequenced. Digoxigenin (DIG)-conjugated complementary RNA (cRNA) probes were synthesized to yield probes in the sense or antisense orientation. Hybridization was performed by modification of a previous protocol (112); in brief, sections of formalin-fixed paraffin-embedded tissue were dewaxed and proteinase K digested, post-fixed and incubated in hybridization solution overnight. Excess probe was rinsed off followed by RNase treatment to remove unbound probe. Hybridized probe was detected with a sheep anti-DIG ALP conjugate, followed by nitroblue tetrazolium chloride and 5-bromo-4-chloro-3-indolyl-phosphate as ALP substrate. Hybridization with sense probes in place of antisense was performed as negative controls. In paper IV, parallel light microscopic (LM) immunohistochemistry (IHC) was used to show that the protein and the gene precursor for COMP co-label. Mounted sections were analyzed with respect to cellular localization of mRNA. The ratio of mRNA positive cells to total number of cells of the same lineage on bone surfaces was determined using point counting on coded sections and their corresponding haematoxylin/eosin-stained sections.

3.4.2 DNA microarrays

In paper III, we used DNA microarray to study differently expressed genes between study groups. A DNA microarray consists of a solid substrate and arrays of probes arranged in grids. Each probe is composed of many identical copies of single-stranded DNAs with a specific gene sequence. We used the oligonucleotide-based Rat Genome 230 2.0 array (containing more than 31,000 probe sets) from Affymetrix Gene Chip®, where probes are generated directly on the substrate by light-directed chemical synthesis. Isolated RNA from the bone samples was reverse-transcribed into cRNA, and the cDNA molecules (“targets”)

were labelled with fluorescent tags (biotin) and hybridized with the probes on the microarray. The amount of fluorescence emitted by each spot on the microarray will be proportional to the amount of mRNA produced by the gene with the DNA sequence identical to the sequence in the spot. Finally, the hybridized microarray was scanned in at the wave-length appropriate to the dyes used to create a value which represents the expression level of a gene. Specific software programs were used for handling and processing of the huge data sets, and the results were expressed as fold changes (FC), e.g. ratio of the mean signals between compared groups. Gene lists were generated with the criteria of $p < 0.05$ and $FC \geq 2$. For expression comparisons of the study groups, profiles were compared using paired t-test.

3.5 PROTEIN ANALYSES - IMMUNOHISTOCHEMISTRY

3.5.1 Qualitative protein analysis

In paper IV, we used a two step IHC technique based on a horseradish peroxidase-labelled polymer conjugated to a secondary antibody for the detection of COMP in sections of long bone. In brief, formalin-fixed, paraffin-embedded specimens were deparaffinized and rehydrated in series of alcohols. To quench endogenous peroxidase activity, sections were incubated with hydrogen peroxide. Subsequently, sections were pretreated with chondroitinase ABC in tris-acetate containing 1% bovine serum albumin (BSA) for antigen retrieval. Incubation with normal goat serum was performed to block non-specific binding before application of the primary antibody. The sections were then incubated with the labelled polymer, and staining was completed by incubation with diaminobenzidine (DAB+) susbstrate-chromogen which results in a brownish precipitate at the antigen site. The sections were finally stained with haematoxylin and eosin/phloxine B. COMP distribution in the epiphyseal growth plate was determined on coded sections using a histologic scoring system and compared between study groups.

3.5.2 Quantitative protein analysis

In general, bone tissues for transmission electronmicroscopic (TEM) IHC were fixed by transcardial *in vivo* perfusion, further fixed in PF or a mixture of PF/glutaraldehyde. After decalcification and dehydration in alcohols during progressive lowering of the temperature, tissue blocks were embedded in an acrylic resin at low temperature. In paper II, some tissue sections were stabilized by high pressure freezing (HPF) followed by freeze substitution (FS); after cervical dislocation of the animals, dissected tissues were subjected to ultrarapid cooling by liquid nitrogen during increasing pressure in a high pressure freezer, which physically vitrifies tissue water without significant formation of ice crystals. By this procedure ultrastructural artefacts which may develop during chemical fixation are avoided (113) and the cell morphology is kept closer to its

living state because soluble cell constituents are maintained (114). Subsequent FS allows dehydration of the frozen samples before resin-embedding at -25°C and was performed with increasing concentrations of methanol.

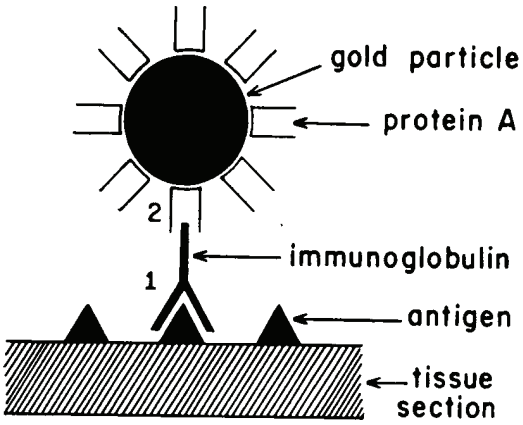

Figure 3.3: Principles of immunolabelling
An ultrathin section placed on a grid is incubated with primary antibodies (1) against the antigen under study. Gold conjugated protein A (2) binds to a single binding site on the Fc part of the primary antibody and can be visualized in the electron microscope. Figure from (1).

The sampling hierarchy was designed based on previous experience with similar analyses using cumulative mean plots for deciding sample size at each level below the animal level (115). Ultrathin sections were cut and mounted on formvar-coated nickel grids. In paper II, some sections were subjected to antigen retrieval by heating in citrate buffer. Immunostaining were performed by overnight incubations with the primary antibody reagents, before incubation with protein A conjugated to 10 nm gold particles. Normal rabbit IgG was used in place of the primary antibodies as negative controls. Before examination, sections were contrasted with uranyl acetate and lead citrate. Electron micrographs of coded sections were sampled in predetermined compartments (which were identified in digital pictures at a final magnification of x 49,000) and regions of interests (ROIs) were drawn by freehand according to the structural limits. After background smoothing and global intensity thresholding, particles occurring within the area of the ROI were counted, and the particle density (particles/μm^2) estimated using a semi-automatic image analysis software program. The mean particle density for each of the predetermined sub/extracellularly compartments was calculated for each animal and used for

statistical comparison of gold labelling density in the compartments between the study groups.

3.6 STATISTICAL METHODS

All data are presented as means and standard deviations, and standard statistical methods were used, i.e. student's t-test, one-way analysis of variance (ANOVA) and multivariate analysis of variance (MANOVA). The level of significance was set to 0.05. All analyses were calculated in SPSS for Windows.

4 SUMMARY OF RESULTS

4. 1 PAPER I

Experimental osteoporosis induced by ovariectomy and vitamin D deficiency does not markedly affect fracture healing in rats
Melhus G*, Solberg LB*, Dimmen S, Madsen JE, Nordsletten L, Reinholt FP
*Contributed equally to the study

The question of whether fracture healing and mechanical properties of the callus are influenced by postmenopausal osteoporosis is still not settled. 72 female Wistar rats were randomized into two groups: OVX and vitamin D_3-deficient diet (OVX-D group) or sham operation and normal rat chow (sham group). After 12 weeks, a closed unilateral tibial midshaft fracture was performed and fixed with an intramedullary nail. Bone loss and callus formation were monitored with DXA; serum levels of estradiol and vitamin D were measured and histomorphometric analyses were performed. Mechanical properties of callus, tibia, femoral shaft, and femoral neck were examined in 3-point cantilever bending 6 weeks after fracture. The OVX-D group showed reduced BMD in the spine and femoral neck, and reduced trabecular bone volume in the femoral head. There were no differences in BMD and mechanical properties of callus between the groups. Except for reduced stiffness of the right femoral neck in the OVX-D group, no differences in the mechanical strength of long bones were detected.

Conclusion of the study: The results suggest that systemic effects of estrogen and vitamin D deficiency are not crucial for fracture healing or mechanical properties of the callus.

4.2 PAPER II

Heat-induced retrieval of immunogold labelling for nucleobindin and osteoadherin from Lowicryl sections of bone.
Solberg LB*, Melhus G*, Brorson SH, Wendel M, Reinholt FP.
*Contributed equally to the study

The preparation, fixation and embedding of bone tissue enabling electronmicroscopic studies of tissue distribution of proteins complicates and may distort localization of antigens by antibodies. Thus, in order to investigate whether heating of bone sections may enhance signalling intensity; the immunogold signal for two bone proteins (NUC and OSAD) was compared in retrieved and non-retrieved sections of PF-fixed normal rat bone. As an additional experiment, the effect of antigen retrieval (for NUC) in sections of

tissue primary stabilized by high pressure freezing with subsequent freeze substitution (HPF-FS) was studied. Finally, the tissue distribution patterns of NUC labeling were compared in non-retrieved HPF-FS sections to that of retrieved and non-retrieved PF-fixed sections. Antigen retrieval in Lowicryl sections of PF-fixed tissues showed significantly enhanced labeling intensity for both proteins in all compartments where they are known to occur. Retrieved PF-fixed sections showed only minor ultrastructural differences compared to non-retrieved ones. Retrieval of HPF-FS sections exhibited no enhancement of labeling but rather a slight reduction, which was significant in the cytoplasm and in cartilage. Furthermore, striking ultrastructural differences were observed in retrieved HPF-FS sections compared to non-retrieved ones with loss of coherence and structure in sections subjected to heating. Comparison of the distribution patterns of Nuc in the sections of PF-fixed and HPF-FS tissues showed discrepancy in most compartments.

Conclusion of the study: Antigen retrieval by heating Lowicryl sections of PF-fixed tissues significantly enhances immunogold labeling in all cell compartments where the bone proteins are known to occur. However, the procedure may distort the tissue distribution pattern of bone proteins.

4.3 PAPER III

Gene expression and distribution of key bone remodelling markers in the callus of estrogen-deficient vitamin D depleted rats
Melhus G, Brorson SH, Baekkevold ES, Andersson G, Jemtland R, Reinholt FP

To investigate whether postmenopausal osteoporosis influences the gene expression and molecular composition of the ECM in the fracture callus, we investigated global gene expression, mRNA synthesis and ultrastructural protein distribution in fracture callus after 3 and 6 weeks of healing for four NCPs in the animal model used in paper I.

Conclusion of the study: Several genes are differently regulated in osteoporosis induced by OVX and vitamin D depletion, mostly in an early stage and the majority in an increased fashion, although no genes encoding NCPs with known function in bone metabolism were differently expressed. On the background of only minor differences in the synthesis and protein expression of OPN, BSP, TRAP and CTK in callus between OVX-D and sham treated animals, our results suggest that the molecular composition of the fracture callus is not markedly skewed in osteoporosis.

4.4 PAPER IV

Chondroadherin-deficient mice present a distinct skeletal phenotype
Melhus G*, Hessle L*, Wenglen C, Brorson SH, Petzold C, Baekkevold ES, Heinegard D, Reinholt FP
* Contributed equally to the study

CHAD, a cartilage matrix protein belonging to the SLRP family, possesses cell binding properties and is suggested to play a role in cartilage homeostasis. We have generated CHAD null mice to study the role of CHAD *in vivo*. These mice show no gross anatomical abnormalities, but exhibit a distinct skeletal phenotype with disturbances of the epiphyseal growth plate, alteration of trabecular and cortical bone parameters with lack of the sex- specific differences seen in WT mice, as well as markedly decreased number of BSP expressing cells in the proximal tibial metaphysis. However, the CHAD null mice presented unaltered expression of OPN, TRAP, CTK and COMP, and normal immunostaining for the latter in the growth plate. Furthermore, ultrastructural analysis showed unaltered protein distribution pattern of BSP and OPN in bone.

Conclusion of the study: These results demonstrate an important role for CHAD in both bone and cartilage homeostasis, clearly visualized by the distinct bone phenotype of CHAD null mice.

5 GENERAL DISCUSSION

5.1 METHODS

The animal models are discussed in the respective papers, and the applied methods are in general well established. However, some aspects are commented upon below.

5.1.1 The model of fracture healing in postmenopausal osteoporosis

The OVX rat is the most widely used laboratory animal model for osteoporosis research. The model is approved by the FDA as clinically relevant in the study of postmenopausal osteoporosis (116). The skeletal changes in the OVX rat share several characteristics to postmenopausal osteoporosis, e.g. bone resorption exceeding bone formation, predominant trabecular bone loss and similar response to treatment with drugs like bisphosphonates, estrogen, PTH and calcitonin (117-118). OVX in rodents does not, however, regularly lead to weakening of cortical bone (119-121) and the frequent low-energy fractures occurring in humans (122) are absent (118). Vitamin D deficiency is very common among the elderly as well as in postmenopausal and osteoporotic women and has been implicated in the development of osteoporosis and ensuing risk of fragility fractures (for references, see (123)). In studies presented in paper I and III, OVX and vitamin D depletion were combined to induce osteoporosis, on the background of the findings by Kaastad et al. showing a significant weakening of the femoral neck in this model (121). Therefore, we considered this model to be particularly relevant in the study of fracture healing in postmenopausal osteoporosis. Although most postmenopausal women with osteoporotic fractures are elderly, advancing age *per se* is associated with impaired fracture healing (124-127). Therefore, to exclude age as a confounding factor, young rats were used.

As expected, loss of bone in trabecular areas was found 3 months after OVX/introduction of vitamin D-deficient diet, as well as decreased bending stiffness of the femoral neck compared to controls. Absence of detectable bone loss and unchanged mechanical function in cortical bone are in line with previous reports; cortical bone loss does occur but slowly and to a lesser extent (117,121,128). However, in spite of cortical thinning, mechanical strength may be preserved as a result of periosteal apposition and altered bone geometry (129). No such geometric compensation was detected in our model.

There are some limitations using the OVX rat as a model for human osteoporosis, e.g. the lack of the Haversian system in cortical bone, the maintained osteoblast function during the late stages of estrogen deficiency and the absence of BMU-based remodelling in young rats (130), as well as the

seeming life-long modelling of bones rather than remodelling which differ from that in human adulthood (131-132).

We used a diaphyseal fracture healing model previously shown to provide stable fractures by intramedullary nailing. Mechanical properties were studied in a 3-point cantilever bending test that has been demonstrated to provide standardized loading until failure and reproducible results (133-135). Intramedullary nailing gives flexible fixation, thereby resulting in indirect healing characterized by periosteal callus formation and endochondral bone formation. However, 6 weeks after fracture in our series, there was a substantial inter-individual variation with respect to macroscopic callus size and morphologic composition accompanied by a relatively high incidence of non-unions.

The indirect healing of fractures is strongly influenced by the amount of interfragmentary movement induced by the load of the fracture site and the stability of the fracture fixation. Thus, a likely explanation for the heterogeneous fracture calluses is that the fractures have been subjected to various degrees of mechanical stability, and non-unions may have occurred as a result of suboptimal positioning of the nail, thereby allowing excessive motion at the fracture site. However, since most non-unions presented little or no visible callus formation, non-unions could also be due to a too rigid nail. Actually, *in vivo* studies have shown stress shielding from the use of rigid internal fixators (136-137) and refractures after removal of these (138). However, complete union in this fracture model using the same type of nail has been reported (135). Furthermore, a too rigid fixation cannot explain the heterogeneity in those animals that achieved union.

After exclusion of non-unions, the sample size for mechanical testing was still considered sufficient to detect a clinically relevant difference in mechanical properties of 20% between the groups. However, no significant differences were observed, but substantially larger standard deviations (in the range of 29% - 55%) were noted for the fractured tibias compared to the intact contralateral controls. This may indicate that the variation was due to inter-individual differences in fracture healing/callus, rather than the bending test itself. Heterogeneity in the callus sample may also have influenced the results reported in paper III. The recruitment of mesenchymal stem cells (MSCs) is a key component in the healing process, and mechanical stimulation is an important factor in determining their cellular fate, i.e. whether they differentiate into osteoblasts, chondrocytes, adipocytes, fibroblasts or myoblasts (139-140). Mechanical stimulation promotes chondrogenetic differentiation and expression of cartilage-related genes (141), and thus, substantial variation in the ratio of cartilage- and bone specific gene expression may have contributed to large standard deviations in the genetic and molecular results. Another aspect of the model is fracture localization; we (as most other authors) examined healing of a diaphyseal fracture since this is easy to establish and can be fixed in a standardized manner. However, long bones are more predisposed to osteoporotic

fractures at the metaphyses rather than at the diaphyses (95,142), and the mechanisms of metaphyseal healing are different from those of diaphyseal bone: In general, diaphyseal fractures heal indirectly with visible periosteal callus formation, whereas metaphyseal fractures usually heal directly with endosteal bone bridging by micro-callus and without significant periosteal callus formation. Furthermore, the periosteum, which plays a central role during fracture healing, displays site-specific differences in long bones (143). However, while trabecular and cortical bone are architecturally different, they are similar at the molecular and biochemical level. The fracture localization is therefore of most relevant for the results in paper I.

5.1.2 The applied methods

DNA microarrays

Several studies using a "gene-by-gene" approach to identify the temporal expression of gene(s) of interest during fracture healing (144-145), in osteoporosis (146) and in fracture healing in osteoporosis (147) have been published. Although this approach shows the spatial distribution of expression, it is not useful in isolating novel genes involved in these processes. Such data can be obtained through the microarray technique. This is a powerful tool to unravel so-far unknown genes involved in osteoporotic fracture healing by allowing the co-ordinated study of the expression of thousands of genes. In paper III, total fracture callus RNA at two different time points was collected, and pooled RNA was used for expression-profiling studies. Although no known NCPs were differently expressed, a variety of genes were found to be differentially regulated in the OVX-D animals. Limitations of our microarray approach include the small number of time points evaluated, the limited sample size (due to ethical considerations and prohibitive costs of the technology), and mixing of the callus RNA samples in each group (due to low levels of RNA in adult rat bone). Due to the latter, inter-individual differences or differences related to bone- and cartilage-specific genes in the callus are not detected, which is of particular relevance in light of the observed morphological heterogeneity of the calluses. Finally, one cannot conclude that changes in mRNA levels by necessity mean parallel changes in protein secretion and tissue distribution as these parameters are regulated also by other mechanisms.

Immunoelectron microscopy and antigen retrieval (paper II)

The aim of TEM IHC is to localize molecules in biological samples at a spatial resolution that cannot be achieved by LM IHC. Fixation/immobilization of specimens can modify both tissue morphology and antigenicity from that of the living state, and thus, a central issue is to preserve the epitope of interest while minimizing the loss of ultrastructural detail. Preparation of tissues for immunogold labelling can be achieved either by 1) chemical fixation with

aldehyde followed by progressive dehydration and embedding at low temperature (148), 2) brief chemical fixation with aldehyde followed by cryofixation and cryosectioning (149), or 3) cryofixation techniques followed by FS and embedding at low temperatures (150). HPF followed by FS is considered to provide the best compromise between preservation of ultrastructural morphology and antigenicity (151-155). However, the HPF-FS technique requires specialized and expensive equipment not available in most laboratories, and the capacity to freeze large series of samples uniformly is limited. Thus, chemical fixation followed by low temperature embedding is often the technique of choice in TEM IHC, and chemical fixation using cross-linking reagents such as PF with or without small concentrations of glutaraldehyde is frequently used for TEM IHC (for references, see (156)). However, effective chemical fixatives that preserve morphology frequently destroy biological activities and/or mask antigens, and consequently, different antigen retrieval techniques have been developed both for LM and TEM IHC (for references, see (157)).

Heat-induced antigen retrieval is one of the most widely used techniques for formalin-fixed paraffin-embedded tissue, but is also applicable on frozen sections (158) and sections prepared for immunoelectron microscopy (159-162). The main mechanism is believed to be cleavage of the intra- and intermolecular crosslinks (i.e. methylene bridges) induced with formaldehyde (163-165). In paper II, we used the HPF-FS technique as a gold standard, to evaluate whether antigen retrieval by heating sections of PF-fixed tissue embedded in the acrylic resin Lowicryl HM23 could increase immunogold labelling for two NCPs in bone tissue without markedly affecting ultrastructural morphology. When the sections were heated in citrate buffer at 95°C for 15 min, significant enhancement of immunogold labelling of both NCPs was observed. Surprisingly, compared to the distribution patterns in HPF-FS sections, retrieved sections of PF-fixed tissue showed alternations in the relative protein distribution between sub- and extracellular compartments. To our knowledge such an effect of antigen retrieval by heating has previously not been reported. The results may also have implications for results of LM IHC following antigen retrieval by heat.

Taken together, our results suggest that although high-temperature heating may disclose antigens in bone tissue fixed by PF and embedded in acrylic resin, heat may distort the native protein distribution and therefore should be used with caution in studies of molecular distribution at the ultrastructural level. Our results support more recent data recommending HPF-FS in TEM IHC when the preservation of tissue ultrastructure in its most native state is the goal (166-167) .

Semi-quantitative immunogold analysis

Immunogold TEM IHC is a powerful method for the detection and localization of tissue antigens at the ultrastructural level and allows quantisation due to the electron dense nature of the gold particles and to the fact that only epitopes at the surface of the section are detected (for references, see (168)). Robust tools for

specimen sampling, stereological estimation and statistical evaluation of subcellular gold-labelling distribution are important design features and allow reproducible results (169). Multistage random sampling is required due to the small specimen size, and guarantees every part of the object under study an equal chance of being sampled (110). The labelling density (number of gold particles per area unit (170)) in different compartments/ ROIs can be compared directly using t-tests (171) or when the relative protein distribution in several compartments are compared between groups such as in paper II and III, multivariate analysis of variance (MANOVA) is the statistical tool of choice (Jon Michael Gran, Department of Biostatistics, Medical Faculty, University of Oslo, personal communication). However, the high magnification required to identify gold particles and compartments by shape and size, contributes to the fact that the collection of information on overall antigen distribution is extremely time-consuming. Therefore, various semi-automated image analysis software programs have been developed for fast and automatic quantification of gold particles. Despite the effectiveness and the advantages of automated particle detection, its quality depends on the operator. Due to simplistic particle detection and quality control algorithms, small, false positive particles may easily go unnoticed unless the operator is aware of this possibility and has been duly trained to optimize threshold levels.

5.2 RESULTS

5.2.1 Fracture healing in osteoporosis (paper I and III)

Osteoporosis and the associated changes in bone metabolism may influence the outcome of fracture healing. However, clinical studies have failed to demonstrate a direct link between the hormone deficiency and the decrease in bone regeneration, as the endocrine status and possible co-morbidities may constitute a considerable bias. To date, no clinical studies reporting impaired/delayed healing in osteoporotic patients compared to age-matched controls have been published. Thus, the current dogma of impaired fracture healing in postmenopausal women is primarily based on increased failure rates of fixation devices (172-173), and experimental studies using the OVX rat model (127,174-179). Although delay in bone healing has been reported in OVX rats at certain stages of fracture repair (127,174,177-179), other published data suggest that some phases of fracture repair in OVX rats are relatively unimpaired. Moreover, the effects of estrogen depletion as well as of other important hormones involved in mineral metabolism are not significantly detrimental to bone regeneration (174-176).

Recent experimental data suggest relatively unaltered healing capacity

Bone density and bone quality, which encompass the structural and material properties of bone, are both important for bone strength (180-181) and the proper

biological functioning of bone (182-183). Bone quality is determined by the characteristic of the matrix (material quality) and the structural characteristics of bone. Material quality plays an important role in the reinforcement of bone strength.

In paper I we show that fracture healing and mechanical properties of callus in OVX-D rats are not markedly influenced by the osteoporotic condition. Several previous studies support our observations by reporting unaltered mechanical properties of callus in OVX rats at certain time points after fracture; e.g. Wheeler et al. (175) report no differences after 4 and 6 weeks, and Cao et al. (176) find no changes after 6 and 16 weeks in OVX rats; their findings do, however, suggest an accelerated and favourable callus remodelling. Furthermore, Kubo et al. (174) report almost identical healing in OVX and controls after 6 weeks but apparent histological osteoporotic changes and decreased BMD in callus after 12 weeks.

However, other studies suggest impaired healing and mechanical properties, e.g. Hao et al. report decreased mineralization and not well connected microstructure in callus after 4, 8, and 12 weeks, accompanied by impaired mechanical properties at the end point, as compared to controls (184). Yet another study, using infrared spectroscopic imaging to identify changes in fracture callus, shows an apparent decrease in mineral to matrix ratio and collagen cross-linking in early stages of fracture healing in OVX rats, but with a gradual normalization until similar values to those of estrogen-treated OVX rats (controls) were obtained after 12 weeks (185), suggesting a OVX-related delay only in early stages of the healing process. In support of the latter, normal enzymatic cross-linking of collagens in callus at the same time point (i.e. 12 weeks after fracture) is recently reported in OVX rats (186), and may be a determinant of the material property of bone (187-188). Thus, as a whole, disparities are found in previous experimental data on fracture repair in osteoporotic bone.

Interestingly, most recently published studies comparing fracture healing in OVX rats and controls provide new evidence for unaltered healing capacity; Shi et al. (189) report indifferent healing with maintenance of mechanical properties of femoral fractures after 2, 3 and 8 weeks, while Saito et al. (186) report only minor differences after 12 weeks' healing of a femoral osteotomy in OVX rats. Yet another study finds no significant differences in callus formation and mechanical properties in OVX rats as compared to controls 5 weeks after a metaphyseal tibia osteotomy, although estrogen prophylaxis in the healing period significantly improved fracture healing in the OVX group (190). However, Ding et al. suggest that OVX influences fracture healing; these authors report decreased vascularisation and lower BMD of callus in OVX rats 1, 2, 4 and 8 weeks after fracture with some influence on mechanical properties after 2 and 8 weeks (i.e. lower ultimate stress but unaltered energy to ultimate load and no

differences in Young's modulus), whereas micro-CT revealed differences in callus composition only at the two early time points (191).

On the other hand, also recent fracture studies in transgenic mice support our results; Egermann et al. (192) investigated fracture healing in senile osteoporosis using SAMP6 mice, a model of senile osteoporosis which display a bone phenotype with reduced trabecular bone volume (193), decreased bone strength (194) and reduced areal BMD (195). The bone marrow-derived MSCs from these mice show a reduced capacity for osteoblast differentiation and increased adipogenesis (196-198) similar to the reported alternations of MSCs from postmenopausal women (199-200). The important role of MSCs in fracture repair is well documented (67,201-202). However, SAMP6 mice exhibited unaltered healing capacity despite the impaired differentiation capacity of BMCs, thus simultaneously calling into question the role of bone marrow-derived MSCs in the repair process and supporting our demonstration of unaffected healing under an osteoporotic condition.

Taken together, recent findings mainly support our results as well as clinical observations that, although fracture fixation is difficult in osteoporosis, the healing potential seems to be relatively unchanged.

The impact of vitamin D deficiency on fracture healing

Prolonged vitamin D deficiency has several skeletal consequences in humans, and may induce decreased bone formation and mineralization, (rickets in children and osteomalacia in adults) or osteopenia/ osteoporosis. Severe vitamin D deficiency results in decreased serum concentration of ionized calcium, a rise in PTH, and calcium malabsorption (203). However, vitamin D insufficiency (low serum vitamin D without rickets or osteomalacia) does not per se cause malabsorption of calcium (204), but is deleterious to bone because it is associated with secondary hyperparathyroidism and signs of increased bone resorption (205). Vitamin D exerts its effects through the vitamin D receptor (VDR). The principal action of the VDR in skeletal growth, maturation, and remodelling concerns its role in intestinal calcium absorption (206). Although human trabecular bone cells respond *in vitro* to exogenous $1,25(OH)_2D_3$ by increasing expression of bone matrix genes such as osteocalcin and BSP (207) and mature osteoblasts express VDRs, studies of vitamin D-deficient rats have failed to demonstrate significant differences in the bone content of several matrix proteins, including osteocalcin, relative to those in normal rats (208). These observations raise questions regarding the importance of vitamin D in adult bone metabolism. On the other hand, administration of active vitamin D analogues do seem to have a positive effect on OVX-induced bone loss by inhibiting bone resorption and maintaining bone formation (209-210)

Neither the effect of vitamin D nor its analogues on fracture healing have been fully established, although vitamin D deficiency has been associated with increased risk of non-unions (211). The administration of vitamin D during fracture healing in normal and OVX rats have shown conflicting results (186,212). To our knowledge, no previous studies have investigated the impact of vitamin D deficiency on fracture healing in OVX rats. All OVX-D rats developed vitamin D deficiency in paper I; 94% showed undetectable levels of 25(OH)D. Previous studies report that when vitamin D-deficient animals are kept normocalemic by experimental or dietary means, no osteomalacia occurs (213) and corroborate that bone in vitamin D deficient rats may be normal when the mineral supply is adequate (213)**.** Thus, due to normal dietary calcium content, the additional effect of vitamin D deficiency may have been minor in our series.

Molecular matrix composition in osteoporotic fracture healing
Until recently there has been relatively limited evidence for altered molecular matrix composition in human osteoporotic bone (214-216), although increased expression of cytokines such as IL1, IL6 and RANKL has been reported (146,217). However, several genes encoding NCPs and other molecules involved in bone metabolism, including OPN, BSP, CTK and TRAP, were reported to be differentially expressed in iliac crest biopsies from postmenopausal women by micro array (Reppe et al., unpublished observations).
In addition, previous experimental data have shown increased mRNA levels of osteoblast-related genes including OPN (218), and augmented number of OPN-expressing osteocytes in bones of OVX rats (219). Furthermore, Hatano et al. investigated estrogen-regulated genes during fracture healing in rats using microarray and found 52 genes to be downregulated by OVX and restored with estrogen, out of which differential mRNA expression was confirmed for 4 of these by qPCR (i.e. collagen type II, extracellular superoxide dismutase, urokinase-type plasminogen activator and ptk-3) (220).
Taken together, we therefore hypothesized that that the molecular composition of the callus in osteoporosis could be skewed with respect to matrix molecules involved in bone remodelling.

However, in paper III we demonstrate, first, that OVX-D rats present no altered expression of genes encoding neither collagens nor NCPs, and second, only minor quantitative differences with respect to mRNA expressing cells and ultrastructural protein distribution of OPN, BSP, TRAP and CTK compared to controls, thus indicating basically unaltered composition of callus in experimental osteoporosis.
Among the latter molecules, OPN and BSP are particularly interesting in the aspects of fracture repair in vitamin D-deficient osteoporotic bone: OPN plays a role in OVX-related bone loss (221) as well as in fracture healing (222) by affecting angiogenesis, callus formation and mechanical strength of callus in

early stages of healing while facilitating later stages of remodelling and ECM organization. BSP, but not OPN, plays a role in primary bone formation and mineralization of newly formed bone during cortical bone healing (223). Both OPN and BSP are under the influence of vitamin D_3, which exerts different transcriptional effects on these genes *in vitro* (stimulates OPN (224), suppresses BSP (225-226)) as well as *in vivo* (transgenic vitamin D_3-deficient mice present increased BSP and decreased OPN expression (227)).

However, the observed lack of altered regulation of these genes in the OVX-D group, supported by ISH and TEM IHC findings may question the importance of vitamin D and estrogen in regulation of these NCPs in the fracture healing process. In support of our findings, unaltered expression of osteocalcin, IGF-1, collagen 1α1 and TRAP have recently been reported in the callus of OVX rats compared to controls (147). Thus, although some data indicate altered molecular callus composition, taken together with the results of paper I, the seemingly unaltered NCP composition of the fracture callus in experimental osteoporosis supports the hypothesis that the fracture healing process is not markedly influenced by OVX in rodents.

On the other hand, recent clinical data indicate altered expression of genes encoding matrix molecules in intact bone from postmenopausal osteoporotic women; a targeted gene expression study show downregulation of genes for ALP, COL1A1, MMP2, MMP9 and MMP13, platelet-derived growth factor alpha polypeptide (PDGFA), nuclear factor of kappa light polypeptide (NFKB1) and upregulation of thrombospondin receptor (CD36), and twist homolog 2 (TWIST2) (228). Another study comprehensively characterizing differential gene expression in human osteoporosis (229), reported alterations in several genes regulating osteoclastogenesis and bone resorption, in particular TREM-2, CCL2, RANK and IL-6 (identified in previous studies (217)), thereby confirming that genes responsible for osteoblast maturation are differentially expressed, in particular CTSB (cathepsin B), TGFB1(TGFβ1) (230-231), but also SPP1 (OPN) and CTGF (connective tissue growth factor). Moreover, microarray analysis of human osteoporotic osteoblasts has revealed 352 potentially differentially regulated genes, out of which four new candidate-genes for osteoporosis were verified in bone by qPCR; two cytokines (pleiotrophin (PTN) and chemokine (C-X-C motif) ligand 2 (CXCL2)), collagen type XV alpha 1 (COL15A1) and BSP (IBSP) (232). Taken together, these studies indicate changes in bone composition at the tissue level, and consequently, altered quality of inorganic and organic matrix in human postmenopausal osteoporosis.

However, the fact that several gene profiling studies on human osteoporotic bone have disclosed different expression of genes, and thus implicated these in the pathogenesis of osteoporosis, does not necessarily mean that the mechanisms of

response to a certain stimulus such as fracture differ from those of healthy bone; the bone trauma and the subsequent repair response may override the osteoporotic condition, allowing important genes to be expressed at a sufficient level to complete the repair process in a physiological manner.

The role of FGF23 and IL-17RA

The fracture healing process is influenced by a variety of molecules other than NCPs which could possibly contribute to altered healing capacity. However, out of the variety of genes encoding cytokines, growth factors and receptors involved in fracture healing and bone metabolism, only fibroblast growth factor 23(FGF23) and interleukin-17 receptor A (IL-17RA) turned out to be differently regulated in the OVX-D group, being down- and upregulated at 3 weeks, respectively. FGF23, a phosphaturic hormone, is part of a newly discovered hormonal bone – parathyroid – kidney axis, which is modulated by PTH, vitamin D and phosphate levels. Recent studies show that $1,25(OH)_2D_3$ regulates FGF23 production through VDRE in the FGF23 promoter (233), being a potent stimulator of FGF23 (234), and that osteoblastic bone formation is a potent modulator of FGF23 production and release into the circulation (235). Interestingly, FGF23 has recently been suggested as a putative marker of fracture healing, and decreased mRNA expression is associated with delayed healing in ovine bone (236). Thus, reduced FGF23 expression in the early phase of fracture healing in the OVX-D group may reflect reduced osteoblastic activity and, consequently, impaired fracture healing. It should be noted that we did not test mechanical properties of callus at this time point.

IL-17A (also known as IL-17) is a proinflammatory cytokine similar to TNFα (237) and may be involved in bone turnover (238). IL-17 is produced by a subset of Th lymphocytes (Th17 cells) (239) and acts upstream of IL-6 and synergize with TNFα to promote inflammation and bone turnover in rheumatoid arthritis (240). The mechanism is at least in part related to the capacity of IL-17 to upregulate the ratio of RANKL to OPG, thereby promoting osteoclastogenesis (241). On the other hand IL-17 seems to be bone-protective in certain situations; IL-17RA null mice exhibit more pronounced bone loss compared to WT mice following OVX (242). Furthermore, these authors report that IL-17 negatively regulates adipogenesis and subsequent leptin expression, which correlates with increased bone destruction during OVX. Thus, the possibility that upregulation of IL-17RA in OVX-D rats could represent a bone protective effect contributing to maintenance of callus strength, cannot be excluded. However, the potential role of IL-17RA needs to be further elucidated.

Taken together, a reasonable explanation for largely unaltered healing capacity in osteoporosis is that the repair process is essential to the individual in an evolutionary aspect, and therefore is given priority in biological systems and allowed to override the osteoporotic condition. Consequently, the immediate

repair response is strong and basically unaltered, while later remodelling of callus may be influenced by the disturbed coupling and by resorption exceeding formation.

5.2.2 The role of chondroadherin in bone and cartilage (paper IV)

CHAD, a member of the SLRP family, is highly expressed in cartilage, but also in other tissues such as bone and tendon. The protein interacts with both collagen and cells and is assumed to play a role in matrix homeostasis (for references, see (243)). Furthermore, CHAD was one of the differentially regulated genes in iliac crest biopsies from osteoporotic women, as analyzed by microarray (Reppe et al, unpublished observations). We have developed mice whose gene for CHAD is deleted. These null mice present a distinct skeletal phenotype, substantiating an important role for CHAD in bone and cartilage metabolism.

Alternations in cortical/trabecular bone parameters

Differences in trabecular/cortical bone parameters were first apparent at the age of 4 months, where the null mice presented significantly higher volumetric BMD, lower cortical thickness but increased trabecular thickness compared to WT mice. Interestingly, the normal differences in these parameters between male and female WT mice were absent in the null mice, indicating that CHAD is important in the sex-specific skeletal development. Similar observations have been reported in OPN knockout mice (244).

Disturbances in the epiphyseal growth plate

CHAD null mice presented markedly disturbances at the epiphyseal growth plate, with a general widening of all zones, but most pronounced in the proliferative zone. Previous studies show that CHAD is synthesized mainly by late proliferative chondrocytes in the epiphyseal growth plate, and deposited close to the cells in the territorial matrix (245). Due to its restricted tissue distribution and the apparent absence of cell spreading and growth of chondrocytes on CHAD-coated surfaces (246), a role in regulation of cell division has been suggested (245). The balance between proliferation and differentiation of chondrocytes is an important regulatory step controlled by multiple signaling molecules, including the Ihh/PTHrP feedback loop. Interestingly, Ihh, which is upstream in the signaling pathway of PTHrP, shows a similar distribution of expression to that of CHAD (247). PTHrP is regulated by Ihh, and the length of the proliferative zone of the growth plate is determined by a combination of the stimulatory effect of Ihh on chondrocyte differentiation and the inhibitory effect of PTHrP on hypertrophic differentiation. On the background of the very distinct localization around a portion of the proliferative chondrocytes and the observed widening of this zone in null mice, it could be speculated that CHAD may influence the Ihh/PTHrP feedback loop and/or participate in the control of chondrocyte differentiation by promoting hypertrophy.

Decreased number of cells expressing BSP mRNA

Interestingly, a markedly reduced number of BSP mRNA-expressing cells were detected in the distal femur metaphysis of CHAD null mice. BSP promotes mineralization (248), and taken together with the slightly increased osteoid surface observed in null mice, this could reflect suboptimal mineralization. Further studies should be performed to elucidate the role of CHAD in the mineralization process. Ongoing work suggests that CHAD influences the cytokine production by osteoblastic cells, thereby reducing the production of osteoclast stimulatory factors such as IL-1, IL-6 and RANKL (16). The increase in volumetric BMD observed in null mice could be due to decreased osteoclastic resorption and supports this hypothesis. However, no quantitative differences with respect to the number of cells expressing the osteoclastic markers TRAP and BSP were noted. Neither did the number of OPN and COMP mRNA-expressing cells vary between the groups, supported by normal immunostaining for COMP in the territorial matrix of chondrocytes in the growth plate. Thus, the lack of CHAD did not induce general changes in synthesis of NCPs at the current detection level.

6 CONCLUSIONS

1. The fracture healing process in experimental postmenopausal osteoporosis does not seem to differ markedly from that in healthy bone, neither at the mechanical nor at the molecular level. The role of IL-17RA and FGF23 should be delineated in future studies.

2. Antibody retrieval by heating increases the signal intensity for NUC and OSAD in Lowicryl sections subjected to TEM IHC. However, the heating results in skewed protein distribution, and thus, the technique cannot be recommended in studies addressing ultrastructural protein distribution in bone tissues.

3. CHAD plays an important role in bone and cartilage turnover in mice, illustrated by the observed skeletal phenotype in CHAD null mice, with alternations in trabecular/cortical bone parameters, widening of the epiphyseal growth plate and decrease in the number of BSP expressing cells.

7 FUTURE PERSPECTIVES

7.1. Fracture healing in postmenopausal osteoporosis

Future studies should focus on improving the OVX-D model to reduce variation so as to allow firmer conclusions. First, the introduction of a metaphyseal fracture model closer mimicking the clinical situation should be considered with respect to mechanical properties. Despite challenges in fixation of such fractures, several recent models have achieved successful stabilization (142,190). Secondly, the surgical technique should be optimized in order to minimize non-unions and to obtain a more reproducible callus size. Thirdly, a proper pilot study should be performed using histomorphometry, micro-CT and mechanical testing at several time points (e.g. at 2, 4, 6, 8, 12, and 16 weeks after fracture) in order to determine the most relevant time points for extended analyses in a larger experiment. One way to establish more homogenous groups may be to start with a larger number of animals in the main experiment, thereby allowing subselection of calluses into groups according to macroscopic callus size (e.g. “small” and ”large” calluses). Similar macroscopic size would reduce the problem of “comparing apples and oranges”, i.e. calluses subjected to various degrees of mechanical forces during healing. By decreasing inter-individual variation in the sample increased power would be anticipated in the statistical analyses. Furthermore, microarray analyses should be performed on whole callus samples at the different time points to reveal candidate genes subjected to detailed analyses at the cellular- and molecular level (e.g. qPCR, ISH, proteomics and semi-quantitative TEM IHC). Detailed histomorphometrical analysis (including osteoblast/osteoclast surfaces and osteoid measurements) should be performed to investigate cell activity and mineralization. For dynamic histomorphometry, double tetracycline labelling (intraperitoneal injection *in vivo* at two time points) is required.

The next step includes further analyses of the differentially regulated genes (encoding FGF23 and IL17RA) in paper III with suggested/potential roles in fracture healing/osteoporosis, qPCR to confirm altered expression, ISH to detect mRNA expressing cells in the callus and LM and TEM IHC to determine differences in localization and quantization at the protein level.

To extend our observations in paper I and III, a detailed supplementary histomorphometric analysis of callus after 3 and 6 weeks of healing is in progress and will be included in the revised manuscript (paper III).

7.2. The role of Chondroadherin in bone and cartilage metabolism

To extend our observations of the skeletal phenotype of CHAD null mice mechanical testing of femurs from 4 months old mice should be performed to delineate the functional impact of the findings by micro-CT. Furthermore, the histomorphometric analyses should be extended by including osteoblast/osteoclast parameters as well as osteoid surface and thickness measurements. During the experiment, double tetracycline labelling should be performed, which enables estimation of dynamic bone remodelling parameters/mineralization, e.g. to measure mineral apposition rate and bone formation rate and allowing calculation of osteoid mineralization and osteoid maturation time.

To confirm reduced BSP expression in osteoblasts, qPCR should be performed. Furthermore, proteomics should be included in future experiments to confirm the presence (quantity) of proteins as well as to identify compensatory alternations of protein concentrations in the null mice. In addition, *in vitro* osteoclast/osteoblast differentiation using mouse BMCs cultures should be evaluated as a supplementary approach.

8 REFERENCES

1. **Hayat M 1989 Colloidal Gold. Principles, Methods and Applications. In: Hayat M (ed.), vol. 1. Academic Press, Inc, Sand Diego, California.**

2. **Stenstrom M, Olander B, Lehto-Axtelius D, Madsen JE, Nordsletten L, Carlsson GA 2000 Bone mineral density and bone structure parameters as predictors of bone strength: an analysis using computerized microtomography and gastrectomy-induced osteopenia in the rat. J Biomech 33(3):289-297.**

3. **Schindeler A, McDonald MM, Bokko P, Little DG 2008 Bone remodeling during fracture repair: The cellular picture. Semin Cell Dev Biol 19(5):459-466.**

4. **Toyosawa S, Shintani S, Fujiwara T, Ooshima T, Sato A, Ijuhin N, Komori T 2001 Dentin matrix protein 1 is predominantly expressed in chicken and rat osteocytes but not in osteoblasts. J Bone Miner Res 16(11):2017-2026.**

5. **Igarashi M, Kamiya N, Ito K, Takagi M 2002 In situ localization and in vitro expression of osteoblast/osteocyte factor 45 mRNA during bone cell differentiation. Histochem J 34(5):255-263.**

6. **Gowen LC, Petersen DN, Mansolf AL, Qi H, Stock JL, Tkalcevic GT, Simmons HA, Crawford DT, Chidsey-Frink KL, Ke HZ, McNeish JD, Brown TA 2003 Targeted disruption of the osteoblast/osteocyte factor 45 gene (OF45) results in increased bone formation and bone mass. J Biol Chem 278(3):1998-2007.**

7. **Yang WC, Lu YB, Kalajzic I, Guo DY, Harris MA, Gluhak-Heinrich J, Kotha S, Bonewald LF, Feng JQ, Rowe DW, Turner CH, Robling AG, Harris SE 2005 Dentin matrix protein 1 gene cis-regulation - Use in osteocytes to characterize local responses to mechanical loading in vitro and in vivo. Journal of Biological Chemistry 280(21):20680-20690.**

8. **Dierkes C, Kreisel M, Schulz A, Steinmeyer J, Wolff JC, Fink L 2009 Catabolic properties of microdissected human endosteal bone lining cells. Calcif Tissue Int 84(2):146-155.**

9. **Reinholt FP, Hultenby K, Oldberg A, Heinegard D 1990 Osteopontin--a possible anchor of osteoclasts to bone. Proc Natl Acad Sci U S A 87(12):4473-4475.**

10. Blair HC, Teitelbaum SL, Ghiselli R, Gluck S 1989 Osteoclastic bone resorption by a polarized vacuolar proton pump. Science 245(4920):855-857.

11. Bromme D, Okamoto K, Wang BB, Biroc S 1996 Human cathepsin O2, a matrix protein-degrading cysteine protease expressed in osteoclasts. Functional expression of human cathepsin O2 in Spodoptera frugiperda and characterization of the enzyme. J Biol Chem 271(4):2126-2132.

12. Salo J, Lehenkari P, Mulari M, Metsikko K, Vaananen HK 1997 Removal of osteoclast bone resorption products by transcytosis. Science 276(5310):270-273.

13. Nesbitt SA, Horton MA 1997 Trafficking of matrix collagens through bone-resorbing osteoclasts. Science 276(5310):266-269.

14. Andersson G, Ek-Rylander B, Hollberg K, Ljusberg-Sjolander J, Lang P, Norgard M, Wang Y, Zhang SJ 2003 TRACP as an osteopontin phosphatase. J Bone Miner Res 18(10):1912-1915.

15. Ek-Rylander B, Andersson G 2010 Osteoclast migration on phosphorylated osteopontin is regulated by endogenous tartrate-resistant acid phosphatase. Exp Cell Res 316(3):443-451.

16. Heinegard D 2009 Proteoglycans and more--from molecules to biology. Int J Exp Pathol 90(6):575-586.

17. Eyre DR, Weis MA, Wu JJ 2006 Articular cartilage collagen: an irreplaceable framework? Eur Cell Mater 12:57-63.

18. Plumb DA, Dhir V, Mironov A, Ferrara L, Poulsom R, Kadler KE, Thornton DJ, Briggs MD, Boot-Handford RP 2007 Collagen XXVII is developmentally regulated and forms thin fibrillar structures distinct from those of classical vertebrate fibrillar collagens. J Biol Chem 282(17):12791-12795.

19. Robey P 2009 The composition of bone. In: Rosen C (ed.) Primer on the metabolic bone diseases and disorders of mineral metabolism, Seventh ed. The American Society for Bone and Mineral Research, Washington, D.C., pp 32-38.

20. Iozzo RV, Moscatello DK, McQuillan DJ, Eichstetter I 1999 Decorin is a biological ligand for the epidermal growth factor receptor. J Biol Chem 274(8):4489-4492.

21. Fisher LW, Fedarko NS 2003 Six genes expressed in bones and teeth encode the current members of the SIBLING family of proteins. Connect Tissue Res 44 Suppl 1:33-40.

22. Mochida Y, Parisuthiman D, Pornprasertsuk-Damrongsri S, Atsawasuwan P, Sricholpech M, Boskey AL, Yamauchi M 2009 Decorin modulates collagen matrix assembly and mineralization. Matrix Biol 28(1):44-52.

23. Shepard JB, Gliga DA, Morrow AP, Hoffman S, Capehart AA 2008 Versican knock-down compromises chondrogenesis in the embryonic chick limb. Anat Rec (Hoboken) 291(1):19-27.

24. Zoeller JJ, McQuillan A, Whitelock J, Ho SY, Iozzo RV 2008 A central function for perlecan in skeletal muscle and cardiovascular development. J Cell Biol 181(2):381-394.

25. Kalamajski S, Aspberg A, Lindblom K, Heinegard D, Oldberg A 2009 Asporin competes with decorin for collagen binding, binds calcium and promotes osteoblast collagen mineralization. Biochem J 423(1):53-59.

26. Matheson S, Larjava H, Hakkinen L 2005 Distinctive localization and function for lumican, fibromodulin and decorin to regulate collagen fibril organization in periodontal tissues. J Periodontal Res 40(4):312-324.

27. Boskey AL, Moore DJ, Amling M, Canalis E, Delany AM 2003 Infrared analysis of the mineral and matrix in bones of osteonectin-null mice and their wildtype controls. J Bone Miner Res 18(6):1005-1011.

28. Qin C, D'Souza R, Feng JQ 2007 Dentin matrix protein 1 (DMP1): new and important roles for biomineralization and phosphate homeostasis. J Dent Res 86(12):1134-1141.

29. Verdelis K, Ling Y, Sreenath T, Haruyama N, MacDougall M, van der Meulen MC, Lukashova L, Spevak L, Kulkarni AB, Boskey AL 2008 DSPP effects on in vivo bone mineralization. Bone 43(6):983-990.

30. Alford AI, Terkhorn SP, Reddy AB, Hankenson KD 2009 Thrombospondin-2 regulates matrix mineralization in MC3T3-E1 pre-osteoblasts. Bone.

31. Seiffert D 1996 Detection of vitronectin in mineralized bone matrix. J Histochem Cytochem 44(3):275-280.

32. Keene DR, Jordan CD, Reinhardt DP, Ridgway CC, Ono RN, Corson GM, Fairhurst M, Sussman MD, Memoli VA, Sakai LY 1997 Fibrillin-1 in human cartilage: developmental expression and formation of special banded fibers. J Histochem Cytochem 45(8):1069-1082.

33. Gorski JP, Wang A, Lovitch D, Law D, Powell K, Midura RJ 2004 Extracellular bone acidic glycoprotein-75 defines condensed mesenchyme regions to be mineralized and localizes with bone sialoprotein during intramembranous bone formation. J Biol Chem 279(24):25455-25463.

34. Luo G, Ducy P, McKee MD, Pinero GJ, Loyer E, Behringer RR, Karsenty G 1997 Spontaneous calcification of arteries and cartilage in mice lacking matrix GLA protein. Nature 386(6620):78-81.

35. Hoang QQ, Sicheri F, Howard AJ, Yang DS 2003 Bone recognition mechanism of porcine osteocalcin from crystal structure. Nature 425(6961):977-980.

36. Segat D, Paulsson M, Smyth N 2001 Matrilins: structure, expression and function. Osteoarthritis Cartilage 9 Suppl A:S29-35.

37. Wagener R, Ehlen HW, Ko YP, Kobbe B, Mann HH, Sengle G, Paulsson M 2005 The matrilins--adaptor proteins in the extracellular matrix. FEBS Lett 579(15):3323-3329.

38. Bellows CG, Aubin JE, Heersche JN 1991 Initiation and progression of mineralization of bone nodules formed in vitro: the role of alkaline phosphatase and organic phosphate. Bone Miner 14(1):27-40.

39. Schinke T, McKee MD, Karsenty G 1999 Extracellular matrix calcification: where is the action? Nat Genet 21(2):150-151.

40. Midura RJ, Wang A, Lovitch D, Law D, Powell K, Gorski JP 2004 Bone acidic glycoprotein-75 delineates the extracellular sites of future bone sialoprotein accumulation and apatite nucleation in osteoblastic cultures. J Biol Chem 279(24):25464-25473.

41. Bonucci E 1992 Comments on the ultrastructural morphology of the calcification process: an attempt to reconcile matrix vesicles, collagen fibrils, and crystal ghosts. Bone Miner 17(2):219-222.

42. Anderson HC 1995 Molecular biology of matrix vesicles. Clin Orthop Relat Res (314):266-280.

43. Bonucci E 1995 Ultrastructural organic-inorganic relationships in calcified tissues: cartilage and bone vs. enamel. Connect Tissue Res 33(1-3):157-162.

44. Robey P 2006 Extracellular matrix and biomineralization of bone. In: Favus M (ed.) Primer on the Metabolic Bone Diseases and Disorders of Mineral Metabolism, Sixth ed. The American Society for Bone and Mineral Research, Washington, D.C., pp 12-19.

45. Anderson HC, Garimella R, Tague SE 2005 The role of matrix vesicles in growth plate development and biomineralization. Front Biosci 10:822-837.

46. Ali SY, Sajdera SW, Anderson HC 1970 Isolation and characterization of calcifying matrix vesicles from epiphyseal cartilage. Proc Natl Acad Sci U S A 67(3):1513-1520.

47. Matsuzawa T, Anderson HC 1971 Phosphatases of epiphyseal cartilage studied by electron microscopic cytochemical methods. J Histochem Cytochem 19(12):801-808.

48. Hui M, Tenenbaum HC 1998 New face of an old enzyme: alkaline phosphatase may contribute to human tissue aging by inducing tissue hardening and calcification. Anat Rec 253(3):91-94.

49. Harrison G, Shapiro IM, Golub EE 1995 The phosphatidylinositol-glycolipid anchor on alkaline phosphatase facilitates mineralization initiation in vitro. J Bone Miner Res 10(4):568-573.

50. Huffman NT, Keightley JA, Chaoying C, Midura RJ, Lovitch D, Veno PA, Dallas SL, Gorski JP 2007 Association of specific proteolytic processing of bone sialoprotein and bone acidic glycoprotein-75 with mineralization within biomineralization foci. J Biol Chem 282(36):26002-26013.

51. Rowe PS, Kumagai Y, Gutierrez G, Garrett IR, Blacher R, Rosen D, Cundy J, Navvab S, Chen D, Drezner MK, Quarles LD, Mundy GR 2004 MEPE has the properties of an osteoblastic phosphatonin and minhibin. Bone 34(2):303-319.

52. Yang Y 2009 Skeletal morphogenesis and embryonic development. In: Rosen C (ed.) Primer on the metabolic bone diseases and disorders of mineral metabolism, Seventh ed. The American Society for Bone and Mineral Research, Washington, D.C., pp 2-10.

53. Gibson GJ, Schor SL, Grant ME 1982 Effects of matrix macromolecules on chondrocyte gene expression: synthesis of a low molecular weight collagen species by cells cultured within collagen gels. J Cell Biol 93(3):767-774.

54. Alini M, Carey D, Hirata S, Grynpas MD, Pidoux I, Poole AR 1994 Cellular and matrix changes before and at the time of calcification in the growth plate studied in vitro: arrest of type X collagen synthesis and net loss of collagen when calcification is initiated. J Bone Miner Res 9(7):1077-1087.

55. Parfitt AM 1994 Osteonal and hemi-osteonal remodeling: the spatial and temporal framework for signal traffic in adult human bone. J Cell Biochem 55(3):273-286.

56. Parfitt AM 2002 Targeted and nontargeted bone remodeling: relationship to basic multicellular unit origination and progression. Bone 30(1):5-7.

57. Rodan GA, Martin TJ 2000 Therapeutic approaches to bone diseases. Science 289(5484):1508-1514.

58. Martin TJ 2004 Paracrine regulation of osteoclast formation and activity: milestones in discovery. J Musculoskelet Neuronal Interact 4(3):243-253.

59. Bell NH 2003 RANK ligand and the regulation of skeletal remodeling. J Clin Invest 111(8):1120-1122.

60. Hofbauer LC, Khosla S, Dunstan CR, Lacey DL, Boyle WJ, Riggs BL 2000 The roles of osteoprotegerin and osteoprotegerin ligand in the paracrine regulation of bone resorption. J Bone Miner Res 15(1):2-12.

61. Hadjidakis DJ, Androulakis, II 2006 Bone remodeling. Ann N Y Acad Sci 1092:385-396.

62. Hofbauer LC, Lacey DL, Dunstan CR, Spelsberg TC, Riggs BL, Khosla S 1999 Interleukin-1beta and tumor necrosis factor-alpha, but not interleukin-6, stimulate osteoprotegerin ligand gene expression in human osteoblastic cells. Bone 25(3):255-259.

63. Moonga BS, Adebanjo OA, Wang HJ, Li S, Wu XB, Troen B, Inzerillo A, Abe E, Minkin C, Huang CL, Zaidi M 2002 Differential effects of interleukin-6 receptor activation on intracellular signaling and bone resorption by isolated rat osteoclasts. J Endocrinol 173(3):395-405.

64. Sims NA, Jenkins BJ, Quinn JM, Nakamura A, Glatt M, Gillespie MT, Ernst M, Martin TJ 2004 Glycoprotein 130 regulates bone turnover and bone size by distinct downstream signaling pathways. J Clin Invest 113(3):379-389.

65. Miao D, He B, Jiang Y, Kobayashi T, Soroceanu MA, Zhao J, Su H, Tong X, Amizuka N, Gupta A, Genant HK, Kronenberg HM, Goltzman D, Karaplis AC 2005 Osteoblast-derived PTHrP is a potent endogenous bone anabolic agent that modifies the therapeutic efficacy of administered PTH 1-34. J Clin Invest 115(9):2402-2411.

66. Barnes GL, Kostenuik PJ, Gerstenfeld LC, Einhorn TA 1999 Growth factor regulation of fracture repair. J Bone Miner Res 14(11):1805-1815.

67. Gerstenfeld LC, Cullinane DM, Barnes GL, Graves DT, Einhorn TA 2003 Fracture healing as a post-natal developmental process: molecular, spatial, and temporal aspects of its regulation. J Cell Biochem 88(5):873-884.

68. Einhorn TA 1998 The cell and molecular biology of fracture healing. Clin Orthop Relat Res (355 Suppl):S7-21.

69. Simon AM, Manigrasso MB, O'Connor JP 2002 Cyclo-oxygenase 2 function is essential for bone fracture healing. J Bone Miner Res 17(6):963-976.

70. Naik AA, Xie C, Zuscik MJ, Kingsley P, Schwarz EM, Awad H, Guldberg R, Drissi H, Puzas JE, Boyce B, Zhang X, O'Keefe RJ 2009 Reduced COX-2 expression in aged mice is associated with impaired fracture healing. J Bone Miner Res 24(2):251-264.

71. Shapiro F 2008 Bone development and its relation to fracture repair. The role of mesenchymal osteoblasts and surface osteoblasts. Eur Cell Mater 15:53-76.

72. Zhang X, Xie C, Lin AS, Ito H, Awad H, Lieberman JR, Rubery PT, Schwarz EM, O'Keefe RJ, Guldberg RE 2005 Periosteal progenitor cell fate in segmental cortical bone graft transplantations: implications for functional tissue engineering. J Bone Miner Res 20(12):2124-2137.

73. Colnot C, Huang S, Helms J 2006 Analyzing the cellular contribution of bone marrow to fracture healing using bone marrow transplantation in mice. Biochem Biophys Res Commun 350(3):557-561.

74. Eghbali-Fatourechi GZ, Lamsam J, Fraser D, Nagel D, Riggs BL, Khosla S 2005 Circulating osteoblast-lineage cells in humans. N Engl J Med 352(19):1959-1966.

75. Rumi MN, Deol GS, Singapuri KP, Pellegrini VD, Jr. 2005 The origin of osteoprogenitor cells responsible for heterotopic ossification following hip surgery: an animal model in the rabbit. J Orthop Res 23(1):34-40.

76. Zimmermann G, Henle P, Kusswetter M, Moghaddam A, Wentzensen A, Richter W, Weiss S 2005 TGF-beta1 as a marker of delayed fracture healing. Bone 36(5):779-785.

77. Ai-Aql ZS, Alagl AS, Graves DT, Gerstenfeld LC, Einhorn TA 2008 Molecular mechanisms controlling bone formation during fracture healing and distraction osteogenesis. J Dent Res 87(2):107-118.

78. Deckers MM, van Bezooijen RL, van der Horst G, Hoogendam J, van Der Bent C, Papapoulos SE, Lowik CW 2002 Bone morphogenetic proteins stimulate angiogenesis through osteoblast-derived vascular endothelial growth factor A. Endocrinology 143(4):1545-1553.

79. Sarahrudi K, Thomas A, Braunsteiner T, Wolf H, Vecsei V, Aharinejad S 2009 VEGF serum concentrations in patients with long bone fractures: a comparison between impaired and normal fracture healing. J Orthop Res 27(10):1293-1297.

80. Zelzer E, Glotzer DJ, Hartmann C, Thomas D, Fukai N, Soker S, Olsen BR 2001 Tissue specific regulation of VEGF expression during bone development requires Cbfa1/Runx2. Mech Dev 106(1-2):97-106.

81. Chen D, Zhao M, Mundy GR 2004 Bone morphogenetic proteins. Growth Factors 22(4):233-241.

82. Nakase T, Yoshikawa H 2006 Potential roles of bone morphogenetic proteins (BMPs) in skeletal repair and regeneration. J Bone Miner Metab 24(6):425-433.

83. Phieffer LS, Goulet JA 2006 Delayed unions of the tibia. J Bone Joint Surg Am 88(1):206-216.

84. Adams CI, Keating JF, Court-Brown CM 2001 Cigarette smoking and open tibial fractures. Injury 32(1):61-65.

85. Henley MB, Chapman JR, Agel J, Harvey EJ, Whorton AM, Swiontkowski MF 1998 Treatment of type II, IIIA, and IIIB open fractures of the tibial shaft: a prospective comparison of unreamed interlocking intramedullary nails and half-pin external fixators. J Orthop Trauma 12(1):1-7.

86. Claes L, Grass R, Schmickal T, Kisse B, Eggers C, Gerngross H, Mutschler W, Arand M, Wintermeyer T, Wentzensen A 2002 Monitoring and healing analysis of 100 tibial shaft fractures. Langenbecks Arch Surg 387(3-4):146-152.

87. Aro HT, Chao EY 1993 Bone-healing patterns affected by loading, fracture fragment stability, fracture type, and fracture site compression. Clin Orthop Relat Res (293):8-17.

88. Castillo RC, Bosse MJ, MacKenzie EJ, Patterson BM 2005 Impact of smoking on fracture healing and risk of complications in limb-threatening open tibia fractures. J Orthop Trauma 19(3):151-157.

89. Vuolteenaho K, Moilanen T, Moilanen E 2008 Non-steroidal anti-inflammatory drugs, cyclooxygenase-2 and the bone healing process. Basic Clin Pharmacol Toxicol 102(1):10-14.

90. Chakkalakal DA, Novak JR, Fritz ED, Mollner TJ, McVicker DL, Garvin KL, McGuire MH, Donohue TM 2005 Inhibition of bone repair in a rat model for chronic and excessive alcohol consumption. Alcohol 36(3):201-214.

91. Meyer MH, Meyer RA, Jr. 2007 Genes with greater up-regulation in the fracture callus of older rats with delayed healing. J Orthop Res 25(4):488-494.

92. Nilsson BE, Edwards P 1969 Age and fracture healing: a statistical analysis of 418 cases of tibial shaft fractures. Geriatrics 24(2):112-117.

93. Smith TK 1987 Prevention of complications in orthopedic surgery secondary to nutritional depletion. Clin Orthop Relat Res (222):91-97.

94. Herskind AM, Christensen K, Norgaard-Andersen K, Andersen JF 1992 Diabetes mellitus and healing of closed fractures. Diabete Metab 18(1):63-64.

95. Claes L, Schmalenbach J, Herrmann M, Olku I, Garcia P, Histing T, Obeid R, Schorr H, Herrmann W, Pohlemann T, Menger MD, Holstein JH 2009 Hyperhomocysteinemia is associated with impaired fracture healing in mice. Calcif Tissue Int 85(1):17-21.

96. Kanis JA, Borgstrom F, De Laet C, Johansson H, Johnell O, Jonsson B, Oden A, Zethraeus N, Pfleger B, Khaltaev N 2005 Assessment of fracture risk. Osteoporos Int 16(6):581-589.

97. Kanis JA 1994 Assessment of fracture risk and its application to screening for postmenopausal osteoporosis: synopsis of a WHO report. WHO Study Group. Osteoporos Int 4(6):368-381.

98. Cummings SR, Black DM, Nevitt MC, Browner W, Cauley J, Ensrud K, Genant HK, Palermo L, Scott J, Vogt TM 1993 Bone density at various sites for prediction of hip fractures. The Study of Osteoporotic Fractures Research Group. Lancet 341(8837):72-75.

99. Johnell O, Kanis JA, Oden A, Johansson H, De Laet C, Delmas P, Eisman JA, Fujiwara S, Kroger H, Mellstrom D, Meunier PJ, Melton LJ, 3rd, O'Neill T, Pols H, Reeve J, Silman A, Tenenhouse A 2005 Predictive value of BMD for hip and other fractures. J Bone Miner Res 20(7):1185-1194.

100. Eklund F, Nordstrom A, Neovius M, Svensson O, Nordstrom P 2009 Variation in fracture rates by country may not be explained by differences in bone mass. Calcif Tissue Int 85(1):10-16.

101. Raisz L 2008 Overview of Pathogenesis. In: Rosen C (ed.) Primer on the Metabolic Bone Diseases and Disorders of Mineral Metabolism, Seventh ed. The American Society for Bone and Mineral Research, Washington, D.C., pp 203-206.

102. Bono CM, Einhorn TA 2003 Overview of osteoporosis: pathophysiology and determinants of bone strength. Eur Spine J 12 Suppl 2:S90-96.

103. Raisz LG 1999 Physiology and pathophysiology of bone remodeling. Clin Chem 45(8 Pt 2):1353-1358.

104. Aaron JE, Makins NB, Sagreiya K 1987 The microanatomy of trabecular bone loss in normal aging men and women. Clin Orthop Relat Res (215):260-271.

105. Lips P, Courpron P, Meunier PJ 1978 Mean wall thickness of trabecular bone packets in the human iliac crest: changes with age. Calcif Tissue Res 26(1):13-17.

106. Eghbali-Fatourechi G, Khosla S, Sanyal A, Boyle WJ, Lacey DL, Riggs BL 2003 Role of RANK ligand in mediating increased bone resorption in early postmenopausal women. J Clin Invest 111(8):1221-1230.

107. Akhter MP, Lappe JM, Davies KM, Recker RR 2007 Transmenopausal changes in the trabecular bone structure. Bone 41(1):111-116.

108. Seeman E 2003 Periosteal bone formation--a neglected determinant of bone strength. N Engl J Med 349(4):320-323.

109. Nordsletten L, Kaastad TS, Madsen JE, Reikeras O, Ovstebo R, Stromme JH, Falch J 1994 The development of femoral osteopenia in ovariectomized rats is not reduced by high intensity treadmill training: a mechanical and densitometric study. Calcif Tissue Int 55(6):436-442.

110. Gundersen HJ, Bendtsen TF, Korbo L, Marcussen N, Moller A, Nielsen K, Nyengaard JR, Pakkenberg B, Sorensen FB, Vesterby A, et al. 1988 Some new, simple and efficient stereological methods and their use in pathological research and diagnosis. Apmis 96(5):379-394.

111. Reinholt FP, Engfeldt B, Hjerpe A, Jansson K 1982 Stereological studies on the epiphyseal growth plate with special reference to the distribution of matrix vesicles. J Ultrastruct Res 80(3):270-279.

112. Baekkevold ES, Yamanaka T, Palframan RT, Carlsen HS, Reinholt FP, von Andrian UH, Brandtzaeg P, Haraldsen G 2001 The CCR7 ligand elc (CCL19) is transcytosed in high endothelial venules and mediates T cell recruitment. J Exp Med 193(9):1105-1112.

113. Shimoni E, Muller M 1998 On optimizing high-pressure freezing: from heat transfer theory to a new microbiopsy device. J Microsc 192(Pt 3):236-247.

114. Edelmann L 2002 Freeze-dried and resin-embedded biological material is well suited for ultrastructure research. J Microsc 207(Pt 1):5-26.

115. Bolender RP 1978 Correlation of morphometry and stereology with biochemical analysis of cell fractions. Int Rev Cytol 55:247-289.

116. Thompson DD, Simmons HA, Pirie CM, Ke HZ 1995 FDA Guidelines and animal models for osteoporosis. Bone 17(4 Suppl):125S-133S.

117. Kalu DN 1991 The ovariectomized rat model of postmenopausal bone loss. Bone Miner 15(3):175-191.

118. Frost HM, Jee WS 1992 On the rat model of human osteopenias and osteoporoses. Bone Miner 18(3):227-236.

119. Gurkan L, Ekeland A, Gautvik KM, Langeland N, Ronningen H, Solheim LF 1986 Bone changes after castration in rats. A model for osteoporosis. Acta Orthop Scand 57(1):67-70.

120. Toolan BC, Shea M, Myers ER, Borchers RE, Seedor JG, Quartuccio H, Rodan G, Hayes WC 1992 Effects of 4-amino-1-hydroxybutylidene bisphosphonate on bone biomechanics in rats. J Bone Miner Res 7(12):1399-1406.

121. Kaastad TS, Reikeras O, Halvorsen V, Falch JA, Obrant KJ, Nordsletten L 2001 Vitamin D deficiency and ovariectomy reduced the strength of the femoral neck in rats. Calcif Tissue Int 69(2):102-108.

122. Bergstrom U, Bjornstig U, Stenlund H, Jonsson H, Svensson O 2008 Fracture mechanisms and fracture pattern in men and women aged 50 years and older: a study of a 12-year population-based injury register, Umea, Sweden. Osteoporos Int 19(9):1267-1273.

123. Holick MF 2007 Vitamin D deficiency. N Engl J Med 357(3):266-281.

124. Bak B, Andreassen TT 1989 The effect of aging on fracture healing in the rat. Calcif Tissue Int 45(5):292-297.

125. Prisby RD, Ramsey MW, Behnke BJ, Dominguez JM, 2nd, Donato AJ, Allen MR, Delp MD 2007 Aging reduces skeletal blood flow, endothelium-dependent vasodilation, and NO bioavailability in rats. J Bone Miner Res 22(8):1280-1288.

126. Lill CA, Hesseln J, Schlegel U, Eckhardt C, Goldhahn J, Schneider E 2003 Biomechanical evaluation of healing in a non-critical defect in a large animal model of osteoporosis. J Orthop Res 21(5):836-842.

127. Meyer RA, Jr., Tsahakis PJ, Martin DF, Banks DM, Harrow ME, Kiebzak GM 2001 Age and ovariectomy impair both the normalization of mechanical properties and the accretion of mineral by the fracture callus in rats. J Orthop Res 19(3):428-435.

128. Iwaniec UT, Moore K, Rivera MF, Myers SE, Vanegas SM, Wronski TJ 2007 A comparative study of the bone-restorative efficacy of anabolic agents in aged ovariectomized rats. Osteoporosis Int 18(3):351-362.

129. Ahlborg HG, Johnell O, Turner CH, Rannevik G, Karlsson MK 2003 Bone loss and bone size after menopause. New Engl J Med 349(4):327-334.

130. Egermann M, Goldhahn J, Schneider E 2005 Animal models for fracture treatment in osteoporosis. Osteoporos Int 16 Suppl 2:S129-138.

131. Wronski TJ, Dann LM, Scott KS, Cintron M 1989 Long-term effects of ovariectomy and aging on the rat skeleton. Calcif Tissue Int 45(6):360-366.

132. Mosekilde L 1995 Assessing bone quality--animal models in preclinical osteoporosis research. Bone 17(4 Suppl):343S-352S.

133. Nordsletten L, Madsen JE, Almaas R, Rootwelt T, Halse J, Konttinen YT, Hukkanen M, Santavirta S 1994 The neuronal regulation of fracture healing. Effects of sciatic nerve resection in rat tibia. Acta Orthop Scand 65(3):299-304.

134. Madsen JE, Hukkanen M, Aune AK, Basran I, Moller JF, Polak JM, Nordsletten L 1998 Fracture healing and callus innervation after peripheral nerve resection in rats. Clin Orthop Relat Res (351):230-240.

135. Dimmen S, Nordsletten L, Madsen JE 2009 Parecoxib and indomethacin delay early fracture healing: a study in rats. Clin Orthop Relat Res 467(8):1992-1999.

136. Terjesen T 1984 Bone healing after metal plate fixation and external fixation of the osteotomized rabbit tibia. Acta Orthop Scand 55(1):69-77.

137. Terjesen T, Apalset K 1988 The influence of different degrees of stiffness of fixation plates on experimental bone healing. J Orthop Res 6(2):293-299.

138. Deluca PA, Lindsey RW, Ruwe PA 1988 Refracture of bones of the forearm after the removal of compression plates. J Bone Joint Surg Am 70(9):1372-1376.

139. Elder SH, Goldstein SA, Kimura JH, Soslowsky LJ, Spengler DM 2001 Chondrocyte differentiation is modulated by frequency and duration of cyclic compressive loading. Ann Biomed Eng 29(6):476-482.

140. Tagil M, Aspenberg P 1999 Cartilage induction by controlled mechanical stimulation in vivo. J Orthop Res 17(2):200-204.

141. Palomares KT, Gleason RE, Mason ZD, Cullinane DM, Einhorn TA, Gerstenfeld LC, Morgan EF 2009 Mechanical stimulation alters tissue differentiation and molecular expression during bone healing. J Orthop Res 27(9):1123-1132.

142. Curtis R, Goldhahn J, Schwyn R, Regazzoni P, Suhm N 2005 Fixation principles in metaphyseal bone-a patent based review. Osteoporosis Int 16:S54-S64.

143. Fan W, Crawford R, Xiao Y 2008 Structural and cellular differences between metaphyseal and diaphyseal periosteum in different aged rats. Bone 42(1):81-89.

144. Bostrom MP, Lane JM, Berberian WS, Missri AA, Tomin E, Weiland A, Doty SB, Glaser D, Rosen VM 1995 Immunolocalization and expression of bone morphogenetic proteins 2 and 4 in fracture healing. J Orthop Res 13(3):357-367.

145. Gersch RP, Lombardo F, McGovern SC, Hadjiargyrou M 2005 Reactivation of Hox gene expression during bone regeneration. J Orthop Res 23(4):882-890.

146. Ralston SH 1994 Analysis of gene expression in human bone biopsies by polymerase chain reaction: evidence for enhanced cytokine expression in postmenopausal osteoporosis. J Bone Miner Res 9(6):883-890.

147. Stuermer EK, Sehmisch S, Rack T, Wenda E, Seidlova-Wuttke D, Tezval M, Wuttke W, Frosch KH, Stuermer KM 2008 Estrogen and raloxifene improve metaphyseal fracture healing in the early phase of osteoporosis. A new fracture-healing model at the tibia in rat. Langenbecks Arch Surg.

148. Carlemalm E, Armbruster BL, Chiovetti R, Garavito RM, Hobot JA, Villiger W, Kellenberger E 1982 Perspectives for achieving improved information by the observation of thin sections in the electron microscope. Tokai J Exp Clin Med 7 Suppl:33-42.

149. Tokuyasu KT 1973 A technique for ultracryotomy of cell suspensions and tissues. J Cell Biol 57(2):551-565.

150. Quintana C 1994 Cryofixation, cryosubstitution, cryoembedding for ultrastructural, immunocytochemical and microanalytical studies. Micron 25(1):63-99.

151. Staehelin LA, Giddings TH, Jr., Kiss JZ, Sack FD 1990 Macromolecular differentiation of Golgi stacks in root tips of Arabidopsis and Nicotiana seedlings as visualized in high pressure frozen and freeze-substituted samples. Protoplasma 157(1-3):75-91.

152. Zhang GF, Staehelin LA 1992 Functional Compartmentation of the Golgi Apparatus of Plant Cells : Immunocytochemical Analysis of High-Pressure Frozen- and Freeze-Substituted Sycamore Maple Suspension Culture Cells. Plant Physiol 99(3):1070-1083.

153. Zhang GF, Driouich A, Staehelin LA 1993 Effect of monensin on plant Golgi: re-examination of the monensin-induced changes in cisternal architecture and functional activities of the Golgi apparatus of sycamore suspension-cultured cells. J Cell Sci 104 (Pt 3):819-831.

154. Driouich A, Faye L, Staehelin LA 1993 The plant Golgi apparatus: a factory for complex polysaccharides and glycoproteins. Trends Biochem Sci 18(6):210-214.

155. Driouich A, Jauneau A, Staehelin LA 1997 7-Dehydrobrefeldin A, a naturally occurring brefeldin A derivative, inhibits secretion and causes a cis-to-trans breakdown of Golgi stacks in plant cells. Plant Physiol 113(2):487-492.

156. Skepper JN 2000 Immunocytochemical strategies for electron microscopy: choice or compromise. J Microsc 199(Pt 1):1-36.

157. D'Amico F, Skarmoutsou E, Stivala F 2009 State of the art in antigen retrieval for immunohistochemistry. J Immunol Methods 341(1-2):1-18.

158. Yamashita S, Okada Y 2005 Application of heat-induced antigen retrieval to aldehyde-fixed fresh frozen sections. Journal of Histochemistry & Cytochemistry 53(11):1421-1432.

159. Hann CR, Springett MJ, Johnson DH 2001 Antigen retrieval of basement membrane proteins from archival eye tissues. J Histochem Cytochem 49(4):475-482.

160. Brorson SH 2002 pH-dependent effect of heat-induced antigen retrieval of epoxy section for electron microscopy. Micron 33(5):481-482.

161. Goode NP, Shires M, Crellin DM, Khan TN, Mooney AF 2004 Post-embedding double-labeling of antigen-retrieved ultrathin sections using a silver enhancement-controlled sequential immunogold (SECSI) technique. J Histochem Cytochem 52(1):141-144.

162. Brorson SH 2001 Heat-induced antigen retrieval of epoxy sections for electron microscopy. Histol Histopathol 16(3):923-930.

163. Rait VK, Xu L, O'Leary TJ, Mason JT 2004 Modeling formalin fixation and antigen retrieval with bovine pancreatic RNase A II. Interrelationship of cross-linking, immunoreactivity, and heat treatment. Lab Invest 84(3):300-306.

164. Yamashita S, Okada Y 2005 Mechanisms of heat-induced antigen retrieval: analyses in vitro employing SDS-PAGE and immunohistochemistry. J Histochem Cytochem 53(1):13-21.

165. Yamashita S, Okada Y 2005 Application of heat-induced antigen retrieval to aldehyde-fixed fresh frozen sections. J Histochem Cytochem 53(11):1421-1432.

166. Brown E, Mantell J, Carter D, Tilly G, Verkade P 2009 Studying intracellular transport using high-pressure freezing and Correlative Light Electron Microscopy. Semin Cell Dev Biol 20(8):910-919.

167. Studer D, Humbel BM, Chiquet M 2008 Electron microscopy of high pressure frozen samples: bridging the gap between cellular ultrastructure and atomic resolution. Histochem Cell Biol 130(5):877-889.

168. D'Amico F, Skarmoutsou E 2008 Quantifying immunogold labelling in transmission electron microscopy. J Microsc 230(Pt 1):9-15.

169. Mayhew TM, Lucocq JM, Griffiths G 2002 Relative labelling index: a novel stereological approach to test for non-random immunogold labelling of organelles and membranes on transmission electron microscopy thin sections. J Microsc 205(Pt 2):153-164.

170. Posthuma G, Slot JW, Geuze HJ 1987 Usefulness of the immunogold technique in quantitation of a soluble protein in ultra-thin sections. J Histochem Cytochem 35(4):405-410.

171. Hollberg K, Nordahl J, Hultenby K, Mengarelli-Widholm S, Andersson G, Reinholt FP 2005 Polarization and secretion of cathepsin K precede tartrate-resistant acid phosphatase secretion to the ruffled border area during the activation of matrix-resorbing clasts. J Bone Miner Metab 23(6):441-449.

172. Barrios C, Brostrom LA, Stark A, Walheim G 1993 Healing complications after internal fixation of trochanteric hip fractures: the prognostic value of osteoporosis. J Orthop Trauma 7(5):438-442.

173. Giannoudis PV, Schneider E 2006 Principles of fixation of osteoporotic fractures. J Bone Joint Surg Br 88B(10):1272-1278.

174. Kubo T, Shiga T, Hashimoto J, Yoshioka M, Honjo H, Urabe M, Kitajima I, Semba I, Hirasawa Y 1999 Osteoporosis influences the late period of fracture healing in a rat model prepared by ovariectomy and low calcium diet. J Steroid Biochem Mol Biol 68(5-6):197-202.

175. Wheeler DL, Eschbach EJ, Montfort MJ, Maheshwari P, McLoughlin SW 2000 Mechanical strength of fracture callus in osteopenic bone at different phases of healing. J Orthop Trauma 14(2):86-92.

176. Cao Y, Mori S, Mashiba T, Westmore MS, Ma L, Sato M, Akiyama T, Shi L, Komatsubara S, Miyamoto K, Norimatsu H 2002 Raloxifene, estrogen, and alendronate affect the processes of fracture repair differently in ovariectomized rats. J Bone Miner Res 17(12):2237-2246.

177. Namkung-Matthai H, Appleyard R, Jansen J, Hao Lin J, Maastricht S, Swain M, Mason RS, Murrell GA, Diwan AD, Diamond T 2001 Osteoporosis influences the early period of fracture healing in a rat osteoporotic model. Bone 28(1):80-86.

178. Wang JW, Li W, Xu SW, Yang DS, Wang Y, Lin M, Zhao GF 2005 Osteoporosis influences the middle and late periods of fracture healing in a rat osteoporotic model. Chin J Traumatol 8(2):111-116.

179. McCann RM, Colleary G, Geddis C, Clarke SA, Jordan GR, Dickson GR, Marsh D 2008 Effect of osteoporosis on bone mineral density and fracture repair in a rat femoral fracture model. J Orthop Res 26(3):384-393.

180. Saito M, Marumo K 2010 Collagen cross-links as a determinant of bone quality: a possible explanation for bone fragility in aging, osteoporosis, and diabetes mellitus. Osteoporos Int 21(2):195-214.

181. Saito M, Fujii K, Soshi S, Tanaka T 2006 Reductions in degree of mineralization and enzymatic collagen cross-links and increases in glycation-induced pentosidine in the femoral neck cortex in cases of femoral neck fracture. Osteoporos Int 17(7):986-995.

182. Uzawa K, Grzesik WJ, Nishiura T, Kuznetsov SA, Robey PG, Brenner DA, Yamauchi M 1999 Differential expression of human lysyl hydroxylase genes, lysine hydroxylation, and cross-linking of type I collagen during osteoblastic differentiation in vitro. J Bone Miner Res 14(8):1272-1280.

183. Saito M, Soshi S, Fujii K 2003 Effect of hyper- and microgravity on collagen post-translational controls of MC3T3-E1 osteoblasts. J Bone Miner Res 18(9):1695-1705.

184. Hao YJ, Zhang G, Wang YS, Qin L, Hung WY, Leung K, Pei FX 2007 Changes of microstructure and mineralized tissue in the middle and late phase of osteoporotic fracture healing in rats. Bone 41(4):631-638.

185. Ouyang H, Sherman PJ, Paschalis EP, Boskey AL, Mendelsohn R 2004 Fourier transform infrared microscopic imaging: effects of estrogen and estrogen deficiency on fracture healing in rat femurs. Appl Spectrosc 58(1):1-9.

186. Saito M, Shiraishi A, Ito M, Sakai S, Hayakawa N, Mihara M, Marumo K 2009 Comparison of effects of alfacalcidol and alendronate on mechanical properties and bone collagen cross-links of callus in the fracture repair rat model. Bone.

187. Saito M, Fujii K, Mori Y, Marumo K 2006 Role of collagen enzymatic and glycation induced cross-links as a determinant of bone quality in spontaneously diabetic WBN/Kob rats. Osteoporos Int 17(10):1514-1523.

188. Oxlund H, Mosekilde L, Ortoft G 1996 Reduced concentration of collagen reducible cross links in human trabecular bone with respect to age and osteoporosis. Bone 19(5):479-484.

189. Shi HF, Cheung WH, Qin L, Leung AH, Leung KS 2009 Low-magnitude high-frequency vibration treatment augments fracture healing in ovariectomy-induced osteoporotic bone. Bone.

190. Kolios L, Hoerster AK, Sehmisch S, Malcherek MC, Rack T, Tezval M, Seidlova-Wuttke D, Wuttke W, Stuermer KM, Stuermer EK 2010 Do estrogen and alendronate improve metaphyseal fracture healing when applied as osteoporosis prophylaxis? Calcif Tissue Int 86(1):23-32.

191. Ding WG, Zhang ZM, Zhang YH, Jiang SD, Jiang LS, Dai LY 2010 Changes of substance P during fracture healing in ovariectomized mice. Regul Pept 159(1-3):28-34.

192. Egermann M, Heil P, Tami A, Ito K, Janicki P, Von Rechenberg B, Hofstetter W, Richards PJ 2009 Influence of defective bone marrow osteogenesis on fracture repair in an experimental model of senile osteoporosis. J Orthop Res.

193. Matsushita M, Tsuboyama T, Kasai R, Okumura H, Yamamuro T, Higuchi K, Kohno A, Yonezu T, Utani A, et al. 1986 Age-related changes in bone mass in the senescence-accelerated mouse (SAM). SAM-R/3 and SAM-P/6 as new murine models for senile osteoporosis. Am J Pathol 125(2):276-283.

194. Silva MJ, Brodt MD, Ettner SL 2002 Long bones from the senescence accelerated mouse SAMP6 have increased size but reduced whole-bone strength and resistance to fracture. J Bone Miner Res 17(9):1597-1603.

195. Takeda T 1999 Senescence-accelerated mouse (SAM): a biogerontological resource in aging research. Neurobiol Aging 20(2):105-110.

196. Jilka RL, Weinstein RS, Takahashi K, Parfitt AM, Manolagas SC 1996 Linkage of decreased bone mass with impaired osteoblastogenesis in a murine model of accelerated senescence. J Clin Invest 97(7):1732-1740.

197. Kodama Y, Takeuchi Y, Suzawa M, Fukumoto S, Murayama H, Yamato H, Fujita T, Kurokawa T, Matsumoto T 1998 Reduced expression of interleukin-11 in bone marrow stromal cells of senescence-accelerated mice (SAMP6): relationship to osteopenia with enhanced adipogenesis. J Bone Miner Res 13(9):1370-1377.

198. Kajkenova O, Lecka-Czernik B, Gubrij I, Hauser SP, Takahashi K, Parfitt AM, Jilka RL, Manolagas SC, Lipschitz DA 1997 Increased adipogenesis and myelopoiesis in the bone marrow of SAMP6, a murine model of defective osteoblastogenesis and low turnover osteopenia. J Bone Miner Res 12(11):1772-1779.

199. Rodriguez JP, Garat S, Gajardo H, Pino AM, Seitz G 1999 Abnormal osteogenesis in osteoporotic patients is reflected by altered mesenchymal stem cells dynamics. J Cell Biochem 75(3):414-423.

200. Rodriguez JP, Montecinos L, Rios S, Reyes P, Martinez J 2000 Mesenchymal stem cells from osteoporotic patients produce a type I collagen-deficient extracellular matrix favoring adipogenic differentiation. J Cell Biochem 79(4):557-565.

201. Kumagai K, Vasanji A, Drazba JA, Butler RS, Muschler GF 2008 Circulating cells with osteogenic potential are physiologically mobilized into the fracture healing site in the parabiotic mice model. J Orthop Res 26(2):165-175.

202. Taguchi K, Ogawa R, Migita M, Hanawa H, Ito H, Orimo H 2005 The role of bone marrow-derived cells in bone fracture repair in a green fluorescent protein chimeric mouse model. Biochem Biophys Res Commun 331(1):31-36.

203. Need AG, O'Loughlin PD, Morris HA, Coates PS, Horowitz M, Nordin BE 2008 Vitamin D metabolites and calcium absorption in severe vitamin D deficiency. J Bone Miner Res 23(11):1859-1863.

204. Need AG, Nordin BE 2008 Misconceptions - vitamin D insufficiency causes malabsorption of calcium. Bone 42(6):1021-1024.

205. Jesudason D, Need AG, Horowitz M, O'Loughlin PD, Morris HA, Nordin BE 2002 Relationship between serum 25-hydroxyvitamin D and bone resorption markers in vitamin D insufficiency. Bone 31(5):626-630.

206. Amling M, Priemel M, Holzmann T, Chapin K, Rueger JM, Baron R, Demay MB 1999 Rescue of the skeletal phenotype of vitamin D receptor-ablated mice in the setting of normal mineral ion homeostasis: formal histomorphometric and biomechanical analyses. Endocrinology 140(11):4982-4987.

207. Atkins GJ, Kostakis P, Pan B, Farrugia A, Gronthos S, Evdokiou A, Harrison K, Findlay DM, Zannettino AC 2003 RANKL expression is related to the differentiation state of human osteoblasts. J Bone Miner Res 18(6):1088-1098.

208. Wientroub S, Fisher LW, Reddi AH, Termine JD 1987 Noncollagenous bone proteins in experimental rickets in the rat. Mol Cell Biochem 74(2):157-162.

209. Shiraishi A, Takeda S, Masaki T, Higuchi Y, Uchiyama Y, Kubodera N, Sato K, Ikeda K, Nakamura T, Matsumoto T, Ogata E 2000 Alfacalcidol inhibits bone resorption and stimulates formation in an ovariectomized rat model of osteoporosis: distinct actions from estrogen. J Bone Miner Res 15(4):770-779.

210. Uchiyama Y, Higuch IY, Takeda S, Masaki T, Shira-Ishi A, Sato K, Kubodera N, Ikeda K, Ogata E 2002 ED-71, a vitamin D analog, is a more potent inhibitor of bone resorption than alfacalcidol in an estrogen-deficient rat model of osteoporosis. Bone 30(4):582-588.

211. Brinker MR, O'Connor DP, Monla YT, Earthman TP 2007 Metabolic and endocrine abnormalities in patients with nonunions. J Orthop Trauma 21(8):557-570.

212. Cao Y, Mori S, Mashiba T, Kaji Y, Manabe T, Iwata K, Miyamoto K, Komatsubara S, Yamamoto T 2007 1Alpha,25-dihydroxy-2beta(3-hydroxypropoxy)vitamin D3 (ED-71) suppressed callus remodeling but did not interfere with fracture healing in rat femora. Bone 40(1):132-139.

213. Toromanoff A, Ammann P, Mosekilde L, Thomsen JS, Riond JL 1997 Parathyroid hormone increases bone formation and improves mineral balance in vitamin D-deficient female rats. Endocrinology 138(6):2449-2457.

214. Young MF 2003 Bone matrix proteins: their function, regulation, and relationship to osteoporosis. Osteoporos Int 14 Suppl 3:S35-42.

215. Grynpas MD, Tupy JH, Sodek J 1994 The distribution of soluble, mineral-bound, and matrix-bound proteins in osteoporotic and normal bones. Bone 15(5):505-513.

216. Ferris BD, Klenerman L, Dodds RA, Bitensky L, Chayen J 1987 Altered organization of non-collagenous bone matrix in osteoporosis. Bone 8(5):285-288.

217. Tsangari H, Findlay DM, Kuliwaba JS, Atkins GJ, Fazzalari NL 2004 Increased expression of IL-6 and RANK mRNA in human trabecular bone from fragility fracture of the femoral neck. Bone 35(1):334-342.

218. Davey RA, Hahn CN, May BK, Morris HA 2000 Osteoblast gene expression in rat long bones: effects of ovariectomy and dihydrotestosterone on mRNA levels. Calcif Tissue Int 67(1):75-79.

219. Ikeda T, Yamaguchi A, Yokose S, Nagai Y, Yamato H, Nakamura T, Tsurukami H, Tanizawa T, Yoshiki S 1996 Changes in biological activity of bone cells in ovariectomized rats revealed by in situ hybridization. J Bone Miner Res 11(6):780-788.

220. Hatano H, Siegel HJ, Yamagiwa H, Bronk JT, Turner RT, Bolander ME, Sarkar G 2004 Identification of estrogen-regulated genes during fracture healing, using DNA microarray. J Bone Miner Metab 22(3):224-235.

221. Yoshitake H, Rittling SR, Denhardt DT, Noda M 1999 Osteopontin-deficient mice are resistant to ovariectomy-induced bone resorption. Proc Natl Acad Sci U S A 96(14):8156-8160.

222. Duvall CL, Taylor WR, Weiss D, Wojtowicz AM, Guldberg RE 2007 Impaired angiogenesis, early callus formation, and late stage remodeling in fracture healing of osteopontin-deficient mice. J Bone Miner Res 22(2):286-297.

223. Monfoulet L, Malaval L, Aubin JE, Rittling SR, Gadeau AP, Fricain JC, Chassande O 2009 Bone sialoprotein, but not osteopontin, deficiency impairs the mineralization of regenerating bone during cortical defect healing. Bone.

224. Prince CW, Butler WT 1987 1,25-Dihydroxyvitamin D3 regulates the biosynthesis of osteopontin, a bone-derived cell attachment protein, in clonal osteoblast-like osteosarcoma cells. Coll Relat Res 7(4):305-313.

225. Oldberg A, Jirskog-Hed B, Axelsson S, Heinegard D 1989 Regulation of bone sialoprotein mRNA by steroid hormones. J Cell Biol 109(6 Pt 1):3183-3186.

226. Chen J, Thomas HF, Sodek J 1996 Regulation of bone sialoprotein and osteopontin mRNA expression by dexamethasone and 1,25-dihydroxyvitamin D3 in rat bone organ cultures. Connect Tissue Res 34(1):41-51.

227. Chen JJ, Jin H, Ranly DM, Sodek J, Boyan BD 1999 Altered expression of bone sialoproteins in vitamin D-deficient rBSP2.7Luc transgenic mice. J Bone Miner Res 14(2):221-229.

228. Balla B, Kosa JP, Kiss J, Borsy A, Podani J, Takacs I, Lazary A, Nagy Z, Bacsi K, Speer G, Orosz L, Lakatos P 2008 Different gene expression patterns in the bone tissue of aging postmenopausal osteoporotic and non-osteoporotic women. Calcif Tissue Int 82(1):12-26.

229. Hopwood B, Tsykin A, Findlay DM, Fazzalari NL 2009 Gene expression profile of the bone microenvironment in human fragility fracture bone. Bone 44(1):87-101.

230. Langdahl BL, Knudsen JY, Jensen HK, Gregersen N, Eriksen EF 1997 A sequence variation: 713-8delC in the transforming growth factor-beta 1 gene has higher prevalence in osteoporotic women than in normal women and is associated with very low bone mass in osteoporotic women and increased bone turnover in both osteoporotic and normal women. Bone 20(3):289-294.

231. Yamada Y, Miyauchi A, Goto J, Takagi Y, Okuizumi H, Kanematsu M, Hase M, Takai H, Harada A, Ikeda K 1998 Association of a polymorphism of the transforming growth factor-beta 1 gene with genetic susceptibility to osteoporosis in postmenopausal Japanese women. J Bone Miner Res 13(10):1569-1576.

232. Trost Z, Trebse R, Prezelj J, Komadina R, Logar DB, Marc J 2009 A microarray based identification of osteoporosis-related genes in primary culture of human osteoblasts. Bone.

233. Liu S, Tang W, Zhou J, Stubbs JR, Luo Q, Pi M, Quarles LD 2006 Fibroblast growth factor 23 is a counter-regulatory phosphaturic hormone for vitamin D. Journal of the American Society of Nephrology 17(5):1305-1315.

234. Burnett-Bowie SA, Henao MP, Dere ME, Lee H, Leder BZ 2009 Effects of hPTH(1-34) infusion on circulating serum phosphate, 1,25-dihydroxyvitamin D, and FGF23 levels in healthy men. J Bone Miner Res 24(10):1681-1685.

235. Samadfam R, Richard C, Nguyen-Yamamoto L, Bolivar I, Goltzman D 2009 Bone formation regulates circulating concentrations of fibroblast growth factor 23. Endocrinology 150(11):4835-4845.

236. Goebel S, Lienau J, Rammoser U, Seefried L, Wintgens KF, Seufert J, Duda G, Jakob F, Ebert R 2009 FGF23 is a putative marker for bone healing and regeneration. J Orthop Res 27(9):1141-1146.

237. Miossec P 2004 IL-17 in rheumatoid arthritis: a new target for treatment or just another cytokine? Joint Bone Spine 71(2):87-90.

238. Gaffen SL 2004 Biology of recently discovered cytokines: interleukin-17--a unique inflammatory cytokine with roles in bone biology and arthritis. Arthritis Res Ther 6(6):240-247.

239. Langrish CL, Chen Y, Blumenschein WM, Mattson J, Basham B, Sedgwick JD, McClanahan T, Kastelein RA, Cua DJ 2005 IL-23 drives a pathogenic T cell population that induces autoimmune inflammation. J Exp Med 201(2):233-240.

240. Lubberts E 2008 IL-17/Th17 targeting: On the road to prevent chronic destructive arthritis? Cytokine 41(2):84-91.

241. Lubberts E, van den Bersselaar L, Oppers-Walgreen B, Schwarzenberger P, Coenen-de Roo CJ, Kolls JK, Joosten LA, van den Berg WB 2003 IL-17 promotes bone erosion in murine collagen-induced arthritis through loss of the receptor activator of NF-kappa B ligand/osteoprotegerin balance. J Immunol 170(5):2655-2662.

242. Goswami J, Hernandez-Santos N, Zuniga LA, Gaffen SL 2009 A bone-protective role for IL-17 receptor signaling in ovariectomy-induced bone loss. Eur J Immunol 39(10):2831-2839.

243. Mansson B, Wenglen C, Morgelin M, Saxne T, Heinegard D 2001 Association of chondroadherin with collagen type II. J Biol Chem 276(35):32883-32888.

244. Franzen A, Hultenby K, Reinholt FP, Onnerfjord P, Heinegard D 2008 Altered osteoclast development and function in osteopontin deficient mice. J Orthop Res 26(5):721-728.

245. Shen Z, Gantcheva S, Mansson B, Heinegard D, Sommarin Y 1998 Chondroadherin expression changes in skeletal development. Biochem J 330 (Pt 1):549-557.

246. Sommarin Y, Larsson T, Heinegard D 1989 Chondrocyte-matrix interactions. Attachment to proteins isolated from cartilage. Exp Cell Res 184(1):181-192.

247. Vortkamp A, Lee K, Lanske B, Segre GV, Kronenberg HM, Tabin CJ 1996 Regulation of rate of cartilage differentiation by Indian hedgehog and PTH-related protein. Science 273(5275):613-622.

248. Hunter GK, Goldberg HA 1994 Modulation of crystal formation by bone phosphoproteins: role of glutamic acid-rich sequences in the nucleation of hydroxyapatite by bone sialoprotein. Biochem J 302 (Pt 1):175-179.

I

This article is removed.

II

This article is removed.

III

GENE EXPRESSION AND DISTRIBUTION OF KEY BONE REMODELING MARKERS IN THE CALLUS OF ESTROGEN-DEFICIENT VITAMIN D DEPLETED RATS

Melhus G[1], Brorson SH[1], Baekkevold ES[1], Andersson G[3], Jemtland R[2], Reinholt FP[1]

[1]Institute of Pathology, University of Oslo, and Division of Pathology, Oslo University Hospital, Rikshospitalet, NO-0027 Oslo, Norway
[2]Endocrine section, Department of Medicine, Oslo University Hospital, Rikshospitalet, Oslo, Norway
[3]Department of Laboratory Medicine, Division of Pathology, F46, Karolinska Institutet, Karolinska University Hospital Huddinge, SE-141 86 Huddinge, Sweden

Correspondence to:
Gunhild Melhus, A3.M006, Institute of Pathology, Oslo University Hospital, Rikshospitalet, Sognsvannsveien 20, NO-0027 Norway
Cell: + 47 920 27 812
Telephone: +47 23 07 14 89
Fax: +47 23 07 15 11
Email: gunhild.melhus@rr-research.no

Running title: Fracture healing in experimental osteoporosis

ABSTRACT

Purpose: An experimental rat model was used to test the hypothesis that in osteoporosis (OP) the molecular composition of the extracellular matrix (ECM) in the fracture callus is disturbed. *Methods:* OP was induced at 10 weeks of age by ovariectomy and vitamin D_3 deficient diet, and sham operated animals fed normal diet served as controls. Three months later a closed tibial fracture was made and stabilized with an intramedullary nail. After 3 and 6 weeks of healing, the animals were sacrificed and the fracture calluses examined with global gene expression, *in situ* mRNA expression and ultrastructural protein distribution of 4 bone remodeling markers, i.e. osteopontin (OPN), bone sialoprotein (BSP), tartrate-resistant acid phosphatase (TRAP), and cathepsin K (CTK). *Results:* The global gene expression showed a relative small number of differently regulated genes, mostly upregulated and at 3 weeks. The 4 chosen markers were not differently regulated and only minor differences in the *in situ* mRNA expression and ultrastructural protein distribution were detected. *Conclusion:* The gene expression and composition of fracture calluses are not generally disturbed in experimental OP.

KEYWORDS

Fracture healing, osteoporosis, global gene expression, non-collagenous matrix proteins

INTRODUCTION

Osteoporosis (OP) is a multifactorial metabolic bone disease characterized by reduced bone density and quality, resulting in loss of mechanical strength and increased susceptibility to fracture. Women undergo a rapid phase of bone loss starting 2 to 3 years before ovarian failure, remaining up to 5 years after menopause, and in many cases, with postmenopausal OP as the final outcome [1, 2]. However, whether or to which extent this disrupted balance between bone formation and bone resorption [3, 4] influences healing of fractures in OP individuals remains to be answered.

Fracture healing is a complex process taking place in order to fully restore anatomic and functional structure following injury, involving cell proliferation and differentiation, chemotaxis and synthesis of extracellular matrix (ECM). Although delayed healing of femoral neck fractures in OP patients has been reported [5], clinical data are limited. Due to ethical concerns and multiple confounding factors, most studies have been performed in animal models of postmenopausal OP. The ovariectomized (OVX) rat model has been approved by FDA [6] as a relevant model for the study of postmenopausal OP, mimicking postmenopausal trabecular bone loss when examined over relatively short periods of time. Impaired fracture healing has been reported in this model in early [7] and late stages [8], as evaluated by radiographic, histomorphometric and mechanical parameters. However, we recently demonstrated preserved BMD and mechanical strength of callus 6 weeks after fracture in experimental OP [9], in line with the findings by Kubo et al. at the same time point [8]. In support, Wheeler et al. [10] reports no difference between OVX and sham rats in mechanical strength of callus at 4, 6 and 8 weeks after fracture. Thus, data are conflicting and, moreover only a limited number of studies look into the molecular events involved in fracture repair in OP.

An additional predictor in the development of postmenopausal OP is vitamin D deficiency, which also may influence bone repair. Vitamin D deficiency is common among women with OP [11] and women with fractures regardless of

age [12], leading to accelerated bone resorption. In support, OVX rats with vitamin D depletion develop site-specific bone loss similar to what is observed in women with postmenopausal OP [13]. Additionally, oral administration of $1,25(OH)_2$ vitamin D_3 has recently been shown to improve fracture healing in OVX rats [14]. Interestingly, both estrogen [15] and vitamin D [16, 17] influences the expression and synthesis of ECM proteins and such proteins play important roles in mediating cellular function and may serve as important modulators of bone regeneration.

Thus, we hypothesized that lack of estrogen and vitamin D deficiency influences the global gene expression as well as the synthesis and ultrastructural distribution of ECM molecules in the fracture callus, and consequently, the capacity of fracture repair. To test this hypothesis, we examined the global gene expression, and the *in situ* mRNA expression as well as ultrastructural protein distribution of two major phosphoproteins in bone, i.e. osteopontin (OPN) and bone sialoprotein (BSP), and two osteoclast enzymes, i.e. tartrate-resistant acid phosphatase (TRAP) and cathepsin K (CTK), in the callus 3 and 6 weeks after tibial fracture of vitamin D depleted OVX rats. Sham operated age-matched controls were used for comparison.

METHODS

Animals and tissue preparation

All animal procedures were approved by the Norwegian Animal Research Authority. The experimental animal model was the same as previously [9]. In brief, 43 female Wistar rats (10 weeks of age with a mean body weight of 235 g (range 197-272 g)) were randomly assigned to two groups; Ovx-D (ovariectomy followed by vitamin D_3-deficient diet and 3 months observation) or sham treated (abdominal skin incision and normal diet in the same period of time). Bone loss was validated by DXA *in vivo* before a closed fracture was made in the tibial midshaft and fixed with an intramedullary nail. Animals were killed at 3 and 6 weeks after fracture, and blood was collected before death. Animals for microarray analyses were killed by a phenobarbital overdose and

the dissected tibias were snap-frozen in liquid nitrogen. In the remaining animals, tissue was fixed by *in vivo* perfusion of 0.1 M phosphate-buffered 2% PFA during deep anaesthesia, the tibias dissected free from muscle and soft tissue and the nail carefully removed from a proximal port. Tibias were immersed in 2% PFA/0.5% glutaraldehyde/0.1 M phosphate-buffer and decalcified in 7% EDTA/0.5% PFA. Bone samples for transmission electron microscopic (TEM) analyses were subjected to low-temperature embedding in Lowicryl HM23 (Chemische Werke Lowi GmbH, Waldkraiburg, Germany) according to our established protocol [18]. Decalcified bone samples for *in situ* hybridization were embedded in paraffin according to a routine protocol.

RNA isolation

Calluses were cut from the tibial diaphyses, homogenized in Trizol reagent (Invitrogen, Carlsbad, CA) and total RNA was isolated according to manufacturer's protocol as previously described [19]. RNA was further purified using QIAGEN RNeasy micro kit (Qiagen, Valencia, CA). Assessment of the concentration and quality of the total RNA samples were performed by spectrophotometry and Agilent 2100 Bioanalyzer (Agilent Technologies, Santa Clara, CA).

***In situ* hybridization (ISH)**

Total RNA was reverse-transcribed to cDNA using oligonucleotide primers listed in table 1. cDNAs were cloned with a Dual Promoter TA Cloning Kit (Invitrogen) and sequenced (Seqlab, Göttingen, Germany), and digoxigenin (DIG)-conjugated complementary RNA (cRNA) probes were synthesized with a DIG-labelling kit (Roche Diagnostics AS, Oslo, Norway) using T7 or Sp6 RNA polymerase to yield probes in the sense or antisense orientation. For TRAP, cloning [20] and DIG-labelling [21] were performed as previously described. Hybridization was performed by modification of a previously described protocol [22]. Briefly, dewaxed and proteinase K-digested sections of paraffin-embedded callus samples were post-fixed in 4% PFA. Following

prehybridization (60 min, RT) in 50% formamide/2x SSC, sections were hybridized (over night, 42°C) with 5 ng probe in 50% formamide/2x SSC/7.5% dextran sulphate. High stringency washing was performed, and unbound probe was removed by RNAse-treatment (Ambion, Austin, USA). Hybridized probe was detected using an alkaline (AP)-conjugated sheep anti-DIG antibody followed by the AP-substrate nitroblue tetrazolium chloride/5-bromo-4-chloro-3-indolyl-phosphate (Roche Diagnostics).

Immunohistochemistry and immunogold labeling

70 nm sections were cut from Lowicryl HM23-embedded tissue and mounted on formvar-coated nickel grids, and immunogold labeling was performed as previously described [18]. Briefly, after blocking with 5% BSA in PBS, grid-mounted sections were incubated overnight with the primary polyclonal antibodies; anti-BSP (Chemicon, Temecula, CA), anti-TRAP (Immunodiagnostics Systems Ltd, Boldon, UK), anti-cathepsin K (Santa Cruz Biotechnology, Inc., CA.) and anti-OPN (raised in rabbits against a peptide sequence of the N-terminal end of the molecule). Bound antibodies were visualized by 90 min. incubation with 10 nm colloidal gold conjugated with protein A. Non-specific rabbit-IgG was used as a negative control.

Analyses

Microarray:

The analysis was performed essentially as previously described [19], except that biotin-labelled cRNA probes were hybridized to GeneChip® Rat Genome 230 2.0 Array (Affymetrix UK Ltd., UK). The quality of the RNA and cRNA probes were assessed by measuring the ratio between 5' and 3' mRNAs for beta-actin and GAPDH according to the Affymetrix-based test, and found to be highly satisfactory.

Light microscopy and ISH:

Light microscopy was performed on paraffin-embedded callus specimens hybridized DIG-labeled cRNA probes for OPN, BSP, TRAP and CTK. Seven to 10 digital images (x 20) were sampled per callus section. Point counting of mRNA positive cells facing bone surfaces was performed using a semiautomatic image analyzer program (AnalySIS pro, Digital Soft Imaging System, Munster, Germany) with grid size of 25 μm x 25 μm [23]. In a parallel set of haematoxylin-stained sections, the corresponding callus area was identified and the total amount of mononuclear cells attached to bone surfaces counted (x 20). The ratio mRNA positive cells/total amount of bone surface cells was calculated for each set of corresponding images.

TEM and immunogold analyses:

Micrographs were obtained by systematic random sampling of cells/surrounding matrix and analyzed using the semiautomatic interactive image analyzer software AnalySIS® pro (Soft Imaging System, Munster, Germany). All identified osteoclasts and at least 4 osteoblasts in one to 3 sections per animal were included in the analyses. An osteoclast was defined as a multinuclear giant cell attached to a matrix surface with characteristic membrane domains, i.e. ruffled border (RB) and/or clear zone (CZ) and an abundance of mitochondria in their cytoplasm [24]. An osteoblast was defined as a mononuclear cell attached to osteoid/bone matrix with a characteristic abundance of ER and Golgi complexes. A minimum of 4 images were sampled in each predetermined subcellular region according to our previously experience with protein distribution for BSP, OPN, TRAP and CTK [25, 26]. The gold particle density was calculated in the regions of interest (ROIs) according to the structural limits in the micrographs. Sections incubated with gold-labeled antibodies against BSP and OPN were analyzed with respect to both osteoblasts and osteoclasts, while only osteoclasts were studied in TRAP and CTK-labeled sections. The results are based on the analysis of up to 42 and 24 osteoclasts at 3 and 6 weeks of healing, respectively. For osteoblasts, a

minimum of 20 cells were analyzed in each group at 3 weeks, and 12 at 6 weeks.

Statistics

Morphological results are given as mean with standard deviation (SD) in parentheses. One-way analysis of variance (ANOVA) and multivariate analysis of variance (MANOVA) were used for light and electron microscopic data, respectively. For the latter, interest was focused on whether the overall distribution pattern for each of the 4 proteins differed between the groups. Thus, for a protein, only differences in overall comparison between the groups using MANOVA, and not differences in tests between subjects, were considered. A *p*-value of less than 0.05 was considered significant.

Statistical analysis of gene expression profiling:

The 16 scanned chip images originating from the bone samples were processed using GCOS 1.4 (Affymetrix). The CEL files were imported into Array Assist software (v5.2.0; Iobion Informatics LLC, LaJolla, CA) and normalized using the PLIER (Probe Logarithmic Intensity Error) algorithm in Array Assist to calculate relative signal values for each probe set. In order to filtrate for low signal values, the MAS5 algorithm in Array Assist was used to create a data set of Absolute Calls, showing the number of present and absent calls for each probe set. The filtration was performed by eliminating probe sets containing $\geq$ 13 absent calls across the data set, resulting in a reduction of probe sets from 31,099 to 21,947. For expression comparisons of different groups, profiles were compared using paired t-test. The results are expressed as fold changes (FC), i.e. ratio of the mean signals between compared groups. Gene lists were generated with the criteria of $p < 0.05$ and $FC \geq 2$.

RESULTS

Animal model of postmenopausal OP

Ovx-D animals presented vitamin D_3- and estrogen deficiency as well as decreased BMD in the vertebra and the femoral neck in comparison with sham treated ($p < 0.001$) [9]. The BMD of the callus areas did not differ between the groups at any time point (data not shown). After randomization, but prior to OVX and introduction of diet, the mean body weight was 4.7% lower in the Ovx-D group compared to sham ($p = 0.02$). However, despite pair feeding the Ovx-D group gained more weight compared to sham treated. The mean body weight was 8.6% and 12.9% higher in the Ovx-D group after 3 and 6 weeks, respectively ($p < 0.001$).

Serum levels of 25-Hydroxyvitamin D and Estradiol

25(OH)D $\leq$ 25 nmol/l in serum was considered as vitamin D deficiency. The Ovx-D group presented levels of 25(OH)D $\leq$ 18 nmol/l, and 94.4% showed undetectable (i.e. $\leq$ 13 nmol/l) levels of 25(OH)D. Postmenopausal estrogen levels was defined as serum estradiol < 0.10 nmol/l (Hormone Laboratory, Aker University Hospital, Oslo, Norway). All Ovx-D animals presented serum estradiol in the range of the reference values for postmenopausal state (i.e. $\leq$ 0.08 nmol/l).

Fracture callus morphology

The fracture calluses demonstrated hard callus formation with intense osteogenesis after 3 weeks in both groups. However, there was large inter-individual variation in size and ratio of intramembranous to endochondral bone formation; some calluses exhibited mainly cartilage/fibrous tissue in the space between the areas of subperiosteal bone formation, while others exhibited predominantly intramembranous bone formation beneath the periosteum adjacent to the fracture site (fig.1). Resorbing clasts were observed both on cartilaginous and osseous surfaces. By light microscopy no obvious differences were detected between Ovx-D and sham treated rats with respect to matrix

resorption activity, vascular invasion or endochondral ossification. At 6 weeks of healing, the same light microscopic heterogeneity was evident. However, a general tendency towards a decline in the remodeling activity was observed.

Gene profiling

At 3 weeks of healing, 155 annotated genes and 88 expressed sequence tags (ESTs) were differently regulated in Ovx-D versus sham, out of which 35 genes were downregulated and 120 upregulated. At 6 weeks, 22 genes and 8 ESTs were differently regulated, out of which 6 genes were downregulated and 16 upregulated in Ovx-D (fig. 1 and suppl. table 2). No significant differences in the mRNA levels for OPN, BSP, TRAP or CTK between the groups or between the different time points were detected (table 2). Among genes with suggested or known roles in bone metabolism, fibroblast growth factor 23 (FGF23) was down-regulated ($p=0.02$) and interleukin 17 (IL-17) receptor A was upregulated ($p=0.01$) in the OP group at 3 weeks.

Localization of OPN, BSP, TRAP and CTK mRNA

OPN and BSP mRNA were detected predominantly in osteoblastic cells and in some chondrocytes in the bone-cartilage transitional zone, but were undetectable in resorbing multinuclear cells. However, BSP mRNA expression in osteoclast progenitors cannot be excluded. CTK and TRAP mRNA were detected in multinucleated cells attached to bone/cartilage surfaces. In addition, several non-attached mononuclear cells, presumably osteoclast progenitors, were positive (fig. 2).

Ratios of mRNA expressing cells on bone surfaces

Compared to sham treated animals, Ovx-D animals exhibited increased ratio of OPN mRNA expressing cells at 3 weeks ($p=0.05$) but decreased ratio of BSP mRNA expressing cells at 6 weeks ($p=0.01$). Ratios for TRAP or CTK did not differ between the two groups. In the Ovx-D group, ratios for BSP ($p=0.04$), OPN ($p=0.01$) and CTK ($p=0.04$) decreased from 3 to 6 weeks. No differences

between the time points were observed among the mRNAs above for sham treated animals (table 3).

Ultrastructural protein distribution

The most intense accumulation of markers for both BSP and OPN was observed at electron dense extracellular areas representing mineralization front/cement lines (fig. 3), and to a lesser extent, diffusely spread, in the mineralized matrix of woven bone. BSP exhibited a characteristic pattern with label being localized to discrete sites in the bone matrix corresponding to areas of early mineral deposition (fig. 3b). Both BSP and OPN labeling showed a tendency towards increased intensity in the matrix facing the CZ of osteoclasts, the latter being most pronounced. No signal for BSP or OPN was found in the cartilaginous areas. Immunoreactivity for TRAP and CTK was consistently increased in the osteoclast cytoplasm and partly also in the matrix facing the RB. Lower levels were observed in the matrix facing the CZ. Intraluminal labeling of vessels was used as a measure of non-specific binding/background and was low throughout the experiments, as was the nuclear labeling (data not shown).

Quantitative immunogold analysis

The immunogold signal for OPN in osteoclasts was different for Ovx-D versus sham animals after 6 weeks ($p = 0.04$) with markedly increased labeling intensity in the matrix facing the RB of osteoclasts in Ovx-D animals, although no differences were observed with respect to osteoblasts at neither time point. For BSP no differences were detected between groups or time points (table 4). CTK showed different distribution with respect to osteoclasts between the groups after 3 weeks ($p=0.03$) with generally increased labeling intensity in all compartments measured for osteoclasts in the Ovx-D animals. Moreover, CTK labeling in the sham treated animals differed from 3 to 6 weeks ($p=0.01$). TRAP distribution did not differ between the groups or between different time

points. Interestingly, TRAP labeling accumulated in the matrix facing the RB of osteoclasts at 3 weeks in both groups, but not at 6 weeks (table 5).

DISCUSSION

The present study addresses fracture healing in vitamin D-depleted OVX rats at the molecular level over a 6 weeks period. Estrogen and vitamin D exert their effects on bone in a spatial manner which differs between metabolic active trabecular bone and weight bearing cortical bone. Although vitamin D initially was reported to stimulate bone resorption *in vitro* [27], more recent *in vivo* findings indicate that active vitamin D analogues rather have an inhibitory effect on bone resorption, at least in a state of high turnover [28]. This inhibitory effect is reported to be less active in trabecular bone [29]. In a similar manner, estrogen deficiency following OVX results in bone loss at discrete sites in the skeleton with most pronounced effect on trabecular bone [30].

Several genes associated with signal transduction, lipid and protein metabolism, ionic and protein transport, neuropeptide and G protein signaling were differently regulated in our Ovx-D rat model. Many of these processes represent metabolic systems capable of maintaining bone homeostasis and tissue turnover. Most genes were expressed in an increased fashion in Ovx-D compared to Sham, in line with other reports on gene profiling of intact bone in OP [31]. Interestingly, no significant differences were detected among genes encoding NCPs with known functions in bone metabolism.

At 3 weeks a 7-fold more genes were differently regulated compared to 6 weeks, and consequently, changes in the healing pattern in OP would be expected in early stages. Among the differently regulated genes, the genes for interleukin 17 (IL-17) receptor A and fibroblast growth factor 23 (FGF23) were up- and downregulated in Ovx-D after 3 weeks, respectively. IL-17 plays a role in bone loss in rheumatoid arthritis [32], and FGF23 has recently been suggested as a putative marker of bone healing; decreased FGF23 mRNA expression being related to delayed fracture healing [33]. However, microarray

data are overall data representing the whole callus and, consequently, differences within the callus are not detected.

In our molecular studies we focused on 4 molecules with roles in bone remodelling taking place in the callus, and, putatively, being influenced by lack of estrogen and vitamin D depletion. E.g. OPN is suggested to play roles both during osteoclast development/activity [34] and during matrix mineralization [35]. Furthermore, OPN null mice are resistant to ovariectomy-induced bone loss [36] and display disturbed fracture healing [37], suggesting a role for OPN during estrogen deficiency-related bone loss as well as in bone repair. Moreover, OPN is under the influence of both estrogen and vitamin D [15, 17]. mRNA expression for OPN, BSP, TRAP and CTK in cell types was distributed as previously described in intact bone tissue [20, 25, 38]. Ovx-D animals presented increased ratio of OPN mRNA expressing cells and indicated decreased ratio of BSP mRNA expressing cells at 3 weeks, and significantly reduced ratio for BSP after 6 weeks of healing. These observations are in line with the reported inverse regulatory role of vitamin D for these proteins *in vivo* [39]. The observed increase in OPN and subsequent decline in BSP indicate suppressed osteoblastic differentiation in the Ovx-D group.

In Ovx-D rats at 3 weeks relative to 6 weeks, there was a significant decline in the ratio of cells expressing mRNAs for OPN, BSP and CTK, but not for TRAP. Thus, the decreased number of cells producing these bone turnover biomarkers in the Ovx-D group at 6 versus 3 weeks indicates a decline in synthetic activity/bone remodeling and a more remodeled callus. The latter supports the findings of Cao et al. [40], reporting a histologically more mature callus with preserved mechanical properties in OP rats versus sham treated rats. Quantitative immunoelectron microscopy showed only minor differences in labeling (table 4, 5). The apparent inconsistence between our ISH and immunogold data is most likely due to the fact that the two data sets represents different aspects of callus turnover; while ISH data represent mRNA expression and thus, protein synthesis, immunogold data reflect the present amount of protein in the tissue, which is the net result of synthesis, secretion

and degradation. That only minor differences of protein synthesis and tissue distribution were detected between the groups is supported by other recent studies [41, 42].

As with any animal model, there are limitations in simulating clinically relevant conditions. The calluses showed considerable heterogeneity both by macroscopic appearance and by histology. Mechanical instability during fracture healing promotes cellular differentiation in the direction of endochondral bone formation [43], suggesting variable degrees of fracture fixation in our experiment. Since mechanical stress is shown to influence the mRNA expression in bone cells [44], this may have influenced our results by causing a relatively large variation among the samples. Furthermore, minimal trauma-fractures in OP patients are mostly localized to the proximal femur, the vertebral column and distal forearm [45], i.e. areas of high trabecular to cortical ratio. Thus, the present study concerns fracture healing in cortical bone and it is possible that this type of bone healing is less influenced by estrogen- and vitamin D deficiency.

In summary, several genes are differently regulated in OP induced by ovariectomy and vitamin D depletion, mostly in an early stage and the majority in an increased fashion, although no genes encoding NCPs with known function in bone metabolism were differently expressed. On the background of only minor differences in the synthesis and protein expression of OPN, BSP, TRAP and CTK in callus between Ovx-D and sham treated animals, our results suggest that the molecular composition of the fracture callus is not markedly skewed in OP.

ACKNOWLEDGEMENTS

The work was financially supported by EU (OSTEOGENE, FP6-502941), University of Oslo (“Småforsk”), and the Norwegian Association against Osteoporosis. Ole Kristoffer Olstad is acknowledged for performing the microarray analyses; Linda T. Dorg, Linda I. Solfjell and Maria Norgård for

excellent technical support. Finally, Jan Erik Madsen and Sigbjorn Dimmen are acknowledged for help with animal surgery.

REFERENCES

1. Eastelle R (2006) Pathogenesis of postmenopausal osteoporosis . In: Favus M (ed) Primer on the metabolic bone diseases and disorders of mineral metabolism. American Society for Bone and Mineral Research, Washington DC, p 259-262
2. Recker R, Lappe J, Davies K, Heaney R (2000) Characterization of perimenopausal bone loss: a prospective study. J Bone Miner Res 15:1965-1973
3. Rodan GA (1991) Mechanical loading, estrogen deficiency, and the coupling of bone formation to bone resorption. J Bone Miner Res 6:527-530
4. Raisz LG (2005) Pathogenesis of osteoporosis: concepts, conflicts, and prospects. J Clin Invest 115:3318-3325
5. Nikolaou VS, Efstathopoulos N, Kontakis G, Kanakaris NK, Giannoudis PV (2009) The influence of osteoporosis in femoral fracture healing time. Injury 40:663-668
6. Thompson DD, Simmons HA, Pirie CM, Ke HZ (1995) FDA Guidelines and animal models for osteoporosis. Bone 17:125S-133S
7. Namkung-Matthai H, Appleyard R, Jansen J, Hao Lin J, Maastricht S, Swain M, Mason RS, Murrell GA, Diwan AD, Diamond T (2001) Osteoporosis influences the early period of fracture healing in a rat osteoporotic model. Bone 28:80-86
8. Kubo T, Shiga T, Hashimoto J, Yoshioka M, Honjo H, Urabe M, Kitajima I, Semba I, Hirasawa Y (1999) Osteoporosis influences the late period of fracture healing in a rat model prepared by ovariectomy and low calcium diet. J Steroid Biochem Mol Biol 68:197-202
9. Melhus G, Solberg LB, Dimmen S, Madsen JE, Nordsletten L, Reinholt FP (2007) Experimental osteoporosis induced by ovariectomy and

vitamin D deficiency does not markedly affect fracture healing in rats. Acta Orthop 78:393-403

10. Wheeler DL, Eschbach EJ, Montfort MJ, Maheshwari P, McLoughlin SW (2000) Mechanical strength of fracture callus in osteopenic bone at different phases of healing. J Orthop Trauma 14:86-92
11. Lips P, Hosking D, Lippuner K, Norquist JM, Wehren L, Maalouf G, Ragi-Eis S, Chandler J (2006) The prevalence of vitamin D inadequacy amongst women with osteoporosis: an international epidemiological investigation. J Intern Med 260:245-254
12. Steele B, Serota A, Helfet DL, Peterson M, Lyman S, Lane JM (2008) Vitamin D Deficiency: A Common Occurrence in Both High-and Low-energy Fractures. Hss J 4:143-148
13. Kaastad TS, Reikeras O, Halvorsen V, Falch JA, Obrant KJ, Nordsletten L (2001) Vitamin D deficiency and ovariectomy reduced the strength of the femoral neck in rats. Calcif Tissue Int 69:102-108
14. Fu L, Tang T, Miao Y, Hao Y, Dai K (2009) Effect of 1,25-dihydroxy vitamin D3 on fracture healing and bone remodeling in ovariectomized rat femora. Bone 44:893-898
15. Young MF IK, Kerr JM, Heegaard AM (1993) Molecular and cellular biology of the major noncollagenous proteins in bone In:Academic Press, Orlando, p 191-234
16. Oldberg A, Jirskog-Hed B, Axelsson S, Heinegard D (1989) Regulation of bone sialoprotein mRNA by steroid hormones. J Cell Biol 109:3183-3186
17. Yoon K, Buenaga R, Rodan GA (1987) Tissue specificity and developmental expression of rat osteopontin. Biochem Biophys Res Commun 148:1129-1136
18. Hultenby K, Reinholt FP, Oldberg A, Heinegard D (1991) Ultrastructural immunolocalization of osteopontin in metaphyseal and cortical bone. Matrix 11:206-213

19. Reppe S, Stilgren L, Olstad OK, Brixen K, Nissen-Meyer LS, Gautvik KM, Abrahamsen B (2006) Gene expression profiles give insight into the molecular pathology of bone in primary hyperparathyroidism. Bone 39:189-198
20. Ek-Rylander B, Bill P, Norgard M, Nilsson S, Andersson G (1991) Cloning, sequence, and developmental expression of a type 5, tartrate-resistant, acid phosphatase of rat bone. J Biol Chem 266:24684-24689
21. Lang P, Schultzberg M, Andersson G (2001) Expression and distribution of tartrate-resistant purple acid phosphatase in the rat nervous system. J Histochem Cytochem 49:379-396
22. Baekkevold ES, Yamanaka T, Palframan RT, Carlsen HS, Reinholt FP, von Andrian UH, Brandtzaeg P, Haraldsen G (2001) The CCR7 ligand elc (CCL19) is transcytosed in high endothelial venules and mediates T cell recruitment. J Exp Med 193:1105-1112
23. Gundersen HJ, Bendtsen TF, Korbo L, Marcussen N, Moller A, Nielsen K, Nyengaard JR, Pakkenberg B, Sorensen FB, Vesterby A, et al. (1988) Some new, simple and efficient stereological methods and their use in pathological research and diagnosis. Apmis 96:379-394
24. Nordahl J, Andersson G, Reinholt FP (1998) Chondroclasts and osteoclasts in bones of young rats: comparison of ultrastructural and functional features. Calcif Tissue Int 63:401-408
25. Nordahl J, Hollberg K, Mengarelli-Widholm S, Andersson G, Reinholt FP (2000) Morphological and functional features of clasts in low phosphate, vitamin D-deficiency rickets. Calcif Tissue Int 67:400-407
26. Hollberg K, Nordahl J, Hultenby K, Mengarelli-Widholm S, Andersson G, Reinholt FP (2005) Polarization and secretion of cathepsin K precede tartrate-resistant acid phosphatase secretion to the ruffled border area during the activation of matrix-resorbing clasts. J Bone Miner Metab 23:441-449

27. Raisz LG, Trummel CL, Holick MF, DeLuca HF (1972) 1,25-dihydroxycholecalciferol: a potent stimulator of bone resorption in tissue culture. Science 175:768-769
28. Shiraishi A, Takeda S, Masaki T, Higuchi Y, Uchiyama Y, Kubodera N, Sato K, Ikeda K, Nakamura T, Matsumoto T, Ogata E (2000) Alfacalcidol inhibits bone resorption and stimulates formation in an ovariectomized rat model of osteoporosis: distinct actions from estrogen. J Bone Miner Res 15:770-779
29. Baldock PA, Thomas GP, Hodge JM, Baker SU, Dressel U, O'Loughlin PD, Nicholson GC, Briffa KH, Eisman JA, Gardiner EM (2006) Vitamin D action and regulation of bone remodeling: suppression of osteoclastogenesis by the mature osteoblast. J Bone Miner Res 21:1618-1626
30. Baldock PA, Need AG, Moore RJ, Durbridge TC, Morris HA (1999) Discordance between bone turnover and bone loss: effects of aging and ovariectomy in the rat. J Bone Miner Res 14:1442-1448
31. Xiao Y, Fu H, Prasadam I, Yang YC, Hollinger JO (2007) Gene expression profiling of bone marrow stromal cells from juvenile, adult, aged and osteoporotic rats: with an emphasis on osteoporosis. Bone 40:700-715
32. Yu JJ, Ruddy MJ, Conti HR, Boonanantanasarn K, Gaffen SL (2008) The interleukin-17 receptor plays a gender-dependent role in host protection against Porphyromonas gingivalis-induced periodontal bone loss. Infect Immun 76:4206-4213
33. Goebel S, Lienau J, Rammoser U, Seefried L, Wintgens KF, Seufert J, Duda G, Jakob F, Ebert R (2009) FGF23 is a putative marker for bone healing and regeneration. J Orthop Res 27:1141-1146
34. Franzen A, Hultenby K, Reinholt FP, Onnerfjord P, Heinegard D (2008) Altered osteoclast development and function in osteopontin deficient mice. J Orthop Res 26:721-728

35. Boskey AL, Maresca M, Ullrich W, Doty SB, Butler WT, Prince CW (1993) Osteopontin-hydroxyapatite interactions in vitro: inhibition of hydroxyapatite formation and growth in a gelatin-gel. Bone Miner 22:147-159
36. Yoshitake H, Rittling SR, Denhardt DT, Noda M (1999) Osteopontin-deficient mice are resistant to ovariectomy-induced bone resorption. Proc Natl Acad Sci U S A 96:8156-8160
37. Duvall CL, Taylor WR, Weiss D, Wojtowicz AM, Guldberg RE (2007) Impaired angiogenesis, early callus formation, and late stage remodeling in fracture healing of osteopontin-deficient mice. J Bone Miner Res 22:286-297
38. Hultenby K, Reinholt FP, Norgard M, Oldberg A, Wendel M, Heinegard D (1994) Distribution and synthesis of bone sialoprotein in metaphyseal bone of young rats show a distinctly different pattern from that of osteopontin. Eur J Cell Biol 63:230-239
39. Chen JJ, Jin H, Ranly DM, Sodek J, Boyan BD (1999) Altered expression of bone sialoproteins in vitamin D-deficient rBSP2.7Luc transgenic mice. J Bone Miner Res 14:221-229
40. Cao Y, Mori S, Mashiba T, Westmore MS, Ma L, Sato M, Akiyama T, Shi L, Komatsubara S, Miyamoto K, Norimatsu H (2002) Raloxifene, estrogen, and alendronate affect the processes of fracture repair differently in ovariectomized rats. J Bone Miner Res 17:2237-2246
41. Jeong KS, Lee J, Jeong W, Noh DH, Do SH, Kim YK (2005) Measurement of estrogen effect on bone turnover by 2H2O labeling. Calcif Tissue Int 76:365-370
42. Huang J, Wang X, Zhang TL, Wang K (2009) Alterations of ovariectomized rat bone and impact of non-collagenous proteins on mineralization. Joint Bone Spine 76:176-183
43. Gerstenfeld LC, Cullinane DM, Barnes GL, Graves DT, Einhorn TA (2003) Fracture healing as a post-natal developmental process:

molecular, spatial, and temporal aspects of its regulation. J Cell Biochem 88:873-884

44. Palomares KT, Gleason RE, Mason ZD, Cullinane DM, Einhorn TA, Gerstenfeld LC, Morgan EF (2009) Mechanical stimulation alters tissue differentiation and molecular expression during bone healing. J Orthop Res 27:1123-1132

45. Harvey N ES, Cooper C (2006) Epidemiology of osteoporotic fractures In: MJ F (ed) Primer on the metabolic bone diseases and disorders of mineral metabolism. The American society for bone and mineral research Washington, D.C., p 244-248

TABLES

Table 1. Primer sequences for DIG-labeled cRNA probes

Sequence name	Sequence forward	Sequence reverse
cathepsin K	5'-agacgcttacccgtatgtgg-3'	5'-tggagagaagggaagcagag-3'
bsp	5'-atggagatggcgatagttcg-3'	5'-tgaaacccgttcagaaggac-3'
osteopontin	5'-ctctgatcaggacagcaacg-3'	5'-tcagggcccaaaacactatc-3'

Table 2. Gene profiling. OP versus sham treated animals

Gene ID	Gene title	Gene symbol	FC Ovx-D vs. Sham	
			3 weeks	6 weeks
1367942_at	Tartrate-resistant acid phosphatase 5 (TRAP)	Acp5	1.26	1.22
1367581_a_at	Secreted phosphoprotein 1 (OPN)	Spp1	1.74	0.83
1368416_at	Integrin binding sialoprotein (BSP)	Ibsp	0.91	1.00
1369947_at	Cathepsin K (CTK)	Ctsk	1.74	0.91

Fold change (FC) $\geq$ 2. No significant differences between the two groups.

Table 3. Ratios of mRNA expressing cells to the total amount of cells attached to bone surfaces

mRNA	Group	n	3 weeks	6 weeks
TRAP	**Ovx-D**	6/5	0.20 (0.14)	0.068 (0.053)
	Sham	7/4	0.11 (0.052)	0.18 (0.14)
CTK	**Ovx-D**	7/5	0.17 (0.095)*b	0.059 (0.032)
	Sham	7/4	0.18 (0.094)	0.14 (0.14)
OPN	**Ovx-D**	7/5	0.33 (0.15)*a/*b	0.12 (0.047)
	Sham	7/4	0.19 (0.059)	0.12 (0.085)
BSP	**Ovx-D**	7/5	0.21 (0.14)*b	0.022 (0.034)
	Sham	7/4	0.32 (0.19)	0.18 (0.089)*

Results are given as mean (SD). (n): number of animals in OP/sham, (*a) Significant differences between the groups ($p \leq 0.05$), (*b) Significant differences between 3 and 6 weeks in the group ($p \leq 0.05$).

Table 4. Protein distribution of OPN and BSP in the fracture callus at 3 and 6 weeks

		3 weeks				6 weeks			
		OPN		BSP		OPN		BSP	
Cell type	**ROI**	**Ovx-D** n=5	**Sham** n=6	**Ovx-D** n=5	**Sham** n=6	**Ovx-D** n=4	**Sham** n=4	**Ovx-D** n=4	**Sham** n=4
OB	Nuc.	2.38 (3.07)	2.30 (1.00)	4.06 (3.56)	2.98 (1.67)	1.32 (0.92)	1.25 (0.87)	1.70 (0.57)	1.69 (0.70)
	Cyt.	2.84 (3.42)	2.66 (1.18)	3.66 (2.32)	3.69 (1.50)	1.04 (0.41)	0.99 (0.21)	1.41 (0.47)	2.06 (1.37)
	O	1.83 (1.04)	1.94 (1.40)	6.63 (6.83)	2.52 (0.56)	1.89 (0.30)	1.65 (0.87)	1.62 (0.27)	1.83 (0.24)
	MF	57.58 (28.38)	38.11 (12.11)	421.22 (343.93)	311.52 (30.65)	42.43 (5.16)	51.18 (18.89)	176.40 (27.92)	308.72 (58.98)
	WB	3.66 (0.52)	3.56 (2.98)	116.87 (102.09)	75.66 (29.31)	1.75 (0.66)	3.03 (2.37)	32.50 (8.94)	81.51 (39.75)
	BG	0.14 (0.09)	1.26 (0.96)	1.95 (1.47)	1.16 (0.60)	0.19 (0.04)	0.39 (0.18)	17.79 (17.79)	0.40 (0.13)
		n=5	n=5	n=5	n=5	n=3	n=3	n=2 (*n=1)	n=3 (*n=2)
OC	Nuc.	0.90 (0.46)	1.12 (0.26)	3.61 (0.83)	1.99 (0.73)	0.69 (0.18)	0.82 (0.40)	2.58 (-)*	1.90 (0.97)
	Cyt.	1.28 (0.24)	1.77 (1.13)	4.38 (1.65)	2.67 (0.90)	0.89 (0.10)	1.25 (0.22)	4.89 (1.33)	3.18 (0.38)
	RBc	0.69 (0.31)	2.17 (0.36)	2.91 (1.71)	2.58 (0.76)	1.30 (1.17)	1.00 (0.46)	3.73 (1.66)	1.85 (0.47)
	RBm	2.30 (1.75)	2.58 (1.18)	39.87 (33.39)	29.67 (8.45)	26.41 (17.38)	3.55 (1.54)	69.11 (36.10)	16.36 (7.84)
	CZc	0.95 (0.52)	2.83 (0.60)	5.81 (1.12)	5.64 (2.27)	1.47 (-)	1.19 (0.44)	9.02 (-)*	3.86 (0.14)*
	CZm	7.13 (4.29)	6.26 (3.08)	34.74 (23.85)	58.34 (60.52)	3.23 (-)	5.03 (3.50)**	36.80 (-)*	57.99 (28.94)*
	BG	1.21 (1.85)	0.68 (0.18)	2.40 (0.30)	1.76 (1.05)	0.44 (0.09)	0.51 (0.11)	1.43 (0.05)	1.31 (0.25)

Values are mean gold particles per um^2. *reduced number - cell domain not found in all animals. ** $p < 0.05$. Abbreviations; ROI = region of interest/compartment, OB = osteoblast, OC = osteoclast, nuc. = nucleus, cyt. = cell cytoplasm, O = osteoid, MF = mineralization front, WB = woven bone, RBc = cell cytoplasm facing the ruffled border, RBm = extracellular matrix facing the ruffled border, CZc = cell cytoplasm facing the clear zone, CZm = extracellular matrix facing the clear zone, BG = background, i.e. capillary lumen.

Table 5. Protein distribution of TRAP and CTK in the fracture callus at 3 and 6 weeks of healing

		3 weeks				6 weeks			
		TRAP		CTK		TRAP		CTK	
Cell type	**ROI**	**Ovx-D** n=5	**Sham** n=5	**Ovx-D** n=3	**Sham** n=5	**Ovx-D** n=3	**Sham** n=3	**Ovx-D** n=2	**Sham** n=3
OC	Nuc	1.04 (0.44)	0.77 (0.37)	1.22 (0.40)	0.74 (0.17)	1.37 (1.10)	0.60 (0.32)	0.94 (0.05)	1.10 (0.46)
	Cyt	6.60 (1.66)	6.33 (2.70)	6.00 (1.92)**	3.67 (0.25)	4.98 (1.33)	2.93 (0.40)	5.56 (3.77)	4.12 (1.04)
	RBc	2.72 (1.28)	2.64 (1.83)	1.77 (1.04)	1.58 (0.34)	0.78 (0.49)	0.57(0.16)	1.48 (1.28)	1.73 (0.68)
	RBm	12.76 (6.86)	13.76 (9.74)	4.13 (2.43)	3.60 (0.73)	2.46 (0.85)	2.93 (2.00)	5.85 (4.23)	3.07 (1.82)
	CZc	1.54 (0.32)	1.33 (0.70)	1.70 (0.41)	1.98 (0.55)	1.43 (1.12)	0.92 (0.43)	2.07 (1.22)	3.80 (1.84)
	CZm	5.95 (3.34)	12.65 (9.07)	2.82 (1.31)	2.40 (0.27)	2.07 (0.48)	2.78 (2.40)	5.82 (-)	2.50 (1.36)
	BG	1.03 (0.53)	0.65 (0.34)	0.68 (0.39)	0.76 (0.24)	1.10 (0.82)	0.62 (0.21)	0.82 (0.16)	0.88 (0.46)

Values are mean gold particles per um^2 *reduced number - cell domain not found in all animals ** p = 0.05
Abbreviations; ROI = region of interest/compartment, OC = osteoclast, nuc. = nucleus, cyt. = cell cytoplasm, O = osteoid, MF = mineralization front, WB = woven bone, RBc = cell cytoplasm facing the ruffled border, RBm = extracellular matrix facing the ruffled border, CZc = cell cytoplasm facing the clear zone, CZm = extracellular matrix facing the clear zone, BG = background, i.e. capillary lumen.

FIGURES

Fig. 1. Differentially expressed genes in callus of the Ovx-D group

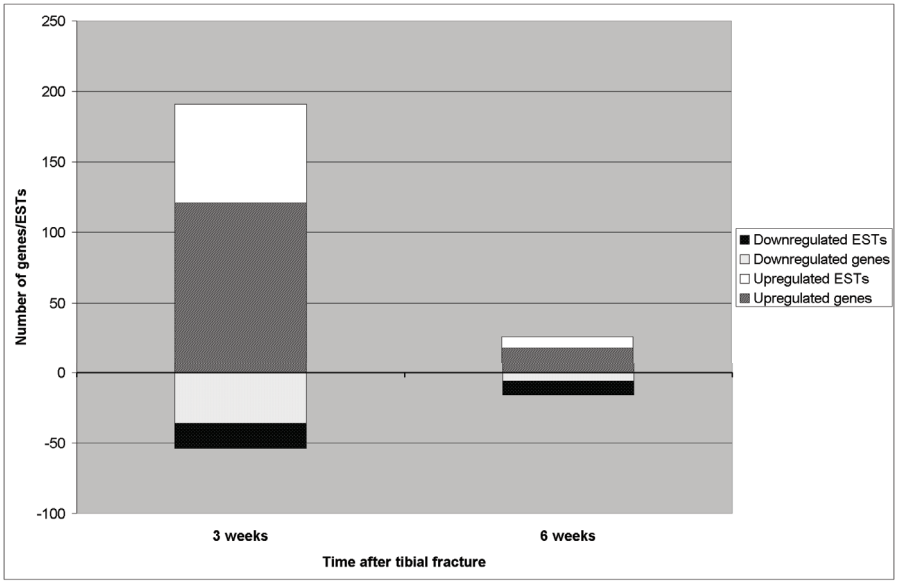

Microarray analysis showed a larger number of annotated genes and expressed sequence tags (ESTs) differently regulated in the Ovx-D group (fold change $\geq$ 2) compared to sham, the majority in an increased fashion and mostly after 3 weeks of healing. $p \leq 0.05$.

Fig. 2. Callus morphology after 3 weeks of healing

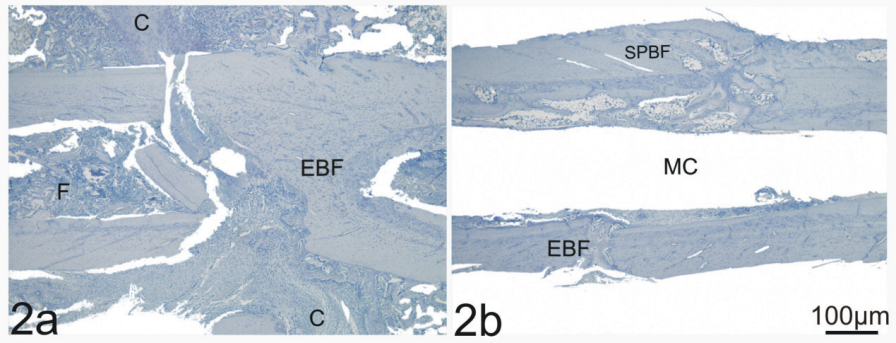

Light microscopic callus morphology showing two different animals in the Ovx-D group at 3 weeks of healing. Both Ovx-D and sham treated animals exhibited relatively large inter-individual variation in the composition and size of callus after 3 as well as 6 weeks of healing. **2a** A large fracture callus with massive accumulation of fibrous tissue (F), cartilage (C) and endosteal bone formation (EBF). **2b** A smaller callus with endosteal and subperiosteal bone formation (SPBF). MC, marrow cavity. H&E, x 4

Fig. 3. Expression of OPN, BSP, TRAP and CTK in the fracture callus

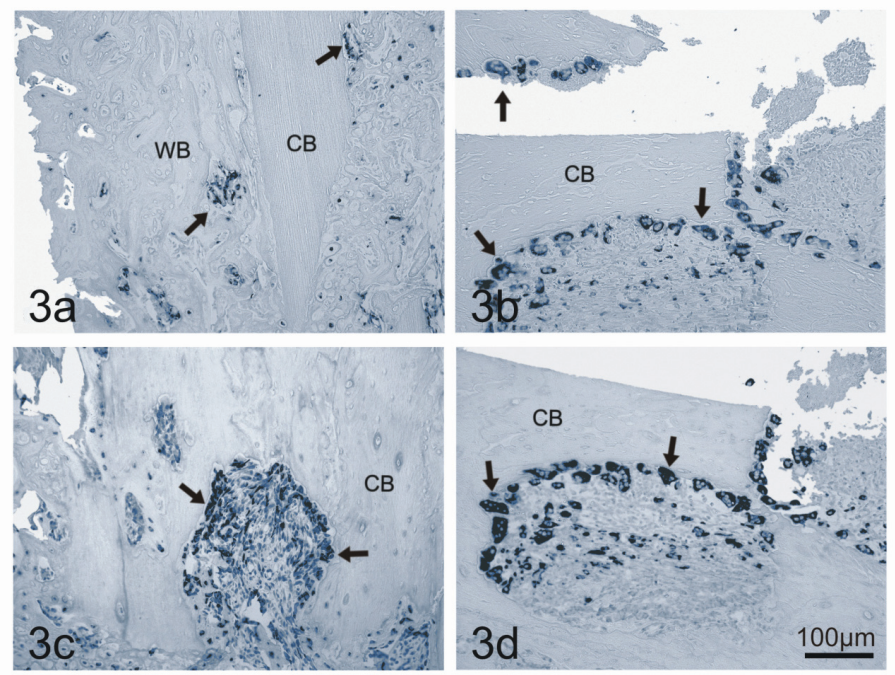

OPN, BSP, TRAP and CTK mRNA positive cells in fracture callus at 3 weeks visualized by *in situ* hybridization. OPN mRNA (**3a**) and BSP mRNA (**3c**) positive osteoblasts, and TRAP mRNA (**3b**) and CTK mRNA (**2d**) positive osteoclasts (*arrows*). WB, woven bone. CB, cortical bone. Paraffin-embedded sections, x 20.

Fig. 4. Ultrastructural distribution of BSP and OPN in mineralized bone

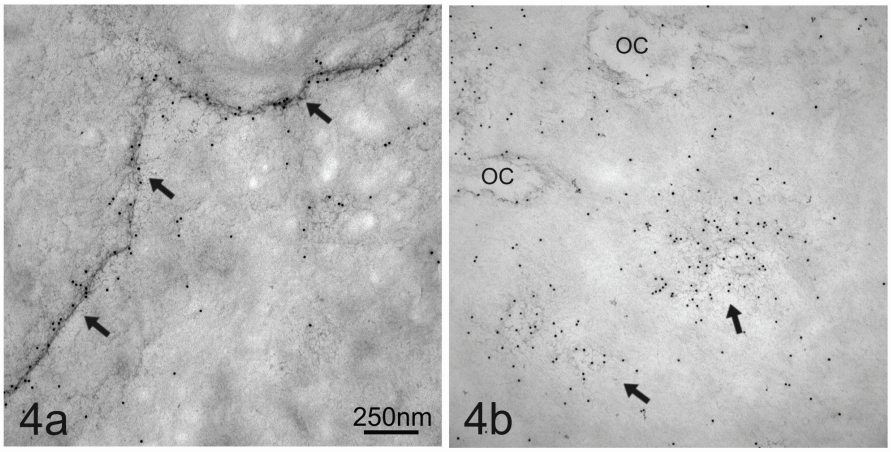

Characteristic ultrastructural protein distribution of OPN and BSP in fracture callus at 3 weeks. **4a** Immunogold signaling for OPN with distinct accumulation along a cement line (*arrows*). **4b** Intense BSP signaling at early focus of mineralization, i.e. “mineralization noduli” (*arrows*). OC, osteocyte canaliculi. Lowicryl HM23 embedded, x 43,000

IV

This article is removed.